FEM/BEM NOTES
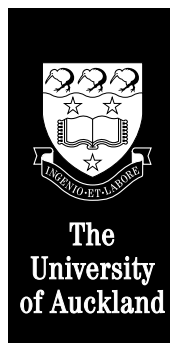
Professor Peter Hunter
p.hunter@auckland.ac.nz

Associate Professor Andrew Pullan
a.pullan@auckland.ac.nz

The University of Auckland

Department of Engineering Science
The University of Auckland
New Zealand

June 17, 2003

Contents

Chapter 1

Finite Element Basis Functions

1.1 Representing a One-Dimensional Field

Consider the problem of finding a mathematical expression $u(x)$ to represent a one-dimensional field *e.g.,* measurements of temperature u against distance x along a bar, as shown in Figure 1.1a.
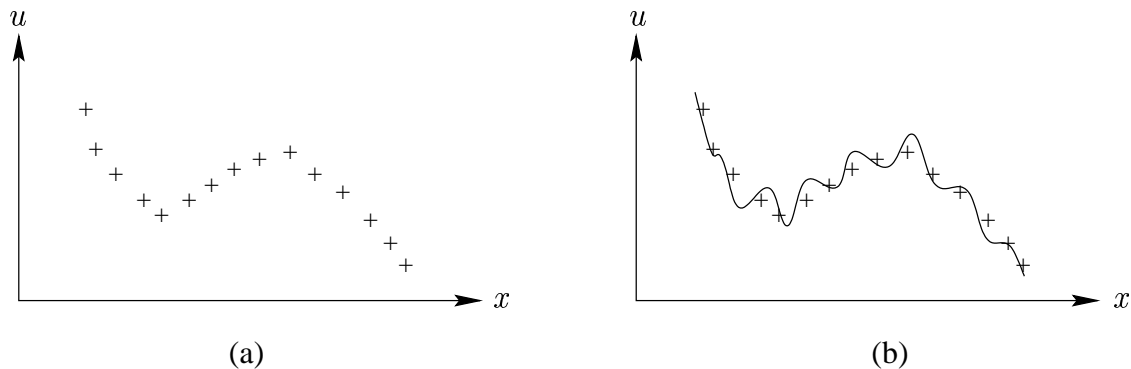
FIGURE 1.1: (a) Temperature distribution $u(x)$ along a bar. The points are the measured temperatures. (b) A least-squares polynomial fit to the data, showing the unacceptable oscillation between data points.

One approach would be to use a polynomial expression $u(x) = a + bx + cx^2 + dx^3 + \ldots$ and to estimate the values of the parameters a, b, c and d from a least-squares fit to the data. As the degree of the polynomial is increased the data points are fitted with increasing accuracy and polynomials provide a very convenient form of expression because they can be differentiated and integrated readily. For low degree polynomials this is a satisfactory approach, but if the polynomial order is increased further to improve the accuracy of fit a problem arises: the polynomial can be made to fit the data accurately, but it oscillates unacceptably between the data points, as shown in Figure 1.1b.

To circumvent this, while retaining the advantages of low degree polynomials, we divide the bar into three subregions and use low order polynomials over each subregion - called *elements*. For later generality we also introduce a parameter s which is a measure of distance along the bar. u is plotted as a function of this arclength in Figure 1.2a. Figure 1.2b shows three linear polynomials in s fitted by least-squares separately to the data in each element.
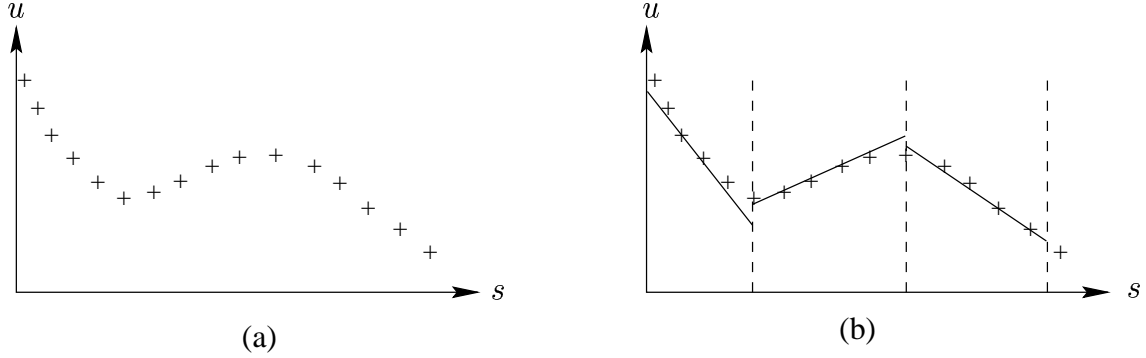
FIGURE 1.2: (a) Temperature measurements replotted against arclength parameter s. (b) The s domain is divided into three subdomains, *elements*, and linear polynomials are independently fitted to the data in each subdomain.

1.2 Linear Basis Functions

A new problem has now arisen in Figure 1.2b: the piecewise linear polynomials are not continuous in u across the boundaries between elements. One solution would be to constrain the parameters a, b, c *etc.* to ensure continuity of u across the element boundaries, but a better solution is to replace the parameters a and b in the first element with parameters u_1 and u_2, which are the values of u at the two ends of that element. We then define a linear variation between these two values by

$$u\left(\xi\right) = \left(1 - \xi\right)u_1 + \xi u_2$$

where $\xi(0 \leq \xi \leq 1)$ is a normalized measure of distance along the curve.

We define

$$\varphi_1\left(\xi\right) = 1 - \xi$$
$$\varphi_2\left(\xi\right) = \xi$$

such that

$$u\left(\xi\right) = \varphi_1\left(\xi\right)u_1 + \varphi_2\left(\xi\right)u_2$$

and refer to these expressions as the *basis* functions associated with the *nodal* parameters u_1 and u_2. The basis functions $\varphi_1\left(\xi\right)$ and $\varphi_2\left(\xi\right)$ are straight lines varying between 0 and 1 as shown in Figure 1.3.

It is convenient always to associate the nodal quantity u_n with *element node* n and to map the temperature U_Δ defined at *global node* Δ onto local node n of element e by using a connectivity matrix $\Delta\left(n, e\right)$ *i.e.,*

$$u_n = U_{\Delta(n,e)}$$

where $\Delta\left(n, e\right) = $ global node number of local node n of element e. This has the advantage that the
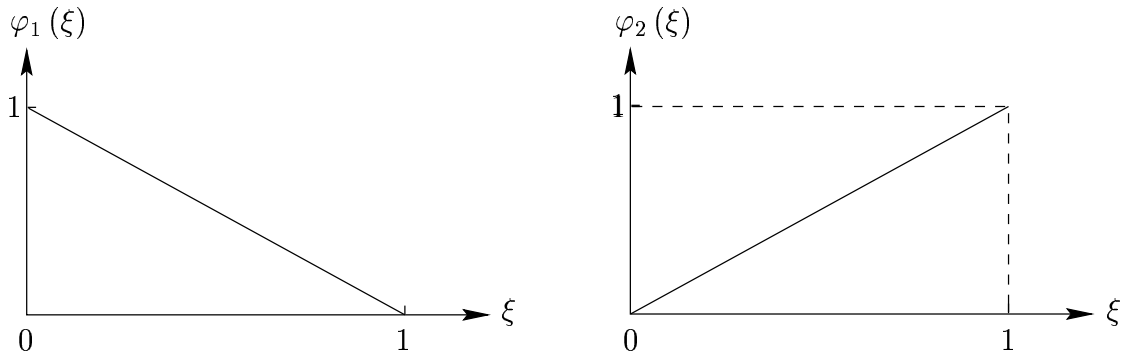
FIGURE 1.3: Linear basis functions $\varphi_1(\xi) = 1 - \xi$ and $\varphi_2(\xi) = \xi$.

interpolation

$$u(\xi) = \varphi_1(\xi) u_1 + \varphi_2(\xi) u_2$$

holds for any element provided that u_1 and u_2 are correctly identified with their global counterparts, as shown in Figure 1.4. Thus, in the first element
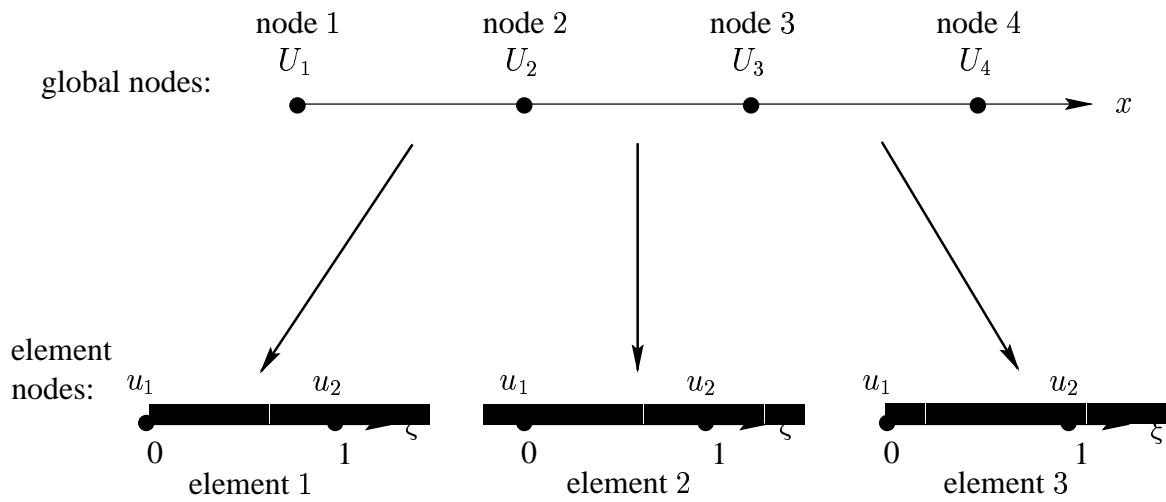
FIGURE 1.4: The relationship between global nodes and element nodes.

$$u(\xi) = \varphi_1(\xi) u_1 + \varphi_2(\xi) u_2 \tag{1.1}$$

with $u_1 = U_1$ and $u_2 = U_2$.

In the second element u is interpolated by

$$u(\xi) = \varphi_1(\xi) u_1 + \varphi_2(\xi) u_2 \tag{1.2}$$

with $u_1 = U_2$ and $u_2 = U_3$, since the parameter U_2 is shared between the first and second elements

the temperature field u is implicitly continuous. Similarly, in the third element u is interpolated by

$$u\left(\xi\right) = \varphi_1\left(\xi\right)u_1 + \varphi_2\left(\xi\right)u_2 \tag{1.3}$$

with $u_1 = U_3$ and $u_2 = U_4$, with the parameter U_3 being shared between the second and third elements. Figure 1.6 shows the temperature field defined by the three interpolations (1.1)–(1.3).
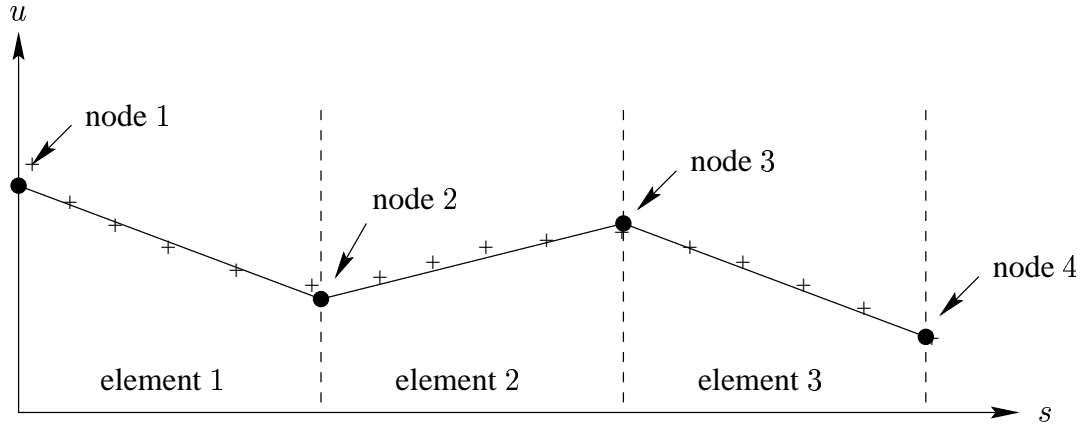
FIGURE 1.5: Temperature measurements fitted with nodal parameters and linear basis functions. The fitted temperature field is now continuous across element boundaries.

1.3   Basis Functions as Weighting Functions

It is useful to think of the basis functions as weighting functions on the nodal parameters. Thus, in element 1

$$\text{at } \xi = 0 \qquad u\left(0\right) = \left(1 - 0\right)u_1 + 0u_2 = u_1$$

which is the value of u at the left hand end of the element and has no dependence on u_2

$$\text{at } \xi = \frac{1}{4} \qquad u\left(\frac{1}{4}\right) = \left(1 - \frac{1}{4}\right)u_1 + \frac{1}{4}u_2 = \frac{3}{4}u_1 + \frac{1}{4}u_2$$

which depends on u_1 and u_2, but is weighted more towards u_1 than u_2

$$\text{at } \xi = \frac{1}{2} \qquad u\left(\frac{1}{2}\right) = \left(1 - \frac{1}{2}\right)u_1 + \frac{1}{2}u_2 = \frac{1}{2}u_1 + \frac{1}{2}u_2$$

which depends equally on u_1 and u_2

$$\text{at } \xi = \frac{3}{4} \qquad u\left(\frac{3}{4}\right) = \left(1 - \frac{3}{4}\right)u_1 + \frac{3}{4}u_2 = \frac{1}{4}u_1 + \frac{3}{4}u_2$$

which depends on u_1 and u_2 but is weighted more towards u_2 than u_1

$$\text{at } \xi = 1 \qquad u\left(1\right) = \left(1 - 1\right)u_1 + 1u_2 = u_2$$

which is the value of u at the right hand end of the region and has no dependence on u_1.

Moreover, these weighting functions can be considered as *global* functions, as shown in Figure 1.6, where the weighting function w_n associated with global node n is constructed from the basis functions in the elements adjacent to that node.
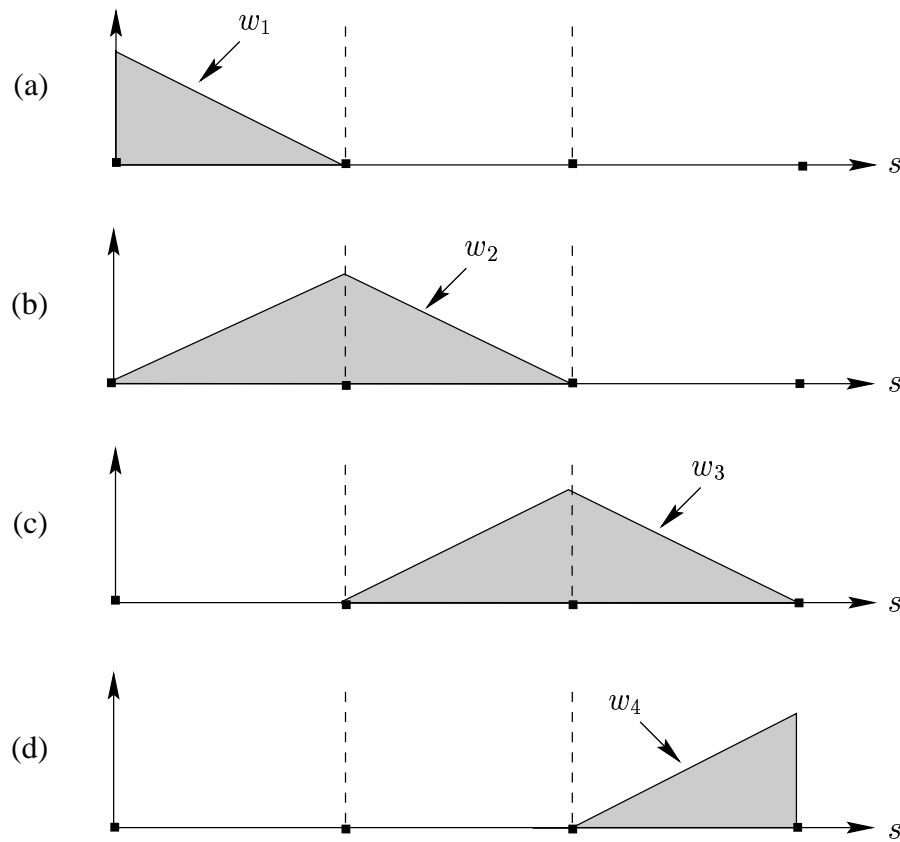
FIGURE 1.6: (a) ... (d) The weighting functions w_n associated with the global nodes $n = 1 \ldots 4$, respectively. Notice the linear fall off in the elements adjacent to a node. Outside the immediately adjacent elements, the weighting functions are defined to be zero.

For example, w_2 weights the global parameter U_2 and the influence of U_2 falls off linearly in the elements on either side of node 2.

We now have a continuous piecewise parametric description of the temperature field $u\left(\xi\right)$ but in order to define $u\left(x\right)$ we need to define the relationship between x and ξ for each element. A convenient way to do this is to define x as an interpolation of the nodal values of x.

For example, in element 1

$$x\left(\xi\right) = \varphi_1\left(\xi\right)x_1 + \varphi_2\left(\xi\right)x_2 \tag{1.4}$$

and similarly for the other two elements. The dependence of temperature on x, $u\left(x\right)$, is therefore

defined by the parametric expressions

$$u(\xi) = \sum_n \varphi_n(\xi) u_n$$

$$x(\xi) = \sum_n \varphi_n(\xi) x_n$$

where summation is taken over all element nodes (in this case only 2) and the parameter ξ (the "element coordinate") links temperature u to physical position x. $x(\xi)$ provides the mapping between the mathematical space $0 \le \xi \le 1$ and the physical space $x_1 \le x \le x_2$, as illustrated in Figure 1.7.
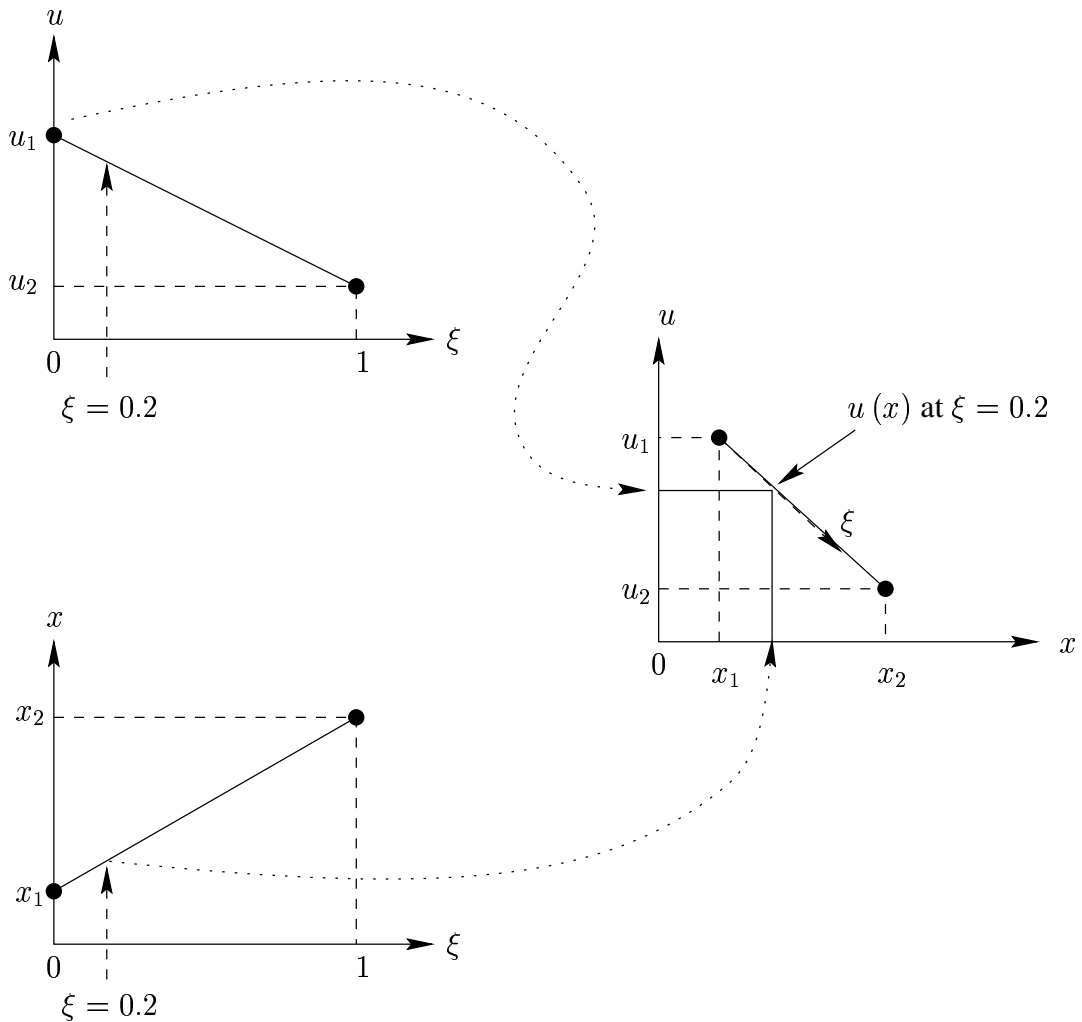
FIGURE 1.7: Illustrating how x and u are related through the normalized element coordinate ξ. The values of $x(\xi)$ and $u(\xi)$ are obtained from a linear interpolation of the nodal variables and then plotted as $u(x)$. The points at $\xi = 0.2$ are emphasized.

1.4   Quadratic Basis Functions

The essential property of the basis functions defined above is that the basis function associated with a particular node takes the value of 1 when evaluated at that node and is zero at every other node in the element (only one other in the case of linear basis functions). This ensures the linear independence of the basis functions. It is also the key to establishing the form of the basis functions for higher order interpolation. For example, a quadratic variation of u over an element requires three nodal parameters u_1, u_2 and u_3

$$u\left(\xi\right) = \varphi_1\left(\xi\right)u_1 + \varphi_2\left(\xi\right)u_2 + \varphi_3\left(\xi\right)u_3 \tag{1.5}$$

The quadratic basis functions are shown, with their mathematical expressions, in Figure 1.8. Notice that since $\varphi_1\left(\xi\right)$ must be zero at $\xi = 0.5$ (node 2), $\varphi_1\left(\xi\right)$ must have a factor $\left(\xi - 0.5\right)$ and since it is also zero at $\xi = 1$ (node 3), another factor is $\left(\xi - 1\right)$. Finally, since $\varphi_1\left(\xi\right)$ is 1 at $\xi = 0$ (node 1) we have $\varphi_1\left(\xi\right) = 2\left(\xi - 1\right)\left(\xi - 0.5\right)$. Similarly for the other two basis functions.

(a) $\varphi_1\left(\xi\right) = 2\left(\xi - 1\right)\left(\xi - 0.5\right)$

(b) $\varphi_2\left(\xi\right) = 4\xi\left(1 - \xi\right)$

(c) $\varphi_3\left(\xi\right) = 2\xi\left(\xi - 0.5\right)$
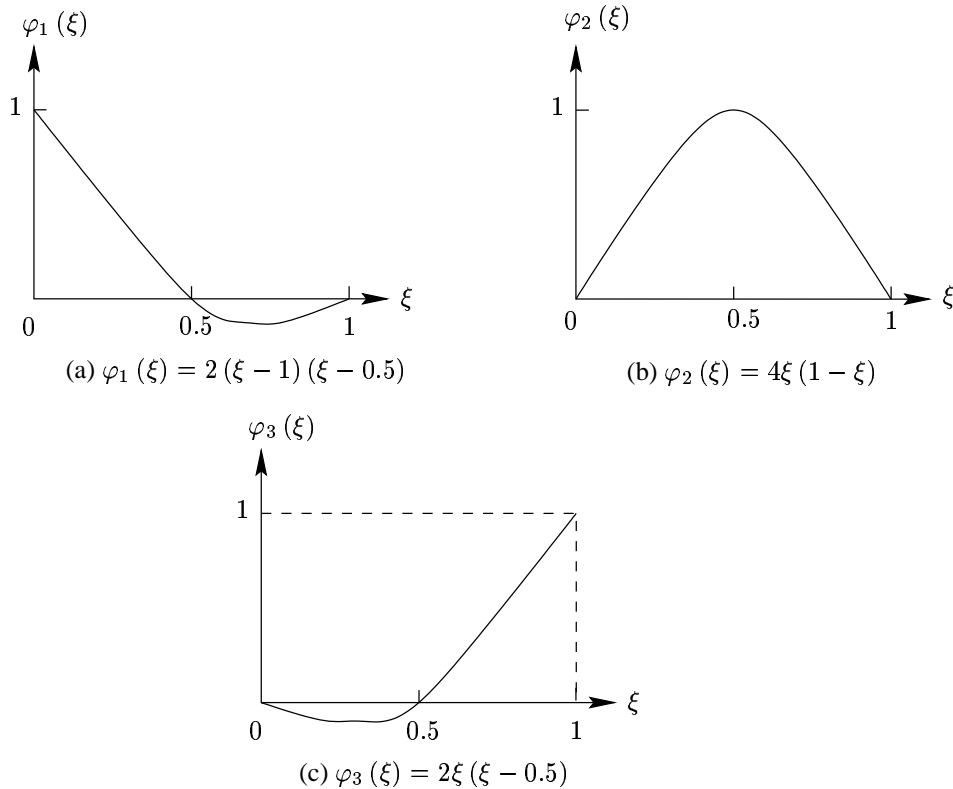
FIGURE 1.8: One-dimensional quadratic basis functions.

1.5   Two- and Three-Dimensional Elements

Two-dimensional bilinear basis functions are constructed from the products of the above one-dimensional linear functions as follows

Let

$$u\left(\xi_1, \xi_2\right) = \varphi_1\left(\xi_1, \xi_2\right) u_1 + \varphi_2\left(\xi_1, \xi_2\right) u_2 + \varphi_3\left(\xi_1, \xi_2\right) u_3 + \varphi_4\left(\xi_1, \xi_2\right) u_4$$

where

$$\begin{aligned}
\varphi_1\left(\xi_1, \xi_2\right) &= \left(1 - \xi_1\right)\left(1 - \xi_2\right) \\
\varphi_2\left(\xi_1, \xi_2\right) &= \xi_1\left(1 - \xi_2\right) \\
\varphi_3\left(\xi_1, \xi_2\right) &= \left(1 - \xi_1\right)\xi_2 \\
\varphi_4\left(\xi_1, \xi_2\right) &= \xi_1\xi_2
\end{aligned} \tag{1.6}$$

Note that $\varphi_1\left(\xi_1, \xi_2\right) = \varphi_1\left(\xi_1\right)\varphi_1\left(\xi_2\right)$ where $\varphi_1\left(\xi_1\right)$ and $\varphi_1\left(\xi_2\right)$ are the one-dimensional linear basis functions. Similarly, $\varphi_2\left(\xi_1, \xi_2\right) = \varphi_2\left(\xi_1\right)\varphi_1\left(\xi_2\right) \ldots$ *etc.*

These four bilinear basis functions are illustrated in Figure 1.9.
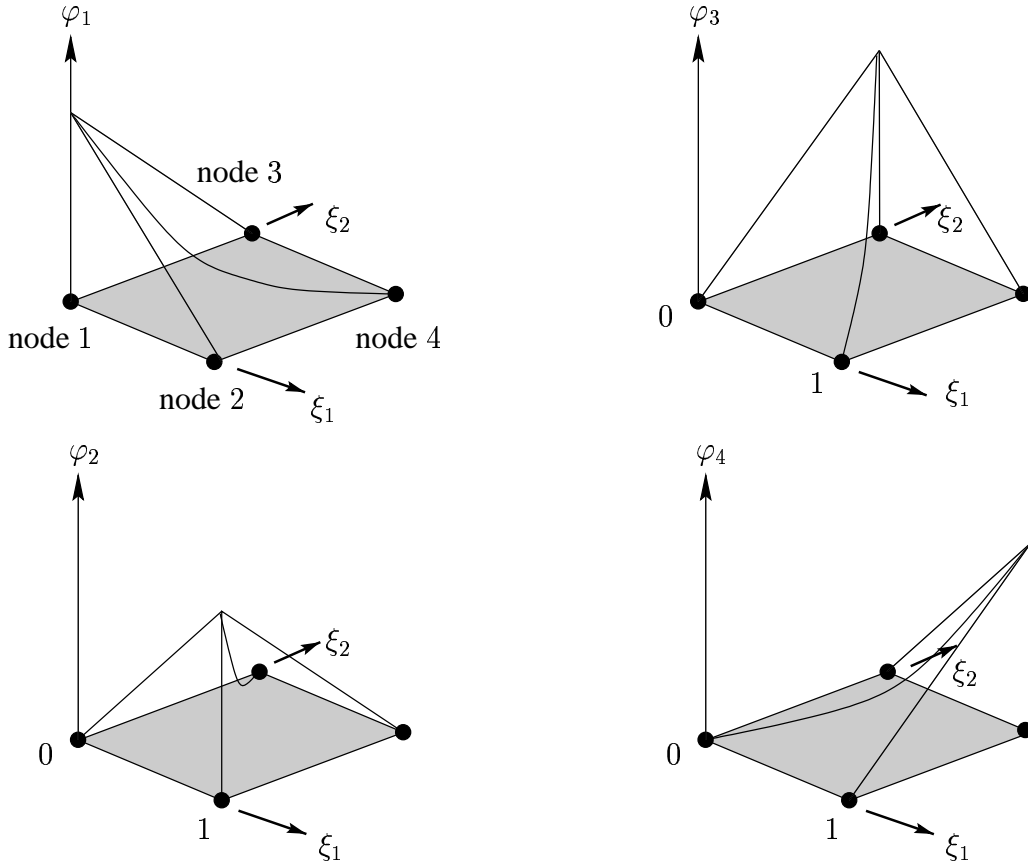
FIGURE 1.9: Two-dimensional bilinear basis functions.

Notice that $\varphi_n\left(\xi_1, \xi_2\right)$ is 1 at node n and zero at the other three nodes. This ensures that the temperature $u\left(\xi_1, \xi_2\right)$ receives a contribution from each nodal parameter u_n weighted by $\varphi_n\left(\xi_1, \xi_2\right)$ and that when $u\left(\xi_1, \xi_2\right)$ is evaluated at node n it takes on the value u_n.

As before the geometry of the element is defined in terms of the node positions $\left(x_n, y_n\right)$, $n =$

$1, \dots, 4$ by

$$x = \sum_n \varphi_n \left(\xi_1, \xi_2\right) x_n$$

$$y = \sum_n \varphi_n \left(\xi_1, \xi_2\right) y_n$$

which provide the mapping between the mathematical space (ξ_1, ξ_2) (where $0 \le \xi_1, \xi_2 \le 1$) and the physical space (x, y).

Higher order 2D basis functions can be similarly constructed from products of the appropriate 1D basis functions. For example, a six-noded (see Figure 1.10) quadratic-linear element (quadratic in ξ_1 and linear in ξ_2) would have

$$u = \sum_{n=1}^{6} \varphi_n \left(\xi_1, \xi_2\right) u_n$$

where

$$\varphi_1 \left(\xi_1, \xi_2\right) = 2 \left(\xi_1 - 1\right) \left(\xi_1 - 0.5\right) \left(1 - \xi_2\right) \qquad \varphi_2 \left(\xi_1, \xi_2\right) = 4\xi_1 \left(1 - \xi_1\right) \left(1 - \xi_2\right) \qquad (1.7)$$

$$\varphi_3 \left(\xi_1, \xi_2\right) = 2\xi_1 \left(\xi_1 - 0.5\right) \left(1 - \xi_2\right) \qquad \varphi_4 \left(\xi_1, \xi_2\right) = 2 \left(\xi_1 - 1\right) \left(\xi_1 - 0.5\right) \xi_2 \qquad (1.8)$$

$$\varphi_5 \left(\xi_1, \xi_2\right) = 4\xi_1 \left(1 - \xi_1\right) \xi_2 \qquad \varphi_6 \left(\xi_1, \xi_2\right) = 2\xi_1 \left(\xi_1 - 0.5\right) \xi_2 \qquad (1.9)$$
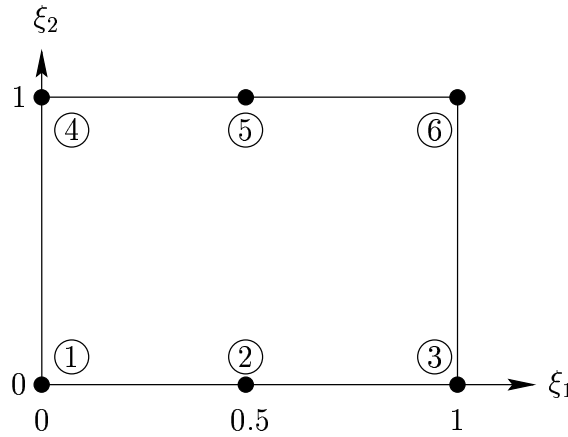
FIGURE 1.10: A 6-node quadratic-linear element (node numbers circled).

Three-dimensional basis functions are formed similarly, *e.g.,* a trilinear element basis has eight nodes (see Figure 1.11) with basis functions

$$\varphi_1 \left(\xi_1, \xi_2, \xi_3\right) = \left(1 - \xi_1\right) \left(1 - \xi_2\right) \left(1 - \xi_3\right) \qquad \varphi_2 \left(\xi_1, \xi_2, \xi_3\right) = \xi_1 \left(1 - \xi_2\right) \left(1 - \xi_3\right) \qquad (1.10)$$

$$\varphi_3 \left(\xi_1, \xi_2, \xi_3\right) = \left(1 - \xi_1\right) \xi_2 \left(1 - \xi_3\right) \qquad \varphi_4 \left(\xi_1, \xi_2, \xi_3\right) = \xi_1 \xi_2 \left(1 - \xi_3\right) \qquad (1.11)$$

$$\varphi_5 \left(\xi_1, \xi_2, \xi_3\right) = \left(1 - \xi_1\right) \left(1 - \xi_2\right) \xi_3 \qquad \varphi_6 \left(\xi_1, \xi_2, \xi_3\right) = \xi_1 \left(1 - \xi_2\right) \xi_3 \qquad (1.12)$$

$$\varphi_7 \left(\xi_1, \xi_2, \xi_3\right) = \left(1 - \xi_1\right) \xi_2 \xi_3 \qquad \varphi_8 \left(\xi_1, \xi_2, \xi_3\right) = \xi_1 \xi_2 \xi_3 \qquad (1.13)$$
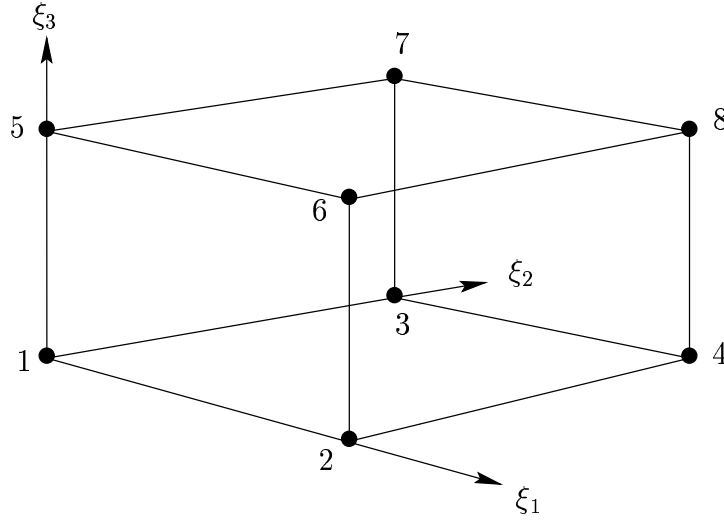
FIGURE 1.11: An 8-node trilinear element.

1.6 Higher Order Continuity

All the basis functions mentioned so far are *Lagrange*[1] basis functions and provide continuity of u across element boundaries but not higher order continuity. Sometimes it is desirable to use basis functions which also preserve continuity of the derivative of u with respect to ξ across element boundaries. A convenient way to achieve this is by defining two additional nodal parameters $\left(\dfrac{du}{d\xi}\right)_n$. The basis functions are chosen to ensure that

$$\frac{du}{d\xi}\bigg|_{\xi=0} = \left(\frac{du}{d\xi}\right)_1 = u'_1 \text{ and } \frac{du}{d\xi}\bigg|_{\xi=1} = \left(\frac{du}{d\xi}\right)_2 = u'_2$$

and since u_n is shared between adjacent elements derivative continuity is ensured. Since the number of element parameters is 4 the basis functions must be cubic in ξ. To derive these cubic *Hermite*[2] basis functions let

$$u(\xi) = a + b\xi + c\xi^2 + d\xi^3,$$
$$\frac{du}{d\xi} = b + 2c\xi + 3d\xi^2,$$

---

[1]Joseph-Louis Lagrange (1736-1813).
[2]Charles Hermite (1822-1901).

and impose the constraints

$$
\begin{aligned}
u\left(0\right) &= a & &= u_1 \\
u\left(1\right) &= a + b + c + d & &= u_2 \\
\frac{du}{d\xi}\left(0\right) &= b & &= u_1' \\
\frac{du}{d\xi}\left(1\right) &= b + 2c + 3d & &= u_2'
\end{aligned}
$$

These four equations in the four unknowns a, b, c and d are solved to give

$$
\begin{aligned}
a &= u_1 \\
b &= u_1' \\
c &= 3u_2 - 3u_1 - 2u_1' - u_2' \\
d &= u_1' + u_2' + 2u_1 - 2u_2
\end{aligned}
$$

Substituting a, b, c and d back into the original cubic then gives

$$
u\left(\xi\right) = u_1 + u_1'\xi + \left(3u_2 - 3u_1 - 2u_1' - u_2'\right)\xi^2 + \left(u_1' + u_2' + 2u_1 - 2u_2\right)\xi^3
$$

or, rearranging,

$$
u\left(\xi\right) = \Psi_1^0\left(\xi\right)u_1 + \Psi_1^1\left(\xi\right)u_1' + \Psi_2^0\left(\xi\right)u_2 + \Psi_2^1\left(\xi\right)u_2' \tag{1.14}
$$

where the four cubic Hermite basis functions are drawn in Figure 1.12.

One further step is required to make cubic Hermite basis functions useful in practice. The derivative $\left(\dfrac{du}{d\xi}\right)_n$ defined at node n is dependent upon the element ξ-coordinate in the two adjacent elements. It is much more useful to define a global node derivative $\left(\dfrac{du}{ds}\right)_n$ where s is arclength and then use

$$
\left(\frac{du}{d\xi}\right)_n = \left(\frac{du}{ds}\right)_{\Delta(n,e)} \cdot \left(\frac{ds}{d\xi}\right)_n \tag{1.15}
$$

where $\left(\dfrac{ds}{d\xi}\right)_n$ is an element *scale factor* which scales the arclength derivative of global node Δ to the ξ-coordinate derivative of element node n. Thus $\dfrac{du}{ds}$ is constrained to be continuous across element boundaries rather than $\dfrac{du}{d\xi}$. A two- dimensional bicubic Hermite basis requires four derivatives per node

$$
u, \frac{\partial u}{\partial \xi_1}, \frac{\partial u}{\partial \xi_2} \text{ and } \frac{\partial^2 u}{\partial \xi_1 \partial \xi_2}
$$
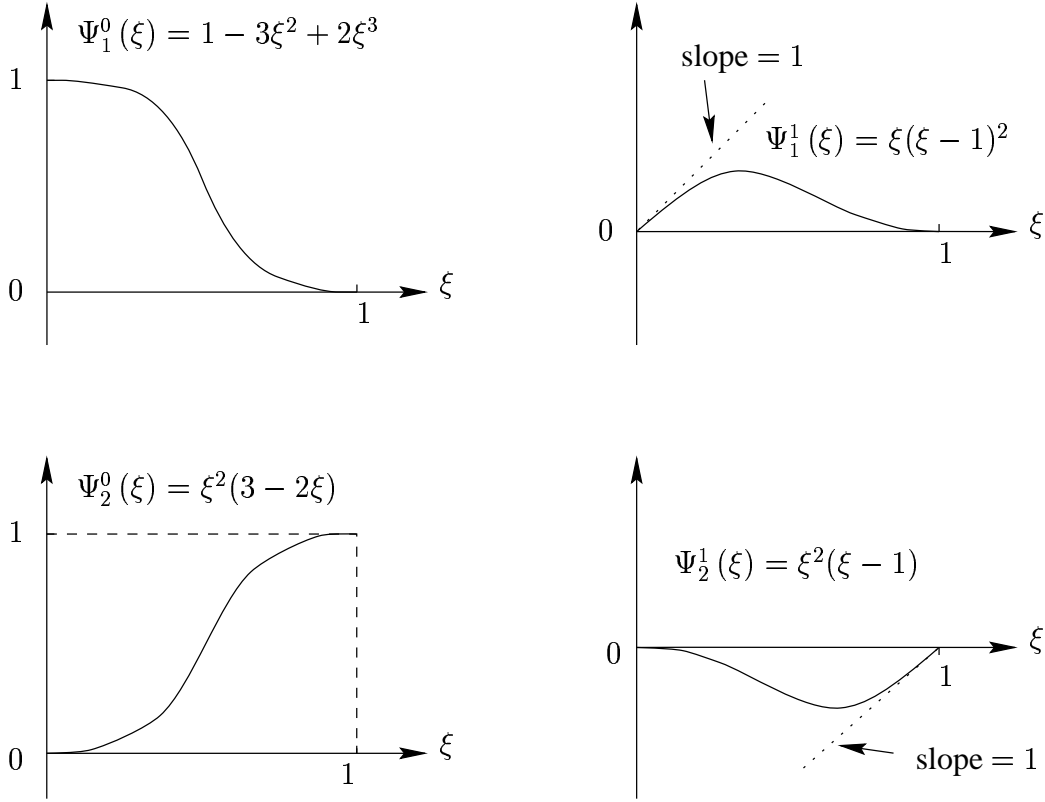
FIGURE 1.12: Cubic Hermite basis functions.

The need for the second-order cross-derivative term can be explained as follows; If u is cubic in ξ_1 and cubic in ξ_2, then $\dfrac{\partial u}{\partial \xi_1}$ is quadratic in ξ_1 and cubic in ξ_2, and $\dfrac{\partial u}{\partial \xi_2}$ is cubic in ξ_1 and quadratic in ξ_2. Now consider the side 1–3 in Figure 1.13. The cubic variation of u with ξ_2 is specified by the four nodal parameters u_1, $\left(\dfrac{\partial u}{\partial \xi_2}\right)_1$, u_3 and $\left(\dfrac{\partial u}{\partial \xi_2}\right)_3$. But since $\dfrac{\partial u}{\partial \xi_1}$ (the normal derivative) is also cubic in ξ_2 along that side and is entirely independent of these four parameters, four additional parameters are required to specify this cubic. Two of these are specified by $\left(\dfrac{\partial u}{\partial \xi_1}\right)_1$ and $\left(\dfrac{\partial u}{\partial \xi_1}\right)_3$, and the remaining two by $\left(\dfrac{\partial^2 u}{\partial \xi_1 \partial \xi_2}\right)_1$ and $\left(\dfrac{\partial^2 u}{\partial \xi_1 \partial \xi_2}\right)_3$.
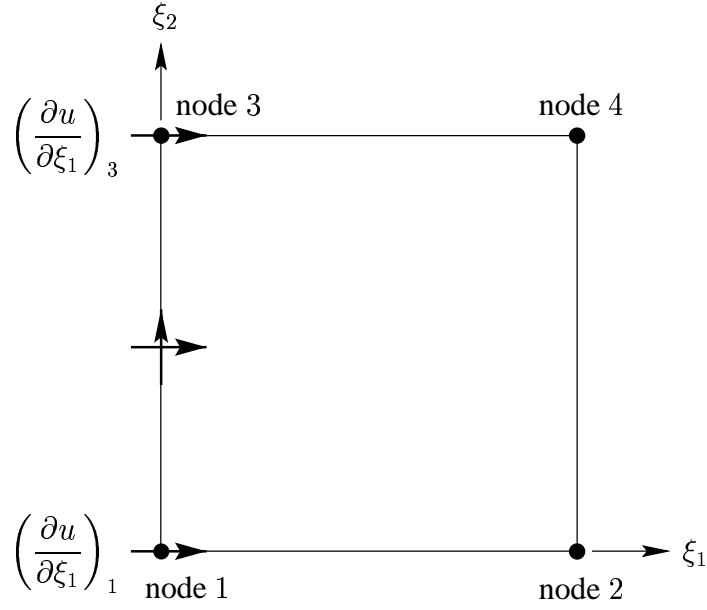
FIGURE 1.13: Interpolation of nodal derivative $\dfrac{\partial u}{\partial \xi_1}$ along side 1–3.

The bicubic interpolation of these nodal parameters is given by

$$
\begin{aligned}
u\left(\xi_{1}, \xi_{2}\right)=\; & \Psi_{1}^{0}\left(\xi_{1}\right) \Psi_{1}^{0}\left(\xi_{2}\right) u_{1}+\Psi_{2}^{0}\left(\xi_{1}\right) \Psi_{1}^{0}\left(\xi_{2}\right) u_{2} \\
& +\Psi_{1}^{0}\left(\xi_{1}\right) \Psi_{2}^{0}\left(\xi_{2}\right) u_{3}+\Psi_{2}^{0}\left(\xi_{1}\right) \Psi_{2}^{0}\left(\xi_{2}\right) u_{4} \\
& +\Psi_{1}^{1}\left(\xi_{1}\right) \Psi_{1}^{0}\left(\xi_{2}\right)\left(\frac{\partial u}{\partial \xi_{1}}\right)_{1}+\Psi_{2}^{1}\left(\xi_{1}\right) \Psi_{1}^{0}\left(\xi_{2}\right)\left(\frac{\partial u}{\partial \xi_{1}}\right)_{2} \\
& +\Psi_{1}^{1}\left(\xi_{1}\right) \Psi_{2}^{0}\left(\xi_{2}\right)\left(\frac{\partial u}{\partial \xi_{1}}\right)_{3}+\Psi_{2}^{1}\left(\xi_{1}\right) \Psi_{2}^{0}\left(\xi_{2}\right)\left(\frac{\partial u}{\partial \xi_{1}}\right)_{4} \\
& +\Psi_{1}^{0}\left(\xi_{1}\right) \Psi_{1}^{1}\left(\xi_{2}\right)\left(\frac{\partial u}{\partial \xi_{2}}\right)_{1}+\Psi_{2}^{0}\left(\xi_{1}\right) \Psi_{1}^{1}\left(\xi_{2}\right)\left(\frac{\partial u}{\partial \xi_{2}}\right)_{2} \\
& +\Psi_{1}^{0}\left(\xi_{1}\right) \Psi_{2}^{1}\left(\xi_{2}\right)\left(\frac{\partial u}{\partial \xi_{2}}\right)_{3}+\Psi_{2}^{0}\left(\xi_{1}\right) \Psi_{2}^{1}\left(\xi_{2}\right)\left(\frac{\partial u}{\partial \xi_{2}}\right)_{4} \\
& +\Psi_{1}^{1}\left(\xi_{1}\right) \Psi_{1}^{1}\left(\xi_{2}\right)\left(\frac{\partial^{2} u}{\partial \xi_{1} \partial \xi_{2}}\right)_{1}+\Psi_{2}^{1}\left(\xi_{1}\right) \Psi_{1}^{1}\left(\xi_{2}\right)\left(\frac{\partial^{2} u}{\partial \xi_{1} \partial \xi_{2}}\right)_{2} \\
& +\Psi_{1}^{1}\left(\xi_{1}\right) \Psi_{2}^{1}\left(\xi_{2}\right)\left(\frac{\partial^{2} u}{\partial \xi_{1} \partial \xi_{2}}\right)_{3}+\Psi_{2}^{1}\left(\xi_{1}\right) \Psi_{2}^{1}\left(\xi_{2}\right)\left(\frac{\partial^{2} u}{\partial \xi_{1} \partial \xi_{2}}\right)_{4}
\end{aligned}
\tag{1.16}
$$

where

$$
\begin{array}{rcl}
\Psi_1^0\left(\xi\right) & = & 1-3\xi^2+2\xi^3 \\
\Psi_1^1\left(\xi\right) & = & \xi\left(\xi-1\right)^2 \\
\Psi_2^0\left(\xi\right) & = & \xi^2\left(3-2\xi\right) \\
\Psi_2^1\left(\xi\right) & = & \xi^2\left(\xi-1\right)
\end{array}
\tag{1.17}
$$

are the one-dimensional cubic Hermite basis functions (see Figure 1.12).

As in the one-dimensional case above, to preserve derivative continuity in physical x-coordinate space as well as in ξ-coordinate space the global node derivatives need to be specified with respect to physical arclength. There are now two arclengths to consider: s_1, measuring arclength along the ξ_1-coordinate, and s_2, measuring arclength along the ξ_2-coordinate. Thus

$$
\begin{array}{rcl}
\left(\dfrac{\partial u}{\partial \xi_1}\right)_n & = & \left(\dfrac{\partial u}{\partial s_1}\right)_{\Delta(n,e)} \cdot \left(\dfrac{\partial s_1}{\partial \xi_1}\right)_n \\[3mm]
\left(\dfrac{\partial u}{\partial \xi_2}\right)_n & = & \left(\dfrac{\partial u}{\partial s_2}\right)_{\Delta(n,e)} \cdot \left(\dfrac{\partial s_2}{\partial \xi_2}\right)_n \\[3mm]
\left(\dfrac{\partial^2 u}{\partial \xi_1 \partial \xi_2}\right)_n & = & \left(\dfrac{\partial^2 u}{\partial s_1 \partial s_2}\right)_{\Delta(n,e)} \cdot \left(\dfrac{ds_1}{d\xi_1}\right)_n \cdot \left(\dfrac{ds_2}{d\xi_2}\right)_n
\end{array}
\tag{1.18}
$$

where $\left(\dfrac{ds_1}{d\xi_1}\right)_n$ and $\left(\dfrac{ds_2}{d\xi_2}\right)_n$ are element *scale factors* which scale the arclength derivatives of global node Δ to the ξ-coordinate derivatives of element node n.

The bicubic Hermite basis is a powerful shape descriptor for curvilinear surfaces. Figure 1.14 shows a four element bicubic Hermite surface in 3D space where each node has the following twelve parameters

$$
x, \frac{\partial x}{\partial s_1}, \frac{\partial x}{\partial s_2}, \frac{\partial^2 x}{\partial s_1 \partial s_2}, y, \frac{\partial y}{\partial s_1}, \frac{\partial y}{\partial s_2}, \frac{\partial^2 y}{\partial s_1 \partial s_2}, z, \frac{\partial z}{\partial s_1}, \frac{\partial z}{\partial s_2} \text{ and } \frac{\partial^2 z}{\partial s_1 \partial s_2}
$$

1.7   Triangular Elements

Triangular elements cannot use the ξ_1 and ξ_2 coordinates defined above for *tensor product* elements (*i.e.,* two- and three- dimensional elements whose basis functions are formed as the product of one-dimensional basis functions). The natural coordinates for triangles are based on area ratios and are called *Area Coordinates* . Consider the ratio of the area formed from the points 2, 3 and $P\left(x,y\right)$ in Figure 1.15 to the total area of the triangle

$$
L_1 = \frac{\text{Area} < P23 >}{\text{Area} < 123 >} = \frac{1}{2}\begin{vmatrix} 1 & x & y \\ 1 & x_2 & y_2 \\ 1 & x_3 & y_3 \end{vmatrix} / \Delta = \left(a_1 + b_1 x + c_1 y\right)/\left(2\Delta\right)
$$
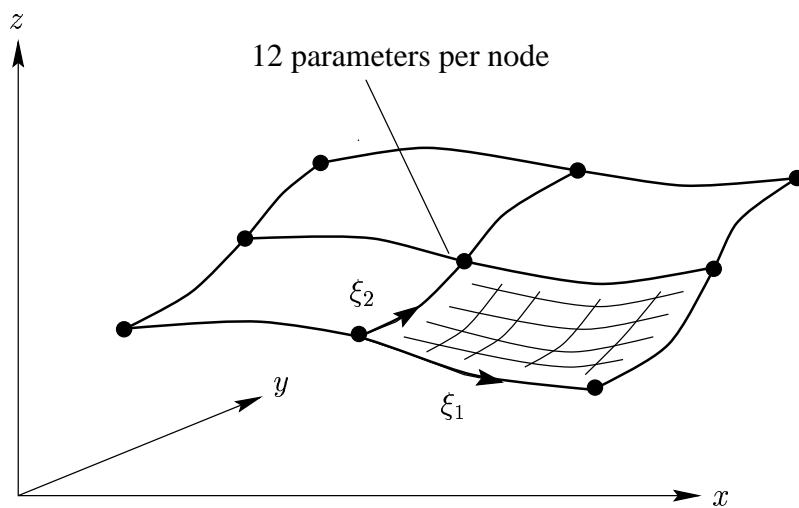
FIGURE 1.14: A surface formed by four bicubic Hermite elements.
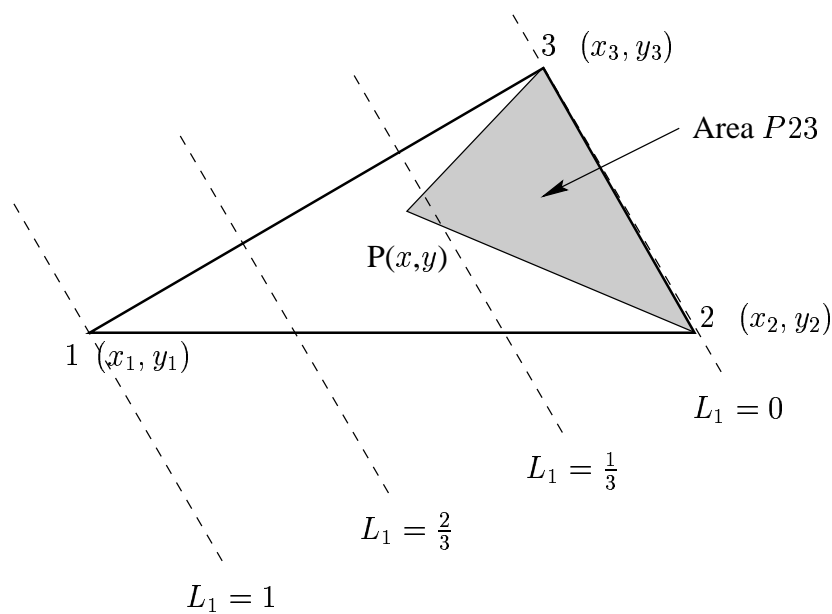
FIGURE 1.15: Area coordinates for a triangular element.

where $\Delta = \frac{1}{2} \begin{vmatrix} 1 & x_1 & y_1 \\ 1 & x_2 & y_2 \\ 1 & x_3 & y_3 \end{vmatrix}$ is the area of the triangle with vertices 123, and $a_1 = x_2 y_3 - x_3 y_2$, $b_1 = y_2 - y_3$, $c_1 = x_3 - x_2$.

Notice that L_1 is linear in x and y. Similarly, area coordinates for the other two triangles containing P and two of the element vertices are

$$L_2 = \frac{\text{Area} < P13 >}{\text{Area} < 123 >} = \frac{1}{2} \begin{vmatrix} 1 & x & y \\ 1 & x_3 & y_3 \\ 1 & x_1 & y_1 \end{vmatrix} / \Delta = (a_2 + b_2 x + c_2 y) / (2\Delta)$$

$$L_3 = \frac{\text{Area} < P12 >}{\text{Area} < 123 >} = \frac{1}{2} \begin{vmatrix} 1 & x & y \\ 1 & x_1 & y_1 \\ 1 & x_2 & y_2 \end{vmatrix} / \Delta = (a_3 + b_3 x + c_3 y) / (2\Delta)$$

where $a_2 = x_3 y_1 - x_1 y_3$, $b_2 = y_3 - y_1$, $c_2 = x_1 - x_3$ and $a_3 = x_1 y_2 - x_2 y_1$, $b_3 = y_1 - y_2$, $c_3 = x_2 - x_1$.

Notice that $L_1 + L_2 + L_3 = 1$.

Area coordinate L_1 varies linearly from $L_1 = 0$ when P lies at node 2 or 3 to $L_1 = 1$ when P lies at node 1 and can therefore be used directly as the basis function for node 1 for a three node triangle. Thus, interpolation over the triangle is given by

$$u(x, y) = \varphi_1(x, y) u_1 + \varphi_2(x, y) u_2 + \varphi_3(x, y) u_3$$

where $\varphi_1 = L_1$, $\varphi_2 = L_2$ and $\varphi_3 = L_3 = 1 - L_1 - L_2$.

Six node quadratic triangular elements are constructed as shown in Figure 1.16.

$$\varphi_1 = L_1 (2L_1 - 1)$$
$$\varphi_2 = L_2 (2L_2 - 1)$$
$$\varphi_3 = L_3 (2L_3 - 1)$$
$$\varphi_4 = 4L_1 L_2$$
$$\varphi_5 = 4L_2 L_3$$
$$\varphi_6 = 4L_3 L_1$$
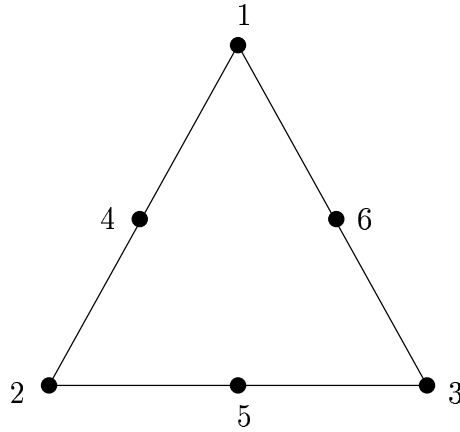
FIGURE 1.16: Basis functions for a six node quadratic triangular element.

1.8 Curvilinear Coordinate Systems

It is sometimes convenient to model the geometry of the region (over which a finite element solution is sought) using an orthogonal curvilinear coordinate system. A 2D circular annulus, for ex-

ample, can be modelled geometrically using one element with cylindrical polar (r, θ)-coordinates, *e.g.,* the annular plate in Figure 1.17a has two global nodes, the first with $r = r_1$ and the second with $r = r_2$.

(a) (b) (c)
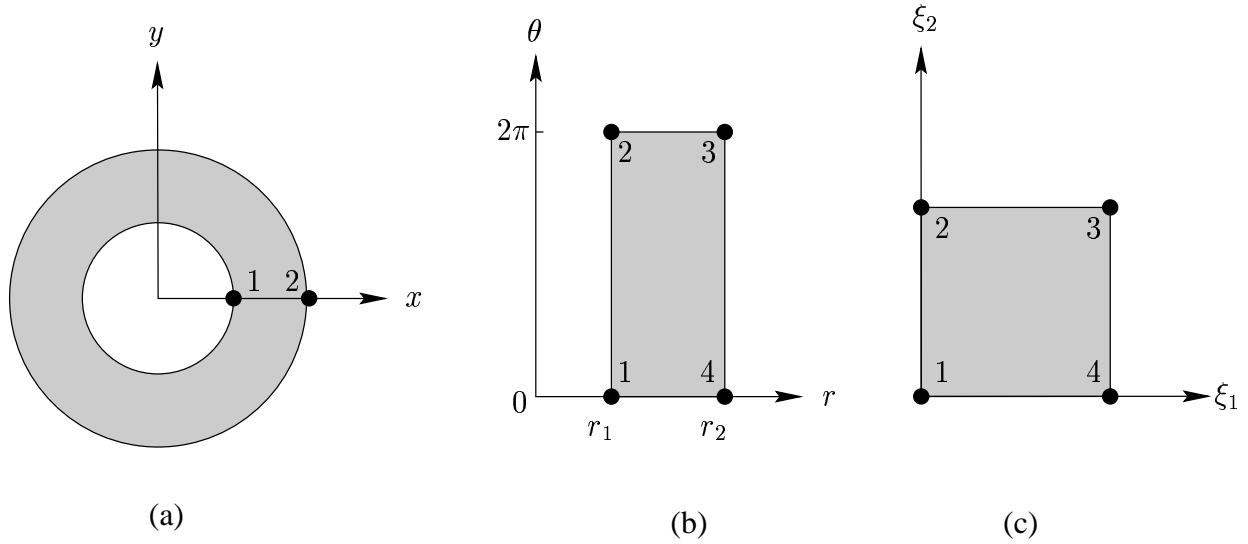
FIGURE 1.17: Defining a circular annulus with one cylindrical polar element. Notice that element vertices 1 and 2 in (r, θ)-space or (ξ_1, ξ_2)-space, as shown in (b) and (c), respectively, map onto the single global node 1 in (x, y)-space in (a). Similarly, element vertices 3 and 4 map onto global node 2.

Global nodes 1 and 2, shown in (x, y)-space in Figure 1.17a, each map to two element vertices in (r, θ)-space, as shown in Figure 1.17b, and in (ξ_1, ξ_2)-space, as shown in Figure 1.17c. The (r, θ) coordinates at any (ξ_1, ξ_2) point are given by a bilinear interpolation of the nodal coordinates r_n and θ_n as

$$r = \varphi_n (\xi_1, \xi_2) \cdot r_n$$
$$\theta = \varphi_n (\xi_1, \xi_2) \cdot \theta_n$$

where the basis functions $\varphi_n (\xi_1, \xi_2)$ are given by (1.6).

Three orthogonal curvilinear coordinate systems are defined here for use in later sections.

Cylindrical polar (r, θ, z) **:**

$$\begin{aligned} x &= r \cos \theta \\ y &= r \sin \theta \\ z &= z \end{aligned} \tag{1.19}$$

Spherical polar (r, θ, ϕ) **:**

$$\begin{aligned} x &= r \cos \theta \cos \phi \\ y &= r \sin \theta \cos \phi \\ z &= r \sin \phi \end{aligned} \tag{1.20}$$

Prolate spheroidal (λ, μ, θ) **:**

$$
\begin{aligned}
x &= d \cosh \lambda \cos \mu \\
y &= d \sinh \lambda \sin \mu \cos \theta \\
z &= d \sinh \lambda \sin \mu \sin \theta
\end{aligned}
\tag{1.21}
$$
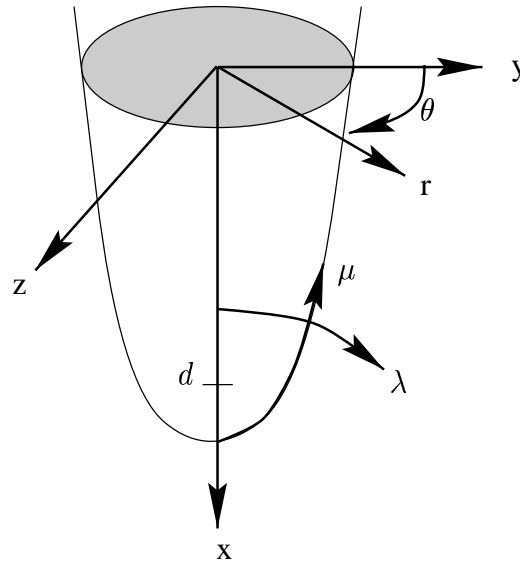
FIGURE 1.18: Prolate spheroidal coordinates.

The prolate spheroidal coordinates rae illustrated in Figure 1.18 and a single prolate spheroidal element is shown in Figure 1.19. The coordinates (λ, μ, θ) are all trilinear in (ξ_1, ξ_2, ξ_3). Only four global nodes are required provided the four global nodes map to eight element nodes as shown in Figure 1.19.
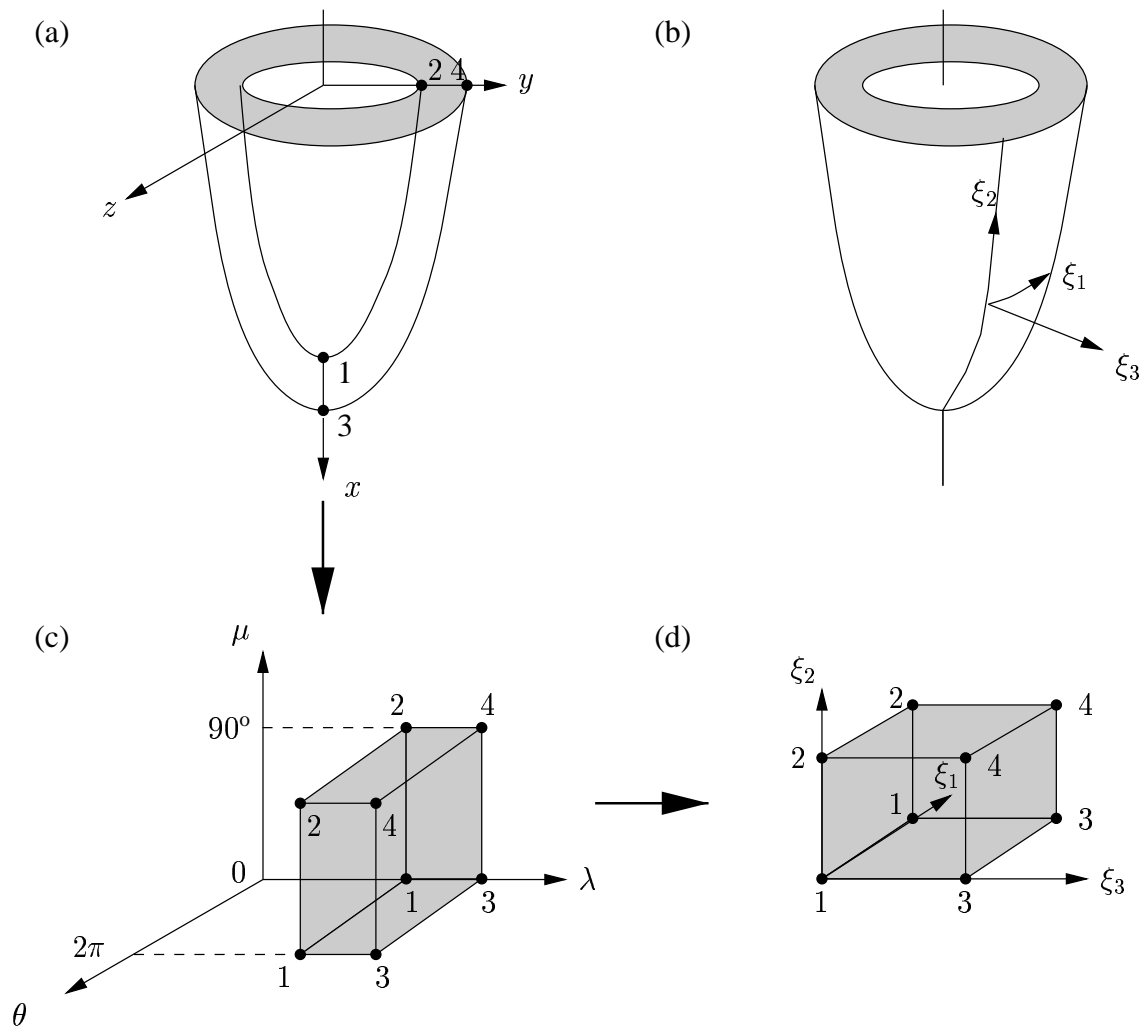
FIGURE 1.19: A single prolate spheroidal element, shown (a) in (x, y, z)-coordinates, (c) in (λ, μ, θ)-coordinates and (d) in (ξ_1, ξ_2, ξ_3)-coordinates, (b) shows the orientation of the ξ_i-coordinates on the prolate spheroid.

1.9   CMISS Examples

1. To define a 2D bilinear finite element mesh run the CMISS example number 111. The nodes should be positioned as shown in Figure 1.20. After defining elements the mesh should appear like the one shown in Figure 1.21.
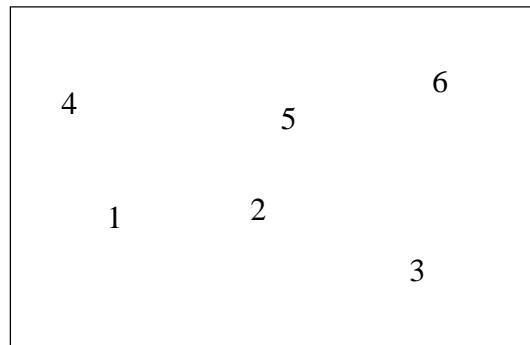
FIGURE 1.20: Node positions for example 111.
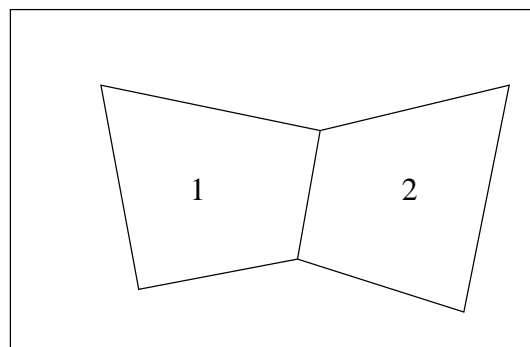
FIGURE 1.21: 2D bilinear finite element mesh for example 111.

2. To refine a mesh run the CMISS example 113. After the first refine the mesh should appear like the one shown in Figure 1.22.

3. To define a quadratic-linear element run the cmiss example 115.

4. To define a 3D trilinear element run CMISS example 121.

5. To define a 2D cubic Hermite-linear finite element mesh run example 114.

6. To define a triangular element mesh run CMISS example 116 (see Figure 1.24).

7. To define a bilinear mesh in cylindrical polar coordinates run CMISS example 122.
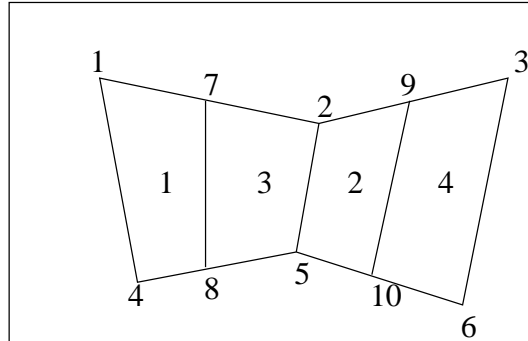
FIGURE 1.22: First refined mesh for example 113
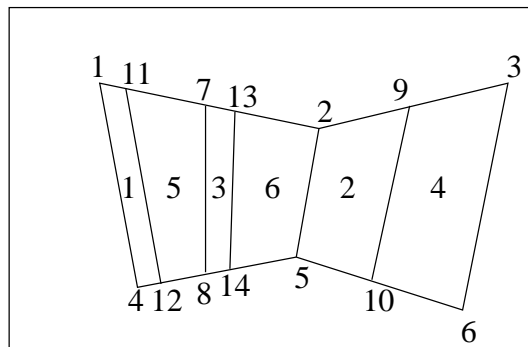
FIGURE 1.23: Second refined mesh for example 113
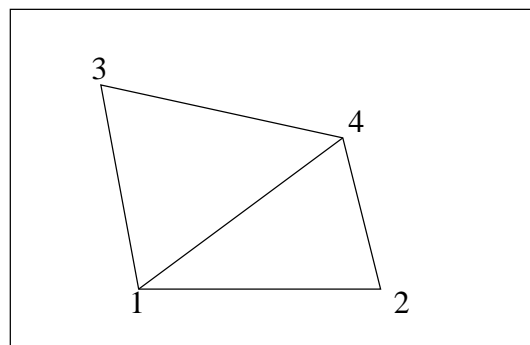
FIGURE 1.24: Defining a triangular mesh for example 116

Chapter 2

Steady-State Heat Conduction

2.1   One-Dimensional Steady-State Heat Conduction

Our first example of solving a partial differential equation by finite elements is the one-dimensional steady-state heat equation. The equation arises from a simple heat balance over a region of conducting material:

Rate of change of heat flux = heat source per unit volume

or

$$\frac{d}{dx} \text{ (heat flux)} + \text{heat sink per unit volume} = 0$$

or

$$\frac{d}{dx} \left(-k \frac{du}{dx} \right) + q(u, x) = 0$$

where u is temperature, $q(u, x)$ the heat sink and k the thermal conductivity (Watts/m/°C).
   Consider the case where $q = u$

$$-\frac{d}{dx} \left(k \frac{du}{dx} \right) + u = 0 \quad 0 < x < 1 \tag{2.1}$$

subject to boundary conditions: $u(0) = 0$ and $u(1) = 1$.
   This equation (with $k = 1$) has an exact solution

$$u(x) = \frac{e}{e^2 - 1} \left(e^x - e^{-x} \right) \tag{2.2}$$

with which we can compare the approximate finite element solutions.
   To solve Equation (2.1) by the finite element method requires the following steps:

1. Write down the integral equation form of the heat equation.

2. Integrate by parts (in 1D) or use Green's Theorem (in 2D or 3D) to reduce the order of derivatives.

3. Introduce the finite element approximation for the temperature field with nodal parameters and element basis functions.

4. Integrate over the elements to calculate the element stiffness matrices and RHS vectors.

5. Assemble the global equations.

6. Apply the boundary conditions.

7. Solve the global equations.

8. Evaluate the fluxes.

2.1.1 Integral equation

Rather than solving Equation (2.1) directly, we form the weighted residual

$$\int R\omega.dx = 0 \tag{2.3}$$

where R is the residual

$$R = -\frac{d}{dx}\left(k\frac{du}{dx}\right) + u \tag{2.4}$$

for an approximate solution u and ω is a weighting function to be chosen below. If u were an exact solution over the whole domain, the residual R would be zero everywhere. But, given that in real engineering problems this will not be the case, we try to obtain an approximate solution u for which the residual or error (*i.e.,* the amount by which the differential equation is not satisfied exactly at a point) is distributed evenly over the domain. Substituting Equation (2.4) into Equation (2.3) gives

$$\int_0^1 \left\{ -\frac{d}{dx}\left(k\frac{du}{dx}\right)\omega + u\omega \right\} dx = 0 \tag{2.5}$$

This formulation of the governing equation can be thought of as forcing the residual or error to be zero in a spatially averaged sense. More precisely, ω is chosen such that the residual is kept orthogonal to the space of functions used in the approximation of u (see step 3 below).

2.1.2 Integration by parts

A major advantage of the integral equation is that the order of the derivatives inside the integral can be reduced from two to one by integrating by parts (or, equivalently for 2D problems, by applying Green's theorem - see later). Thus, substituting $f = \omega$ and $g = -k\frac{du}{dx}$ into the *integration by parts*

formula

$$\int_0^1 f\frac{dg}{dx}\,dx = [f.g]_0^1 - \int_0^1 g\frac{df}{dx}\,dx$$

gives

$$\int_0^1 \omega\frac{d}{dx}\left(-k\frac{du}{dx}\right)\,dx = \left[\omega\left(-k\frac{du}{dx}\right)\right]_0^1 - \int_0^1 \left(-k\frac{du}{dx}\frac{d\omega}{dx}\right)\,dx$$

and Equation (2.5) becomes

$$\int_0^1 \left(k\frac{du}{dx}\frac{d\omega}{dx} + u\omega\right)\,dx = \left[k\frac{du}{dx}\omega\right]_0^1 \tag{2.6}$$

2.1.3 Finite element approximation

We divide the domain $0 < x < 1$ into 3 equal length elements and replace the continuous field variable $u(x)$ within each element by the parametric finite element approximation

$$u(\xi) = \varphi_1(\xi)\,u_1 + \varphi_2(\xi)\,u_2 = \varphi_n(\xi)\,u_n$$
$$x(\xi) = \varphi_1(\xi)\,x_1 + \varphi_2(\xi)\,x_2 = \varphi_n(\xi)\,x_n$$

(summation implied by repeated index) where $\varphi_1(\xi) = 1 - \xi$ and $\varphi_2(\xi) = \xi$ are the linear basis functions for both u and x.

We also choose $\omega = \varphi_m$ (called the *Galerkin*[1] assumption). This forces the residual R to be orthogonal to the space of functions used to represent the dependent variable u, thereby ensuring that the residual, or error, is monotonically reduced as the finite element mesh is refined (see later for a more complete justification of this very important step) .

The domain integral in Equation (2.6) can now be replaced by the sum of integrals taken separately over the three elements

$$\int_0^1 \cdot\,dx = \int_0^{\frac{1}{3}} \cdot\,dx + \int_{\frac{1}{3}}^{\frac{2}{3}} \cdot\,dx + \int_{\frac{2}{3}}^1 \cdot\,dx$$

---

[1]Boris G. Galerkin (1871-1945). Galerkin was a Russian engineer who published his first technical paper on the buckling of bars while imprisoned in 1906 by the Tzar in pre-revolutionary Russia. In many Russian texts the Galerkin finite element method is known as the Bubnov-Galerkin method. He published a paper using this idea in 1915. The method was also attributed to I.G. Bubnov in 1913.

and each element integral is then taken over ξ-space

$$\int\limits_{x_1}^{x_2} \cdot\, dx = \int\limits_{0}^{1} \cdot J\, d\xi$$

where $J = \left| \dfrac{dx}{d\xi} \right|$ is the Jacobian of the transformation from x coordinates to ξ coordinates.

2.1.4 Element integrals

The element integrals arising from the LHS of Equation (2.6) have the form

$$\int\limits_{0}^{1} \left(k\frac{du}{dx}\frac{d\omega}{dx} + u\omega \right) J\, d\xi \tag{2.7}$$

where $u = \varphi_n u_n$ and $\omega = \varphi_m$. Since φ_n and φ_m are both functions of ξ the derivatives with respect to x need to be converted to derivatives with respect to ξ. Thus Equation (2.7) becomes

$$u_n \int\limits_{0}^{1} \left(k\frac{d\varphi_m}{d\xi}\frac{d\xi}{dx}\frac{d\varphi_n}{d\xi}\frac{d\xi}{dx} + \varphi_m\varphi_n \right) J\, d\xi \tag{2.8}$$

Notice that u_n has been taken outside the integral because it is not a function of ξ. The term $\dfrac{d\xi}{dx}$ is evaluated by substituting the finite element approximation $x(\xi) = \varphi_n . X_n$. In this case $x = \dfrac{1}{3}\xi$ or $\dfrac{d\xi}{dx} = 3$ and the Jacobian is $J = \dfrac{dx}{d\xi} = \frac{1}{3}$. The term multiplying the nodal parameters u_n is called the element stiffness matrix, E_{mn}

$$E_{mn} = \int\limits_{0}^{1} \left(k\frac{d\varphi_m}{d\xi}\frac{d\xi}{dx}\frac{d\varphi_n}{d\xi}\frac{d\xi}{dx} + \varphi_m\varphi_n \right) J\, d\xi = \int\limits_{0}^{1} \left(k\frac{d\varphi_m}{d\xi}3\frac{d\varphi_n}{d\xi}3 + \varphi_m\varphi_n \right) \frac{1}{3}\, d\xi$$

where the indices m and n are 1 or 2. To evaluate E_{mn} we substitute the basis functions

$$\varphi_1(\xi) = 1 - \xi \quad \text{or} \quad \frac{d\varphi_1}{d\xi} = -1$$
$$\varphi_2(\xi) = \xi \qquad \text{or} \quad \frac{d\varphi_2}{d\xi} = 1$$
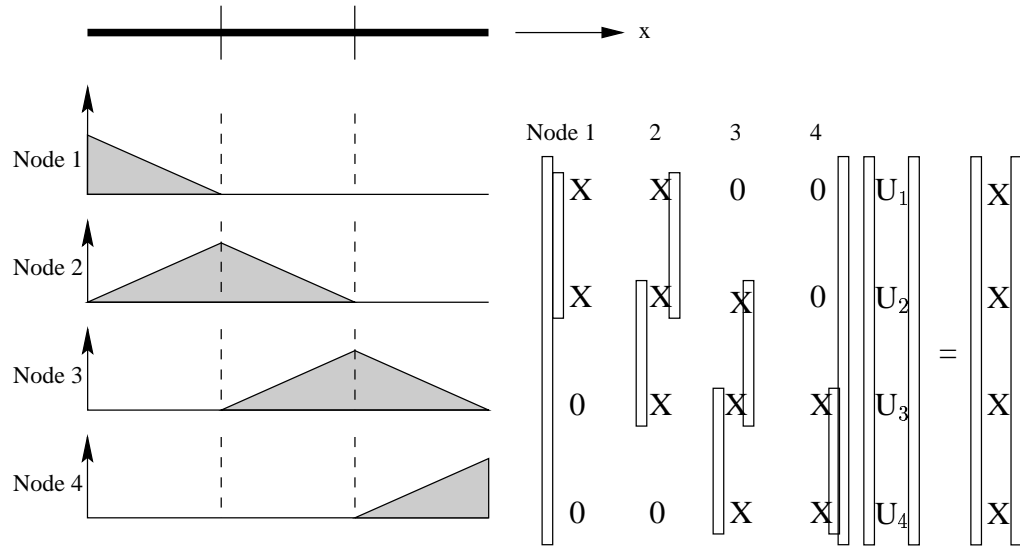
FIGURE 2.1: The rows of the global stiffness matrix are generated from the global weight functions. The bar is shown at the top divided into three elements.

Thus,

$$E_{11} = \frac{1}{3} \int\limits_0^1 \left(9k \left(\frac{d\varphi_1}{d\xi} \right)^2 + (\varphi_1)^2 \right) d\xi = \frac{1}{3} \int\limits_0^1 \left(9k \left(-1 \right)^2 + (1 - \xi)^2 \right) d\xi = \frac{1}{3} \left(9k + \frac{1}{3} \right)$$

and, similarly,

$$E_{12} = E_{21} = \frac{1}{3} \left(-9k + \frac{1}{6} \right)$$

$$E_{22} = \frac{1}{3} \left(9k + \frac{1}{3} \right)$$

$$E_{mn} = \begin{bmatrix} \frac{1}{3} \left(9k + \frac{1}{3} \right) & \frac{1}{3} \left(-9k + \frac{1}{6} \right) \\ \frac{1}{3} \left(-9k + \frac{1}{6} \right) & \frac{1}{3} \left(9k + \frac{1}{3} \right) \end{bmatrix}$$

Notice that the element stiffness matrix is symmetric. Notice also that the stiffness matrix, in this particular case, is the same for all elements. For simplicity we put $k = 1$ in the following steps.

2.1.5   Assembly

The three element stiffness matrices (with $k = 1$) are assembled into one global stiffness matrix. This process is illustrated in Figure 2.1 where rows $1, .., 4$ of the global stiffness matrix (shown here multiplied by the vector of global unknowns) are generalised from the weight function associated with nodes $1, .., 4$.

Note how each element stiffness matrix (the smaller square brackets in Figure 2.1) overlaps

with its neighbour because they share a common global node. The assembly process gives

$$
\begin{bmatrix}
\frac{28}{9} & -\frac{53}{18} & 0 & 0 \\
-\frac{53}{18} & \frac{28}{9} + \frac{28}{9} & -\frac{53}{18} & 0 \\
0 & -\frac{53}{18} & \frac{28}{9} + \frac{28}{9} & -\frac{53}{18} \\
0 & 0 & -\frac{53}{18} & \frac{28}{9}
\end{bmatrix}
\begin{bmatrix}
U_1 \\ U_2 \\ U_3 \\ U_4
\end{bmatrix}
$$

Notice that the first row (generating heat flux at node 1) has zeros multiplying U_3 and U_4 since nodes 3 and 4 have no direct connection through the basis functions to node 1. Finite element matrices are always *sparse* matrices - containing many zeros - since the basis functions are local to elements.

The RHS of Equation (2.6) is

$$
\left[k\frac{du}{dx}\omega \right]_{x=0}^{x=1} = \left(k\frac{du}{dx}\omega \right)\bigg|_{x=1} - \left(k\frac{du}{dx}\omega \right)\bigg|_{x=0} \tag{2.9}
$$

To evaluate these expressions consider the weighting function ω corresponding to each global node (see Fig.1.6). For node 1 ω_1 is obtained from the basis function φ_1 associated with the first node of element 1 and therefore $\omega_1|_{x=0} = 1$. Also, since ω_1 is identically zero outside element 1, $\omega_1|_{x=1} = 0$. Thus Equation (2.9) for node 1 reduces to

$$
\left[k\frac{du}{dx}\omega_1 \right]_{x=0}^{x=1} = -\left(k\frac{du}{dx} \right)\bigg|_{x=0} = \text{flux entering node 1.}
$$

Similarly,

$$
\left[k\frac{du}{dx}\omega_n \right]_{x=0}^{x=1} = 0 \qquad \text{(nodes 2 and 3)}
$$

and

$$
\left[k\frac{du}{dx}\omega_4 \right]_{x=0}^{x=1} = \left(k\frac{du}{dx} \right)\bigg|_{x=1} = \text{flux entering node 4.}
$$

Note: k has been left in these expressions to emphasise that they are heat fluxes.

Putting these global equations together we get

$$
\begin{bmatrix}
\frac{28}{9} & -\frac{53}{18} & 0 & 0 \\
-\frac{53}{18} & \frac{28}{9} + \frac{28}{9} & -\frac{53}{18} & 0 \\
0 & -\frac{53}{18} & \frac{28}{9} + \frac{28}{9} & -\frac{53}{18} \\
0 & 0 & -\frac{53}{18} & \frac{28}{9}
\end{bmatrix}
\begin{bmatrix}
U_1 \\ U_2 \\ U_3 \\ U_4
\end{bmatrix}
=
\begin{bmatrix}
-\left(k\frac{du}{dx} \right)\bigg|_{x=0} \\
0 \\
0 \\
\left(k\frac{du}{dx} \right)\bigg|_{x=1}
\end{bmatrix}
\tag{2.10}
$$

or

$$
\boldsymbol{Ku} = \boldsymbol{f}
$$

where $\boldsymbol{K}$ is the global "stiffness" matrix, $\boldsymbol{u}$ the vector of unknowns and $\boldsymbol{f}$ the global "load" vector.

Note that if the governing differential equation had included a distributed source term that was independent of u, this term would appear - via its weighted integral - on the RHS of Equation (2.10) rather than on the LHS as here. Moreover, if the source term was a function of x, the contribution from each element would be different - as shown in the next section.

2.1.6 Boundary conditions

The boundary conditions $u(0) = 0$ and $u(1) = 1$ are applied directly to the first and last nodal values: *i.e.,* $U_1 = 0$ and $U_4 = 1$. These so-called *essential* boundary conditions then replace the first and last rows in the global Equation (2.10), where the flux terms on the RHS are at present unknown

$$
\begin{array}{llllll}
1^{\text{st}} \text{ equation} & U_1 & & & & = 0 \\
2^{\text{nd}} \text{ equation} & -\frac{53}{18}U_1 & +\frac{56}{9}U_2 & -\frac{53}{18}U_3 & & = 0 \\
3^{\text{rd}} \text{ equation} & & -\frac{53}{18}U_2 & +\frac{56}{9}U_3 & -\frac{53}{18}U_4 & = 0 \\
4^{\text{th}} \text{ equation} & & & & U_4 & = 1
\end{array}
$$

Note that, if a flux boundary condition had been applied, rather than an essential boundary condition, the known value of flux would enter the appropriate RHS term and the value of U at that node would remain an unknown in the system of equations. An applied boundary flux of zero, corresponding to an insulated boundary, is termed a *natural* boundary condition, since effectively no additional constraint is applied to the global equation. At least one essential boundary condition must be applied.

2.1.7 Solution

Solving these equations gives: $U_2 = 0.2885$ and $U_3 = 0.6098$. From Equation (2.2) the exact solutions at these points are 0.2889 and 0.6102, respectively. The finite element solution is shown in Figure 2.2.

2.1.8 Fluxes

The fluxes at nodes 1 and 4 are evaluated by substituting the nodal solutions $U_1 = 0$, $U_2 = 0.2885$, $U_3 = 0.6098$ and $U_4 = 1$ into Equation (2.10)

$$
\text{flux entering node } 1 = -\left. \left(k\frac{du}{dx} \right) \right|_{x=0} = -0.8496 \quad (k = 1; \text{ exact solution } 0.8509)
$$

$$
\text{flux entering node } 4 = \left. \left(k\frac{du}{dx} \right) \right|_{x=1} = 1.3157 \quad (k = 1; \text{ exact solution } 1.3131)
$$

These fluxes are shown in Figure 2.2 as heat entering node 4 and leaving node 1, consistent with heat flow down the temperature gradient.
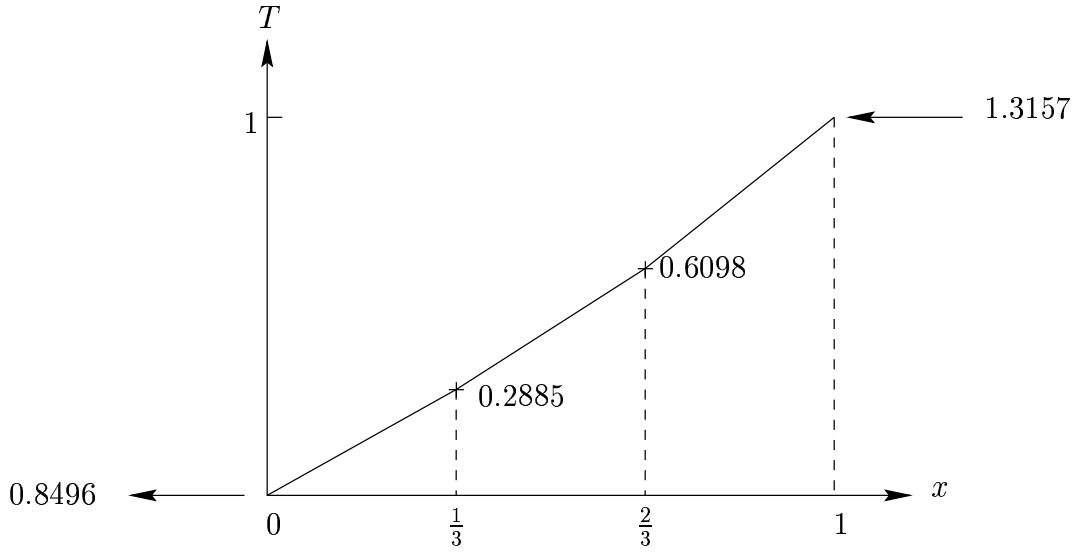
FIGURE 2.2: Finite element solution of one-dimensional heat equation.

2.2 An x-Dependent Source Term

Consider the addition of a source term dependent on x in Equation (2.1):

$$-\frac{d}{dx}\left(k\frac{du}{dx}\right) + u - x = 0 \quad 0 < x < 1$$

Equation (2.6) now becomes

$$\int_0^1 \left(k\frac{du}{dx}\frac{d\omega}{dx} + u\omega\right) dx = \left[k\frac{du}{dx}\omega\right]_0^1 + \int_0^1 x\omega\, dx \tag{2.11}$$

where the x-dependent source term appears on the RHS because it is not dependent on u. Replacing the domain integral for this source term by the sum of three element integrals

$$\int_0^1 x\omega\, dx = \int_0^{\frac{1}{3}} x\omega\, dx + \int_{\frac{1}{3}}^{\frac{2}{3}} x\omega\, dx + \int_{\frac{2}{3}}^1 x\omega\, dx$$

and putting x in terms of ξ gives (with $\frac{dx}{d\xi} = \frac{1}{3}$ for all three elements)

$$\int_0^1 x\omega\, dx = \frac{1}{3}\int_0^1 \frac{\xi}{3}\omega\, d\xi + \frac{1}{3}\int_0^1 \frac{(1+\xi)}{3}\omega\, d\xi + \frac{1}{3}\int_0^1 \frac{(2+\xi)}{3}\omega\, d\xi \tag{2.12}$$

where ω is chosen to be the appropriate basis function within each element. For example, the first term on the RHS of (2.12) corresponding to element 1 is $\dfrac{1}{9}\displaystyle\int_0^1 \xi\varphi_m\,d\xi$, where $\varphi_1 = 1 - \xi$ and $\varphi_2 = \xi$. Evaluating these expressions,

$$\int_0^1 \frac{1}{9}\xi\left(1 - \xi\right)d\xi = \frac{1}{54}$$

and

$$\int_0^1 \frac{1}{9}\xi^2\,d\xi = \frac{1}{27}$$

Thus, the contribution to the element 1 RHS vector from the source term is $\begin{bmatrix} \frac{1}{54} \\ \frac{1}{27} \end{bmatrix}$.

Similarly, for element 2,

$$\int_0^1 \frac{1}{9}\left(1 + \xi\right)\left(1 - \xi\right)d\xi = \frac{2}{27} \quad \text{and} \quad \int_0^1 \frac{1}{9}\left(1 + \xi\right)\xi\,d\xi = \frac{5}{54} \quad \text{gives} \quad \begin{bmatrix} \frac{2}{27} \\ \frac{5}{54} \end{bmatrix}$$

and for element 3,

$$\int_0^1 \frac{1}{9}\left(2 + \xi\right)\left(1 - \xi\right)d\xi = \frac{7}{54} \quad \text{and} \quad \int_0^1 \frac{1}{9}\left(2 + \xi\right)\xi\,d\xi = \frac{5}{54} \quad \text{gives} \quad \begin{bmatrix} \frac{7}{54} \\ \frac{5}{54} \end{bmatrix}$$

Assembling these into the global RHS vector, Equation (2.10) becomes

$$\begin{bmatrix} \frac{28}{9} & -\frac{53}{18} & 0 & 0 \\ -\frac{53}{18} & \frac{56}{9} & -\frac{53}{18} & 0 \\ 0 & -\frac{53}{18} & \frac{56}{9} & -\frac{53}{18} \\ 0 & 0 & -\frac{53}{18} & \frac{28}{9} \end{bmatrix}\begin{bmatrix} U_1 \\ U_2 \\ U_3 \\ U_4 \end{bmatrix} = \begin{bmatrix} -\left(k\dfrac{du}{dx}\right)\Big|_{x=0} \\ 0 \\ 0 \\ \left(k\dfrac{du}{dx}\right)\Big|_{x=1} \end{bmatrix} + \begin{bmatrix} \frac{1}{54} \\ \frac{1}{27} + \frac{2}{27} \\ \frac{5}{54} + \frac{7}{54} \\ \frac{5}{54} \end{bmatrix}$$

2.3   The Galerkin Weight Function Revisited

A key idea in the Galerkin finite element method is the choice of weighting functions which are orthogonal to the equation residual (thought of here as the error or amount by which the equation fails to be exactly zero). This idea is illustrated in Figure 2.3.

In Figure 2.3a an exact vector $\boldsymbol{u}_e$ (lying in 3D space) is approximated by a vector $\boldsymbol{u} = u_1\boldsymbol{\varphi}_1$ where $\boldsymbol{\varphi}_1$ is a basis vector along the first coordinate axis (representing one degree of freedom in the system). The difference between the exact vector $\boldsymbol{u}_e$ and the approximate vector $\boldsymbol{u}$ is the

$$\boldsymbol{u} = u_1\varphi_1 \qquad\qquad \boldsymbol{u} = u_1\varphi_1 + u_2\varphi_2 \qquad\qquad \boldsymbol{u} = u_1\varphi_1 + u_2\varphi_2 + u_3\varphi_3$$

$$\boldsymbol{r} \cdot \varphi_1 = 0 \qquad\qquad \ldots + \boldsymbol{r} \cdot \varphi_2 = 0 \qquad\qquad \ldots + \boldsymbol{r} \cdot \varphi_3 = 0$$
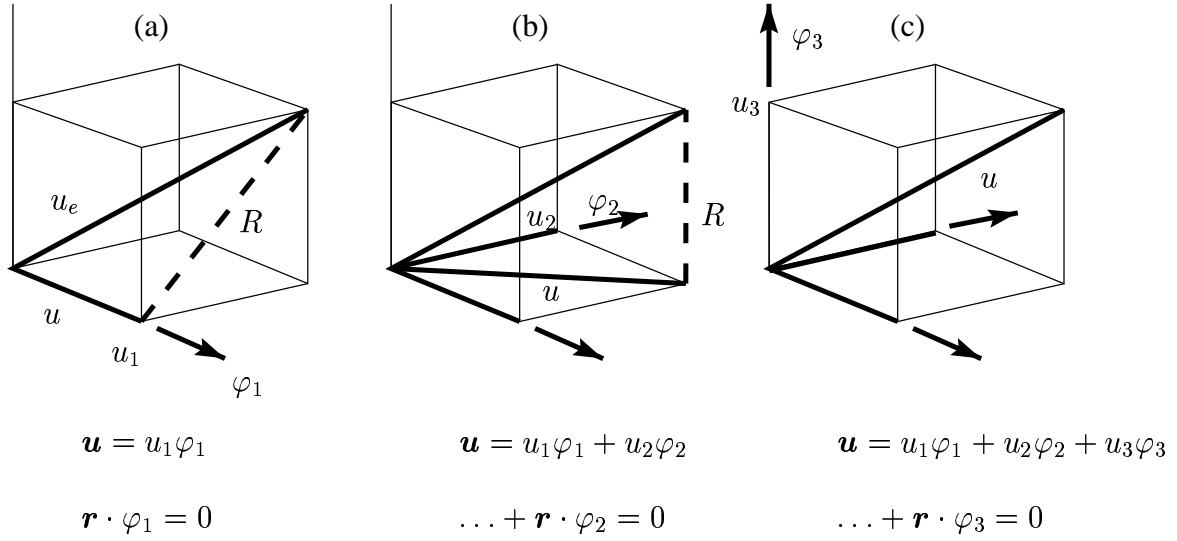
FIGURE 2.3: Showing how the Galerkin method maintains orthogonality between the residual vector $\boldsymbol{r}$ and the set of basis vectors $\boldsymbol{\varphi_i}$ as i is increased from (a) 1 to (b) 2 to (c) 3.

error or residual $\boldsymbol{r} = \boldsymbol{u_e} - \boldsymbol{u}$ (shown by the broken line in Figure 2.3a). The Galerkin technique minimises this residual by making it orthogonal to φ_1 and hence to the approximating vector $\boldsymbol{u}$. If a second degree of freedom (in the form of another coordinate axis in Figure 2.3b) is added, the approximating vector is $\boldsymbol{u} = u_1\boldsymbol{\varphi_1} + u_2\boldsymbol{\varphi_2}$ and the residual is now *also* made orthogonal to φ_2 and hence to $\boldsymbol{u}$. Finally, in Figure 2.3c, a third degree of freedom (a third axis in Figure 2.3c) is permitted in the approximation $\boldsymbol{u} = u_1\varphi_1 + u_2\varphi_2 + u_3\varphi_3$ with the result that the residual (now also orthogonal to φ_3) is reduced to zero and $\boldsymbol{u} = \boldsymbol{u_e}$. For a 3D vector space we only need three axes or basis vectors to represent the true vector $\boldsymbol{u}$, but in the infinite dimensional vector space associated with a spatially continuous field $u(x)$ we need to impose the equivalent orthogonality condition $\left(\int R\varphi \, dx = 0 \right)$ for every basis function φ used in the approximate representation of $u(x)$. The key point is that in this analogy the residual is made orthogonal to the current set of basis vectors - or, equivalently, in finite element analysis, to the set of basis functions used to represent the dependent variable. This ensures that the error or residual is minimal (in a least-squares sense) for the current number of degrees of freedom and that as the number of degrees of freedom is increased (or the mesh refined) the error decreases monotonically.

2.4 Two and Three-Dimensional Steady-State Heat Conduction

Extending Equation (2.1) to two or three spatial dimensions introduces some additional complexity which we examine here. Consider the three-dimensional steady-state heat equation with no source terms:

$$-\frac{\partial}{\partial x}\left(k_x\frac{\partial u}{\partial x}\right) - \frac{\partial}{\partial y}\left(k_y\frac{\partial u}{\partial y}\right) - \frac{\partial}{\partial z}\left(k_z\frac{\partial u}{\partial z}\right) = 0$$

where k_x, k_y and k_z are the thermal diffusivities along the x, y and z axes respectively. If the material is assumed to be isotropic, $k_x = k_y = k_z = k$, and the above equation can be written as

$$-\nabla \cdot (k\nabla u) = 0 \tag{2.13}$$

and, if k is spatially constant (in the case of a homogeneous material), this reduces to Laplace's equation $k\nabla^2 u = 0$. Here we consider the solution of Equation (2.13) over the region Ω, subject to boundary conditions on Γ (see Figure 2.4).

Solution region boundary: Γ

Solution region: Ω
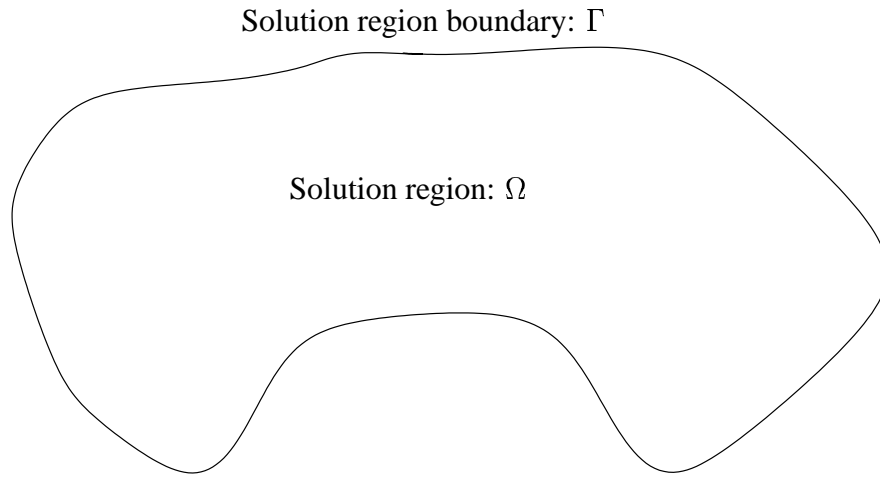
FIGURE 2.4: The region Ω and the boundary Γ.

The weighted integral equation, corresponding to Equation (2.13), is

$$\int_\Omega -\nabla \cdot (k\nabla u)\, \omega\, d\Omega = 0 \tag{2.14}$$

The multi-dimensional equivalent of integration by parts is the Green-Gauss theorem:

$$\int_\Omega (f\nabla \cdot \nabla g + \nabla f \cdot \nabla g)\, d\Omega = \int_\Gamma f\frac{\partial g}{\partial n}\, d\Gamma \tag{2.15}$$

(see p553 in Advanced Engineering Mathematics" by E. Kreysig, 7th edition, Wiley, 1993).

This is used (with $f = \omega$, $g = -ku$ and assuming that k is constant) to reduce the derivative order from two to one as follows:

$$\int_\Omega -\nabla \cdot (k\nabla u)\, \omega\, d\Omega = \int_\Omega k\nabla u \cdot \nabla \omega\, d\Omega - \int_\Gamma k\frac{\partial u}{\partial n}\omega\, d\Gamma \tag{2.16}$$

cf. Integration by parts is $\int_x -\frac{d}{dx}\left(k\frac{du}{dx}\right)\omega\, dx = \int_x k\frac{du}{dx}\frac{d\omega}{dx}\, dx - \left[k\frac{du}{dx}\omega\right]_{x_1}^{x_2}.$

Using Equation (2.16) in Equation (2.14) gives the two-dimensional equivalent of Equation (2.6)

(but with no source term):

$$\int_{\Omega} k \nabla u \cdot \nabla \omega \, d\Omega = \int_{\Gamma} k \frac{\partial u}{\partial n} \omega \, d\Gamma \tag{2.17}$$

subject to u being given on one part of the boundary and $\dfrac{\partial u}{\partial n}$ being given on another part of the boundary.

The integrand on the LHS of (2.17) is evaluated using

$$\nabla u \cdot \nabla \omega = \frac{\partial u}{\partial x_k} \cdot \frac{\partial \omega}{\partial x_k} = \frac{\partial u}{\partial \xi_i} \frac{\partial \xi_i}{\partial x_k} \cdot \frac{\partial \omega}{\partial \xi_j} \frac{\partial \xi_j}{\partial x_k} \tag{2.18}$$

where $u = \varphi_n u_n$ and $\omega = \varphi_m$, as before, and the geometric terms $\dfrac{\partial \xi_i}{\partial x_k}$ are found from the inverse matrix

$$\left[\frac{\partial \xi_i}{\partial x_k} \right] = \left[\frac{\partial x_k}{\partial \xi_i} \right]^{-1}$$

or, for a two-dimensional element,

$$\begin{bmatrix} \dfrac{\partial \xi_1}{\partial x} & \dfrac{\partial \xi_1}{\partial y} \\ \dfrac{\partial \xi_2}{\partial x} & \dfrac{\partial \xi_2}{\partial y} \end{bmatrix} = \begin{bmatrix} \dfrac{\partial x}{\partial \xi_1} & \dfrac{\partial x}{\partial \xi_2} \\ \dfrac{\partial y}{\partial \xi_1} & \dfrac{\partial y}{\partial \xi_2} \end{bmatrix}^{-1} = \frac{1}{\dfrac{\partial x}{\partial \xi_1} \dfrac{\partial y}{\partial \xi_2} - \dfrac{\partial x}{\partial \xi_2} \dfrac{\partial y}{\partial \xi_1}} \begin{bmatrix} \dfrac{\partial y}{\partial \xi_2} & -\dfrac{\partial x}{\partial \xi_2} \\ -\dfrac{\partial y}{\partial \xi_1} & \dfrac{\partial x}{\partial \xi_1} \end{bmatrix}$$

2.5 Basis Functions - Element Discretisation

Let $\Omega = \bigcup\limits_{i=1}^{I} \Omega_i$, *i.e.,* the solution region is the union of the individual elements. In each Ω_i let $u = \varphi_n u_n = \varphi_1 u_1 + \varphi_2 u_2 + \ldots + \varphi_N u_N$ and map each Ω_i to the ξ_1, ξ_2 plane. Figure 2.5 shows an example of this mapping.
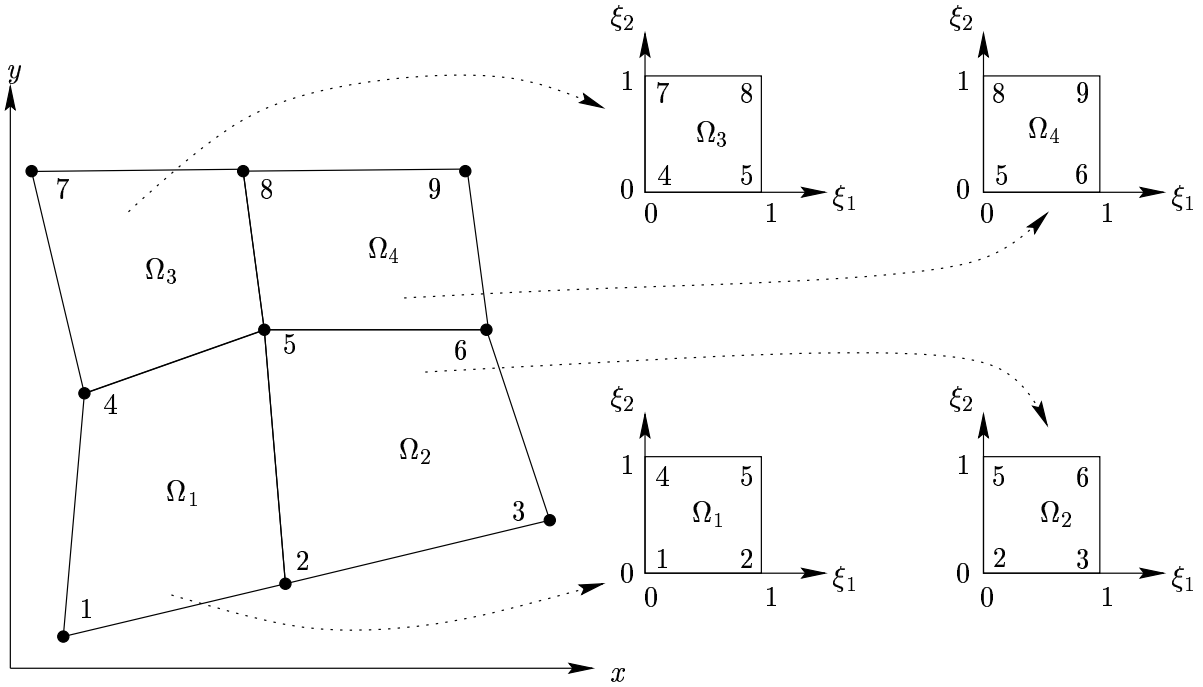
FIGURE 2.5: Mapping each Ω to the ξ_1, ξ_2 plane in a 2×2 element plane.

For each element, the basis functions and their derivatives are:

$$\varphi_1 = (1 - \xi_1)(1 - \xi_2) \qquad \frac{\partial \varphi_1}{\partial \xi_1} = -(1 - \xi_2) \tag{2.19}$$

$$\frac{\partial \varphi_1}{\partial \xi_2} = -(1 - \xi_1) \tag{2.20}$$

$$\tag{2.21}$$

$$\varphi_2 = \xi_1(1 - \xi_2) \qquad \frac{\partial \varphi_2}{\partial \xi_1} = 1 - \xi_2 \tag{2.22}$$

$$\frac{\partial \varphi_1}{\partial \xi_2} = -\xi_1 \tag{2.23}$$

$$\tag{2.24}$$

$$\varphi_3 = (1 - \xi_1)\xi_2 \qquad \frac{\partial \varphi_3}{\partial \xi_1} = -\xi_2 \tag{2.25}$$

$$\frac{\partial \varphi_3}{\partial \xi_2} = 1 - \xi_1 \tag{2.26}$$

$$\tag{2.27}$$

$$\varphi_4 = \xi_1 \xi_2 \qquad \frac{\partial \varphi_4}{\partial \xi_1} = \xi_2 \tag{2.28}$$

$$\frac{\partial \varphi_4}{\partial \xi_2} = \xi_1 \tag{2.29}$$

2.6 Integration

The equation is

$$\int_\Omega k \nabla u \cdot \nabla \omega \, d\Omega = \int_\Gamma k \frac{\partial u}{\partial n} \omega \, d\Gamma \tag{2.30}$$

i.e.,

$$\int_\Omega k \left(\frac{\partial u}{\partial x} \frac{\partial \omega}{\partial x} + \frac{\partial u}{\partial y} \frac{\partial \omega}{\partial y} \right) d\Omega = \int_\Gamma k \frac{\partial u}{\partial n} \omega \, d\Gamma \tag{2.31}$$

u has already been approximated by $\varphi_n u_n$ and ω is a weight function but what should this be chosen to be? For a *Galerkin* formulation choose $\omega = \varphi_m$ *i.e.,* weight function is one of the basis functions used to approximate the dependent variable.

This gives

$$\sum_i u_n \int_\Omega k \left(\frac{\partial \varphi_n}{\partial x} \frac{\partial \varphi_m}{\partial x} + \frac{\partial \varphi_n}{\partial y} \frac{\partial \varphi_m}{\partial y} \right) d\Omega = \int_\Gamma k \frac{\partial u}{\partial n} \varphi_m \, d\Gamma \tag{2.32}$$

where the stiffness matrix is E_{mn} where $m = 1, \ldots, 4$ and $n = 1, \ldots, 4$ and F_m is the (element) load vector.

The names originated from earlier finite element applications and extension of spring systems, *i.e.,* $F = kx$ where k is the stiffness of spring and F is the force/load.

This yields the system of equations $E_{mn} u_n = F_m$. *e.g.,* heat flow in a unit square (see Figure 2.6).
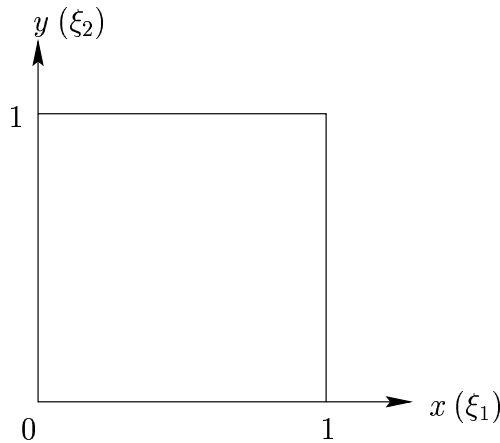
FIGURE 2.6: Considering heat flow in a unit square.

The first component E_{11} is calculated as

$$E_{11} = k \int\limits_0^1 \int\limits_0^1 (1-y)^2 + (1-x)^2 \, dxdy$$

$$= \frac{2}{3}k$$

and similarly for the other components of the matrix.

Note that if the element was not the unit square we would need to transform from (x,y) to (ξ_1, ξ_2) coordinates. In this case we would have to include the Jacobian of the transformation and also use the chain rule to calculate $\frac{\partial \varphi_i}{\partial x_j}$. e.g., $\frac{\partial \varphi_n}{\partial x} = \frac{\partial \varphi_n}{\partial \xi_1}\frac{\partial \xi_1}{\partial x} + \frac{\partial \varphi_n}{\partial \xi_2}\frac{\partial \xi_2}{\partial x} = \frac{\partial \varphi_n}{\partial \xi_i}\frac{\partial \xi_i}{\partial x}$.

The system of $E_{mn}u_n = F_m$ becomes

$$k \begin{bmatrix} \frac{2}{3} & -\frac{1}{6} & -\frac{1}{6} & -\frac{1}{3} \\ -\frac{1}{6} & \frac{2}{3} & -\frac{1}{3} & -\frac{1}{6} \\ -\frac{1}{6} & -\frac{1}{3} & \frac{2}{3} & -\frac{1}{6} \\ -\frac{1}{3} & -\frac{1}{6} & -\frac{1}{6} & \frac{2}{3} \end{bmatrix} \begin{bmatrix} u_1 \\ u_2 \\ u_3 \\ u_4 \end{bmatrix} = RHS \qquad \text{(Right Hand Side)} \qquad (2.33)$$

Note that the Galerkin formulation generates a symmetric stiffness matrix (this is true for self adjoint operators which are the most common).

Given that boundary conditions can be applied and it is possible to solve for unknown nodal temperatures or fluxes. However, typically there is more than one element and so the next step is required.

2.7 Assemble Global Equations

Each element stiffness matrix must be assembled into a global stiffness matrix. For example, consider 4 elements (each of unit size) and nine nodes. Each element has the same element stiffness matrix as that given above. This is because each element is the same size, shape and interpolation.

$$\begin{bmatrix} \frac{2}{3} & -\frac{1}{6} & & -\frac{1}{6} & & -\frac{1}{3} & & & \\ -\frac{1}{6} & \frac{2}{3}+\frac{2}{3} & -\frac{1}{6} & -\frac{1}{3} & -\frac{1}{6}-\frac{1}{6} & -\frac{1}{3} & & & \\ & -\frac{1}{6} & \frac{2}{3} & & -\frac{1}{3} & -\frac{1}{6} & & & \\ -\frac{1}{6} & -\frac{1}{3} & & \frac{2}{3}+\frac{2}{3} & -\frac{1}{6}-\frac{1}{6} & & -\frac{1}{6} & -\frac{1}{3} & \\ -\frac{1}{3} & -\frac{1}{6}-\frac{1}{6} & -\frac{1}{3} & -\frac{1}{6}-\frac{1}{6} & \frac{2}{3}+\frac{2}{3}+\frac{2}{3}+\frac{2}{3} & -\frac{1}{6}-\frac{1}{6} & -\frac{1}{3} & -\frac{1}{6}-\frac{1}{6} & -\frac{1}{3} \\ & -\frac{1}{3} & -\frac{1}{6} & & -\frac{1}{6}-\frac{1}{6} & \frac{2}{3}+\frac{2}{3} & & -\frac{1}{3} & -\frac{1}{6} \\ & & & -\frac{1}{6} & -\frac{1}{3} & & \frac{2}{3} & -\frac{1}{6} & \\ & & & -\frac{1}{3} & -\frac{1}{6}-\frac{1}{6} & -\frac{1}{3} & -\frac{1}{6} & \frac{2}{3}+\frac{2}{3} & -\frac{1}{6} \\ & & & & -\frac{1}{3} & -\frac{1}{6} & & -\frac{1}{6} & \frac{2}{3} \end{bmatrix} \begin{bmatrix} u_1 \\ u_2 \\ u_3 \\ u_4 \\ u_5 \\ u_6 \\ u_7 \\ u_8 \\ u_9 \end{bmatrix} = RHS$$

$$(2.34)$$
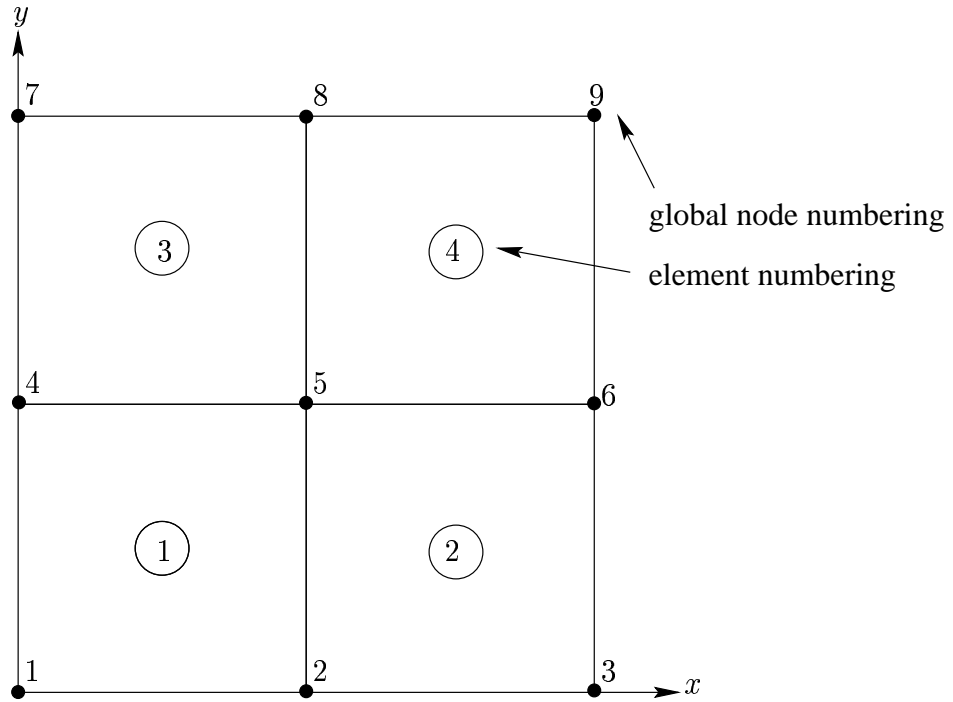
FIGURE 2.7: Assembling 4 unit sized elements into a global stiffness matrix.

This yields the system of equations

$$
\begin{bmatrix}
\frac{2}{3} & -\frac{1}{6} & & -\frac{1}{6} & -\frac{1}{3} & & & & \\
-\frac{1}{6} & \frac{4}{3} & -\frac{1}{6} & -\frac{1}{3} & -\frac{1}{3} & -\frac{1}{3} & & & \\
& -\frac{1}{6} & \frac{2}{3} & & -\frac{1}{3} & -\frac{1}{6} & & & \\
-\frac{1}{6} & -\frac{1}{3} & & \frac{4}{3} & -\frac{1}{3} & & -\frac{1}{6} & -\frac{1}{3} & \\
-\frac{1}{3} & -\frac{1}{3} & -\frac{1}{3} & -\frac{1}{3} & \frac{8}{3} & -\frac{1}{3} & -\frac{1}{3} & -\frac{1}{3} & -\frac{1}{3} \\
& -\frac{1}{3} & -\frac{1}{6} & & -\frac{1}{3} & \frac{4}{3} & & -\frac{1}{3} & -\frac{1}{6} \\
& & & -\frac{1}{6} & -\frac{1}{3} & & \frac{2}{3} & -\frac{1}{6} & \\
& & & -\frac{1}{3} & -\frac{1}{3} & -\frac{1}{3} & -\frac{1}{6} & \frac{4}{3} & -\frac{1}{6} \\
& & & & -\frac{1}{3} & -\frac{1}{6} & & -\frac{1}{6} & \frac{2}{3}
\end{bmatrix}
\begin{bmatrix}
u_1 \\ u_2 \\ u_3 \\ u_4 \\ u_5 \\ u_6 \\ u_6 \\ u_7 \\ u_8 \\ u_9
\end{bmatrix}
= RHS
$$

Note that the matrix is symmetric. It should also be clear that the matrix will be sparse if there is a larger number of elements.

From this system of equations, boundary conditions can be applied and the equations solved. To solve, firstly boundary conditions are applied to reduce the size of the system.

If at global node i, u_i is known, we can remove the ith equation and replace it with the known value of u_i. This is because the RHS at node i is known but the RHS equation is uncoupled from other equations so the equation can be removed. Therefore the size of the system is reduced. The final system to solve is only as big as the number of unknown values of u.

As an example to illustrate this consider fixing the temperature (u) at the left and right sides of the plate in Figure 2.7 and insulating the top (node 8) and the bottom (node 2). This means that

there are only 3 unknown values of u at nodes (2,5 and 8), therefore there is a 3×3 matrix to solve. The RHS is known at these three nodes (see below). We can then solve the 3×3 matrix and then multiply out the original matrix to find the unknown RHS values.

The RHS is 0 at nodes 2 and 8 because it is insulated. To find out what the RHS is at node 5 we need to examine the RHS expression $\int\limits_{\Gamma} \dfrac{\partial u}{\partial n} \omega \, d\Gamma = 0$ at node 5. This is zero as flux is always 0 at internal nodes. This can be explained in two ways.
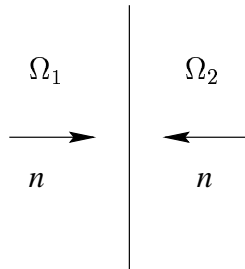
FIGURE 2.8: "Cancelling" of flux in internal nodes.

Correct way: Γ does not pass through node 5 and each basis function that is not zero at 5 is zero on Γ

Other way: $\dfrac{\partial u}{\partial n}$ is opposite in neighbouring elements so it cancels (see Figure 2.8).

2.8   Gaussian Quadrature

The element integrals arising from two- or three-dimensional problems can seldom be evaluated analytically. Numerical integration or *quadrature* is therefore required and the most efficient scheme for integrating the expressions that arise in the finite element method is Gauss-Legendre quadrature.

Consider first the problem of integrating $f(\xi)$ between the limits 0 and 1 by the sum of weighted samples of $f(\xi)$ taken at points $\xi_1, \xi_2, \ldots, \xi_I$ (see Figure 2.3):

$$\int\limits_{0}^{1} f(\xi) \, d\xi = \sum_{i=1}^{I} W_i f(\xi_i) + E$$

Here W_i are the weights associated with sample points ξ_i - called *Gauss points* - and E is the error in the approximation of the integral. We now choose the Gauss points and weights to exactly integrate a polynomial of degree $2I - 1$ (since a general polynomial of degree $2I - 1$ has $2I$ arbitrary coefficients and there are $2I$ unknown Gauss points and weights).

For example, with $I = 2$ we can exactly integrate a polynomial of degree 3:
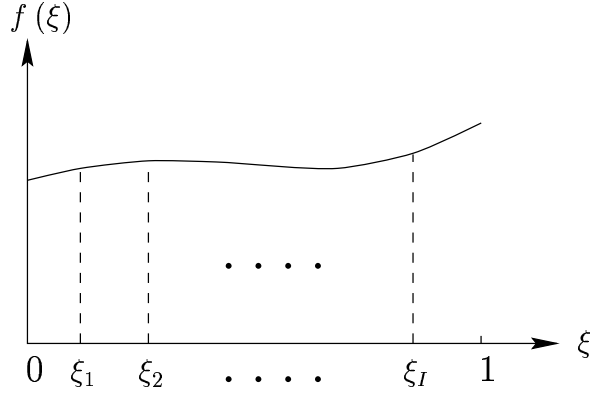
FIGURE 2.9: Gaussian quadrature. $f(\xi)$ is sampled at I Gauss points $\xi_1, \xi_2 \ldots \xi_I$.

$$\text{Let} \quad \int_0^1 f(\xi)\, d\xi = W_1 f(\xi_1) + W_2 f(\xi_2)$$

and choose $f(\xi) = a + b\xi + c\xi^2 + d\xi^3$. Then

$$\int_0^1 f(\xi)\, d\xi = a \int_0^1 d\xi + b \int_0^1 \xi\, d\xi + c \int_0^1 \xi^2\, d\xi + d \int_0^1 \xi^3\, d\xi \tag{2.35}$$

Since a, b, c and d are arbitrary coefficients, each integral on the RHS of 2.35 must be integrated exactly. Thus,

$$\int_0^1 d\xi = 1 = W_1.1 + W_2.1 \tag{2.36}$$

$$\int_0^1 \xi\, d\xi = \frac{1}{2} = W_1.\xi_1 + W_2.\xi_2 \tag{2.37}$$

$$\int_0^1 \xi^2\, d\xi = \frac{1}{3} = W_1.\xi_1^2 + W_2.\xi_2^2 \tag{2.38}$$

$$\int_0^1 \xi^3\, d\xi = \frac{1}{4} = W_1.\xi_1^3 + W_2.\xi_2^3 \tag{2.39}$$

These four equations yield the solution for the two Gauss points and weights as follows:

From symmetry and Equation (2.36),

$$W_1 = W_2 = \frac{1}{2}.$$

Then, from (2.37),

$$\xi_2 = 1 - \xi_1$$

and, substituting in (2.38),

$$\xi_1^2 + (1 - \xi_1)^2 = \frac{2}{3}$$

$$2\xi_1^2 - 2\xi_1 + \frac{1}{3} = 0,$$

giving

$$\xi_1 = \frac{1}{2} \pm \frac{1}{2\sqrt{3}}.$$

Equation (2.39) is satisfied identically. Thus, the two Gauss points are given by

$$\begin{aligned}
\xi_1 &= \frac{1}{2} - \frac{1}{2\sqrt{3}}, \\
\xi_2 &= \frac{1}{2} + \frac{1}{2\sqrt{3}}, \\
W_1 &= W_2 = \frac{1}{2}
\end{aligned} \tag{2.40}$$

A similar calculation for a 5th degree polynomial using three Gauss points gives

$$\begin{aligned}
\xi_1 &= \frac{1}{2} - \frac{1}{2}\sqrt{\frac{3}{5}}, & W_1 &= \frac{5}{18} \\
\xi_2 &= \frac{1}{2}, & W_2 &= \frac{4}{9} \\
\xi_3 &= \frac{1}{2} + \frac{1}{2}\sqrt{\frac{3}{5}}, & W_3 &= \frac{5}{18}
\end{aligned} \tag{2.41}$$

2 For two- or three-dimensional Gaussian quadrature the Gauss point positions are simply the values given above along each ξ_i-coordinate with the weights scaled to sum to 1 *e.g.,* for 2x2 Gauss quadrature the 4 weights are all $\frac{1}{4}$. The number of Gauss points chosen for each ξ_i-direction is governed by the complexity of the integrand in the element integral (2.8). In general two- and three-dimensional problems the integral is not polynomial (owing to the $\frac{\partial \xi_i}{\partial x_j}$ terms which come from the

inverse of the matrix $\left[\dfrac{\partial x_i}{\partial \xi_j}\right]$) and no attempt is made to achieve exact integration. The quadrature error must be balanced against the discretization error. For example, if the two-dimensional basis is cubic in the ξ_1-direction and linear in the ξ_2-direction, three Gauss points would be used in the ξ_1-direction and two in the ξ_2-direction.

2.9 CMISS Examples

1. To solve for the steady state temperature distribution inside a plate run CMISS example 311

2. To solve for the steady state temperature distribution inside an annulus run CMISS example 312

3. To investigate the convergence of the steady state temperature distribution with mesh refinement run CMISS examples 3141, 3142, 3143 and 3144.

Chapter 3

The Boundary Element Method

3.1 Introduction

Having developed the basic ideas behind the finite element method, we now develop the basic ideas of the boundary element method. There are several key differences between these two methods, one of which involves the choice of weighting function (recall the Galerkin finite element method used as a weighting function one of the basis functions used to approximate the solution variable). Before launching into the boundary element method we must briefly develop some ideas that are central to the weighting function used in the boundary element method.

3.2 The Dirac-Delta Function and Fundamental Solutions

Before one applies the boundary element method to a particular problem one must obtain a *fundamental solution* (which is similar to the idea of a particular solution in ordinary differential equations and is the weighting function). Fundamental solutions are tied to the Dirac[1] Delta function and we deal with both here.

3.2.1 Dirac-Delta function

What we do here is very non-rigorous. To gain an intuitive feel for this unusual function, consider the following sequence of force distributions applied to a large plate as shown in Figure 3.1

$$w_n\left(x\right) = \begin{cases} \frac{n}{2} & |x| < \frac{1}{n} \\ 0 & |x| > \frac{1}{n} \end{cases}$$

---

[1]Paul A.M. Dirac (1902-1994) was awarded the Nobel Prize (with Erwin Schrodinger) in 1933 for his work in quantum mechanics. Dirac introduced the idea of the "Dirac Delta" intuitively, as we will do here, around 1926-27. It was rigorously defined as a so-called generalised function by Schwartz in 1950-51, and strictly speaking we should talk about the "Dirac Delta Distribution".

Each has the property that

$$\int_{-\infty}^{\infty} w_n(x)\,dx = 1 \qquad (\textit{i.e.,} \text{ the total force applied is unity})$$

but as n increases the area of force application decreases and the force/unit area increases.
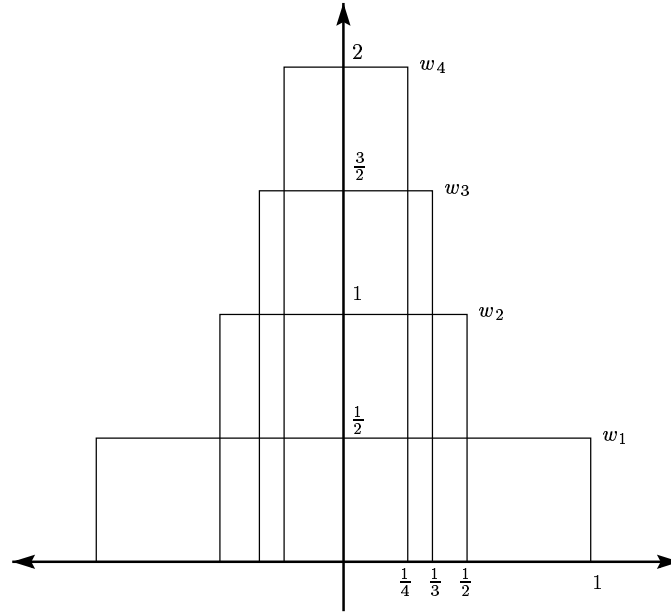
FIGURE 3.1: Illustrations of unit force distributions w_n.

As n gets larger we can easily see that the area of application of the force becomes smaller and smaller, the magnitude of the force increases but the total force applied remains unity. If we imagine letting $n \to \infty$ we obtain an idealised "point" force of unit strength, given the symbol $\delta(x)$, acting at $x = 0$. Thus, in a nonrigorous sense we have

$$\delta(x) = \lim_{n \to \infty} w_n(x) \quad \text{the Dirac Delta``function''.}$$

This is not a function that we are used to dealing with because we have $\delta(x) = 0$ if $x \neq 0$ and "$\delta(0) = \infty$" *i.e.,* the "function" is zero everywhere except at the origin, where it is infinite. However, we have $\int_{-\infty}^{\infty} \delta(x)\,dx = 1$ since each $\int_{-\infty}^{\infty} w_n(x)\,dx = 1$.

The Dirac delta "function" is not a function in the usual sense, and it is more correctly referred to as the Dirac delta distribution. It also has the property that for any continuous function $h(x)$

$$\int_{-\infty}^{\infty} \delta(x)\,h(x)\,dx = h(0) \tag{3.1}$$

A rough proof of this is as follows

$$\int\limits_{-\infty}^{\infty} \delta\left(x\right) h\left(x\right)\ dx = \lim_{n \to \infty} \int\limits_{-\infty}^{\infty} w_n\left(x\right) h\left(x\right)\ dx \quad \text{by definition of } \delta\left(x\right)$$

$$= \lim_{n \to \infty} \frac{n}{2} \int\limits_{-\frac{1}{n}}^{\frac{1}{n}} h\left(x\right)\ dx \qquad \text{by definition of } w_n\left(x\right)$$

$$= \lim_{n \to \infty} \frac{n}{2} h\left(\xi\right) \frac{2}{n} \qquad \text{by the Mean Value Theorem, where } \xi \in \left(-\frac{1}{n}, \frac{1}{n}\right)$$

$$= h\left(0\right) \qquad \text{since } \xi \in \left(-\frac{1}{n}, \frac{1}{n}\right) \text{ and as } n \to \infty,\ \xi \to 0$$

The above result (Equation (3.1)) is often used as the defining property of the Dirac delta in more rigorous derivations. One does not usually talk about the values of the Dirac delta at a particular point, but rather its integral behaviour. Some properties of the Dirac delta are listed below

$$\int\limits_{-\infty}^{\infty} \delta\left(\xi - x\right) h\left(x\right)\ dx = h\left(\xi\right) \tag{3.2}$$

(Note: $\delta\left(\xi - x\right)$ is the Dirac delta distribution centred at $x = \xi$ instead of $x = 0$)

$$\delta\left(\xi - x\right) = H'\left(\xi - t\right) \tag{3.3}$$

where $H\left(\xi - t\right) = \begin{cases} 0 & \text{if } \xi < t \\ 1 & \text{if } \xi > t \end{cases}$ (*i.e.,* the Dirac Delta function is the slope of the Heaviside[2] step function.)

$$\delta\left(\xi - x, \eta - y\right) = \delta\left(\xi - x\right) \delta\left(\eta - y\right) \tag{3.4}$$

(*i.e.,* the two dimensional Dirac delta is just a product of two one-dimensional Dirac deltas.)

3.2.2 Fundamental solutions

We develop here the fundamental solution (also called the freespace Green's[3] function) for Laplace's Equation in two variables. The fundamental solution of a particular equation is the weighting function that is used in the boundary element formulation of that equation. It is therefore important to be able to find the fundamental solution for a particular equation. Most of the common equations

---

[2]Oliver Heaviside (1850-1925) was a British physicist, who pioneered the mathematical study of electrical circuits and helped develop vector analysis.

[3]George Green (1793-1841) was a self-educated miller's son. Most widely known for his integral theorem (the Green-Gauss theorem).

have well-known fundamental solutions (see Appendix 3.16). We briefly illustrate here how to find a simple fundamental solution.

Consider solving the Laplace Equation $\dfrac{\partial^2 u}{\partial x^2} + \dfrac{\partial^2 u}{\partial y^2} = 0$ in some domain $\Omega \in \Re^2$.

The fundamental solution for this equation (analogous to a particular solution in ODE work) is a solution of

$$\frac{\partial^2 \omega}{\partial x^2} + \frac{\partial^2 \omega}{\partial y^2} + \delta\left(\xi - x, \eta - y\right) = 0 \tag{3.5}$$

in $\Re^2$ (*i.e.,* we solve the above without reference to the original domain Ω or original boundary conditions). The method is to try and find solution to $\nabla^2 \omega = 0$ in $\Re^2$ which contains a singularity at the point (ξ, η). This is not as difficult as it sounds. We expect the solution to be symmetric about the point (ξ, η) since $\delta\left(\xi - x, \eta - y\right)$ is symmetric about this point. So we adopt a local polar coordinate system about the *singular point* (ξ, η).

Let

$$r = \sqrt{\left(\xi - x\right)^2 + \left(\eta - y\right)^2}$$

Then, from Section 1.8 we have

$$\nabla^2 \omega = \frac{1}{r} \frac{\partial}{\partial r}\left(r \frac{\partial \omega}{\partial r}\right) + \frac{1}{r^2} \frac{\partial^2 \omega}{\partial \theta^2} \tag{3.6}$$

For $r > 0, \delta\left(\xi - x, \eta - y\right) = 0$ and owing to symmetry, $\dfrac{\partial^2 \omega}{\partial \theta^2}$ is zero. Thus Equation (3.6) becomes

$$\frac{1}{r} \frac{\partial}{\partial r}\left(r \frac{\partial \omega}{\partial r}\right) = 0$$

This can be solved by straight (one-dimensional) integration. The solution is

$$\omega = A \log r + B \tag{3.7}$$

Note that this function is singular at $r = 0$ as required.

To find A and B we make use of the integral property of the Delta function. From Equation (3.5) we must have

$$\int_D \nabla^2 \omega \, dD = -\int_D \delta \, dD = -1 \tag{3.8}$$

where D is any domain containing $r = 0$.

We choose a simple domain to allow us to evaluate the above integrals. If D is a small disk of
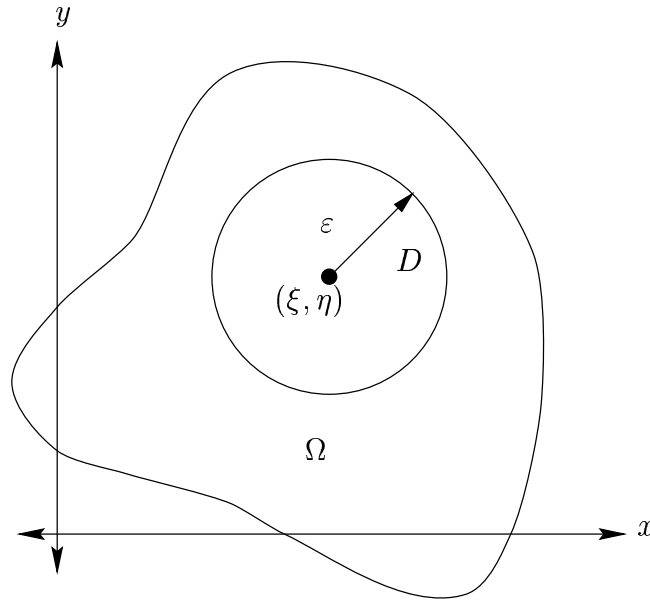
FIGURE 3.2: Domain used to evaluate fundamental solution coefficients.

radius $\varepsilon > 0$ centred at $r = 0$ (Figure 3.2) then from the Green-Gauss theorem

$$\int_D \nabla^2 \omega \, dD = \int_{\partial D} \frac{\partial \omega}{\partial n} \, dS \qquad \partial D \text{ is the surface of the disk } D$$

$$= \int_{\partial D} \frac{\partial \omega}{\partial r} \, dS \qquad \text{since } D \text{ is a disk centred at } r = 0 \text{ so } n \text{ and } r \text{ are in the same direction}$$

$$= \frac{A}{\varepsilon} 2\pi\varepsilon \qquad \text{from Equation (3.7), and the fact that } D \text{ is a disc of radius } \varepsilon$$

$$= 2\pi A$$

Therefore, from Equation (3.8)

$$A = -\frac{1}{2\pi}.$$

So we have

$$\omega = -\frac{1}{2\pi} \log r + B$$

B remains arbitrary but usually put equal to zero, so that the fundamental solution for the two-dimensional Laplace Equation is

$$\omega = -\frac{1}{2\pi} \log r \quad \left(= \frac{1}{2\pi} \log \frac{1}{r} \right) \tag{3.9}$$

where $r = \sqrt{(\xi - x)^2 + (\eta - y)^2}$ (singular at the point (ξ, η)).

The fundamental solution for the three-dimensional Laplace Equation can be found by a similar technique. The result is

$$\omega = \frac{1}{4\pi r}$$

where r is now a distance measured in three-dimensions.

3.3   The Two-Dimensional Boundary Element Method

We are now at a point where we can develop the boundary element method for the solution of $\nabla^2 u = 0$ in a two-dimensional domain Ω. The basic steps are in fact quite similar to those used for the finite element method (refer Section 2.1). We firstly must form an integral equation from the Laplace Equation by using a weighted integral equation and then use the Green-Gauss theorem. From Section 2.4 we have seen that

$$0 = \int_{\Omega} \nabla^2 u.\omega \, d\Omega = \int_{\partial\Omega} \frac{\partial u}{\partial n} \omega \, d\Gamma - \int_{\Omega} \nabla u.\nabla\omega \, d\Omega \tag{3.10}$$

This was the starting point for the finite element method. To derive the starting equation for the boundary element method we use the Green-Gauss theorem again on the second integral. This gives

$$\begin{aligned}
0 &= \int_{\partial\Omega} \frac{\partial u}{\partial n} \omega \, d\Gamma - \int_{\Omega} \nabla u.\nabla\omega \, d\Omega \\
&= \int_{\partial\Omega} \frac{\partial u}{\partial n} \omega \, d\Gamma - \int_{\partial\Omega} u\frac{\partial \omega}{\partial n} \, d\Gamma + \int_{\Omega} u\nabla^2\omega \, d\Omega
\end{aligned} \tag{3.11}$$

For the Galerkin FEM we chose ω, the weighting function, to be φ_m, one of the basis functions used to approximate u. For the boundary element method we choose ω to be the fundamental solution of Laplace's Equation derived in the previous section *i.e.,*

$$\omega = -\frac{1}{2\pi} \log r$$

where $r = \sqrt{(\xi - x)^2 + (\eta - y)^2}$ (singular at the point $(\xi, \eta) \in \Omega$).

Then from Equation (3.11), using the property of the Dirac delta

$$\int_{\Omega} u\nabla^2\omega \, d\Omega = -\int_{\Omega} u\delta\left(\xi - x, \eta - y\right) d\Omega = -u\left(\xi, \eta\right) \quad (\xi, \eta) \in \Omega \tag{3.12}$$

i.e., the domain integral has been replaced by a point value.

Thus Equation (3.11) becomes

$$u\left(\xi, \eta\right) + \int_{\partial\Omega} u\frac{\partial\omega}{\partial n}\, d\Gamma = \int_{\partial\Omega} \frac{\partial u}{\partial n}\omega\, d\Gamma \quad \left(\xi, \eta\right) \in \Omega \tag{3.13}$$

This equation contains only boundary integrals (and no domain integrals as in Finite Elements) and is referred to as a boundary integral equation. It relates the value of u at some point inside the solution domain to integral expressions involving u and $\dfrac{\partial u}{\partial n}$ over the boundary of the solution domain. Rather than having an expression relating the value of u at some point inside the domain to boundary integrals, a more useful expression would be one relating the value of u at some point *on the boundary* to boundary integrals. We derive such an expression below.

The previous equation (Equation (3.13)) holds if $\left(\xi, \eta\right) \in \Omega$ (*i.e.,* the singularity of Dirac Delta function is inside the domain). If $\left(\xi, \eta\right)$ is outside Ω then

$$\int_{\Omega} u\nabla^2\omega\, d\Omega = -\int_{\Omega} u\delta\left(\xi - x, \eta - y\right)\, d\Omega = 0$$

since the integrand of the second integral is zero at every point except $\left(\xi, \eta\right)$ and this point is outside the region of integration. The case which needs special consideration is when the singular point $\left(\xi, \eta\right)$ is on the boundary of the domain Ω. This case also happens to be the most important for numerical work as we shall see. The integral expression we will ultimately obtain is simply Equation (3.13) with $u\left(\xi, \eta\right)$ replaced by $\dfrac{1}{2}u\left(\xi, \eta\right)$. We can see this in a non-rigorous way as follows. When $\left(\xi, \eta\right)$ was inside the domain, we integrated around the entire singularity of the Dirac Delta to get $u\left(\xi, \eta\right)$ in Equation (3.13). When $\left(\xi, \eta\right)$ is on the boundary we only have half of the singularity contained inside the domain, so we integrate around one-half of the singularity to get $\dfrac{1}{2}u\left(\xi, \eta\right)$. Rigorous details of where this coefficient $\dfrac{1}{2}$ comes from are given below.

Let P denote the point $\left(\xi, \eta\right) \in \Omega$. In order to be able to evaluate $\displaystyle\int_{\Omega} u\nabla^2\omega\, d\Omega$ in this case we enlarge Ω to include a disk of radius ε about P (Figure 3.3). We call this enlarged region Ω' and let $\Gamma' = \Gamma_{-\varepsilon} \cup \Gamma_{\varepsilon}$.

Now, since P is inside the enlarged region Ω', Equation (3.13) holds for this enlarged domain *i.e.,*

$$u\left(P\right) + \int_{\Gamma_{-\varepsilon}\cup\Gamma_{\varepsilon}} u\frac{\partial\omega}{\partial n}\, d\Gamma = \int_{\Gamma_{-\varepsilon}\cup\Gamma_{\varepsilon}} \frac{\partial u}{\partial n}\omega\, d\Gamma \tag{3.14}$$

We must now investigate this equation as $\lim_{\varepsilon\downarrow 0}$. There are 4 integrals to consider, and we look at each of these in turn.
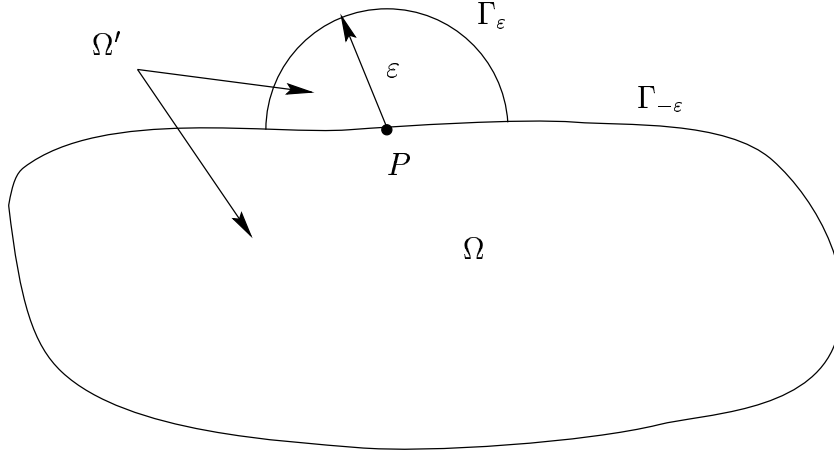
FIGURE 3.3: Illustration of enlarged domain when singular point is on the boundary.

Firstly consider

$$
\int_{\Gamma_\varepsilon} u \frac{\partial \omega}{\partial n} \, d\Gamma = \int_{\Gamma_\varepsilon} u \frac{\partial}{\partial n} \left(-\frac{1}{2\pi} \log r \right) d\Gamma \qquad \text{by definition of } \omega
$$

$$
= \int_{\Gamma_\varepsilon} u \frac{\partial}{\partial r} \left(-\frac{1}{2\pi} \log r \right) d\Gamma \qquad \text{since } \frac{\partial}{\partial n} \equiv \frac{\partial}{\partial r} \text{ on } \Gamma_\varepsilon
$$

$$
= -\frac{1}{2\pi} \int_{\Gamma_\varepsilon} \frac{u}{r} \, d\Gamma
$$

$$
= -\frac{1}{2\pi} \frac{1}{\varepsilon} \int_{\Gamma_\varepsilon} u \, d\Gamma \qquad \text{since } r = \varepsilon \text{ on } \Gamma_\varepsilon
$$

$$
\rightarrow -\frac{1}{2\pi} \frac{1}{\varepsilon} u(P) \pi \varepsilon
$$

by the mean value theorem for a surface with a unique tangent at P.
    Thus

$$
\lim_{\varepsilon \downarrow 0} \int_{\Gamma_\varepsilon} u \frac{\partial \omega}{\partial n} \, d\Gamma = \lim_{\varepsilon \downarrow 0} \left(-\frac{1}{2\pi} \frac{u(P)}{\varepsilon} \pi \varepsilon \right) = -\frac{u(P)}{2} \qquad (3.15)
$$

By a similar process we obtain

$$
\lim_{\varepsilon \downarrow 0} \int_{\Gamma_\varepsilon} \omega \frac{\partial u}{\partial n} \, d\Gamma = \lim_{\varepsilon \downarrow 0} \left(-\frac{1}{2\pi} \frac{\partial u}{\partial n} (P) \pi \varepsilon \log \varepsilon \right) = 0 \qquad (3.16)
$$

since $\lim_{\varepsilon \log \varepsilon \downarrow 0}$ as $\lim_{\varepsilon \downarrow 0}$.

It only remains to consider the integrand over $\Gamma_{-\varepsilon}$. For "nice" integrals (which includes the integrals we are dealing with here) we have

$$\lim_{\varepsilon \downarrow 0} \left(\int_{\Gamma_{-\varepsilon}} (\text{nice integrand}) \, d\Gamma \right) = \int_{\Gamma} (\text{nice integrand}) \, d\Gamma$$

since $\Gamma_{-\varepsilon} \to \Gamma$ as $\lim_{\varepsilon \downarrow 0}$.

Note: If the integrand is too badly behaved we cannot always replace $\Gamma_{-\varepsilon}$ by Γ in the limit and one must deal with Cauchy Principal Values. (refer Section 4.8)

Thus we have

$$\lim_{\varepsilon \to 0} \left(\int_{\Gamma_{-\varepsilon}} \frac{\partial u}{\partial n} \omega \, d\Gamma \right) = \int_{\Gamma} \frac{\partial u}{\partial n} \omega \, d\Gamma \qquad (3.17)$$

$$\lim_{\varepsilon \to 0} \left(\int_{\Gamma_{-\varepsilon}} \frac{\partial \omega}{\partial n} u \, d\Gamma \right) = \int_{\Gamma} \frac{\partial \omega}{\partial n} u \, d\Gamma \qquad (3.18)$$

Combining Equations (3.14)–(3.18) we get

$$u\left(P\right) + \int_{\Gamma} u \frac{\partial \omega}{\partial n} \, d\Gamma = \frac{1}{2} u\left(P\right) + \int_{\Gamma} \frac{\partial u}{\partial n} \omega \, d\Gamma$$

or

$$\frac{1}{2} u\left(P\right) + \int_{\Gamma} u \frac{\partial \omega}{\partial n} \, d\Gamma = \int_{\Gamma} \frac{\partial u}{\partial n} \omega \, d\Gamma$$

where $P = (\xi, \eta) \in \partial\Omega$ (*i.e.*, singular point is on the boundary of the region).

Note: The above is true if the point P is at a smooth point (*i.e.*, a point with a unique tangent) on the boundary of Ω. If P happens to lie at some nonsmooth point e.g. a corner, then the coefficient $\frac{1}{2}$ is replaced by $\frac{\alpha}{2\pi}$ where α is the internal angle at P (Figure 3.4).
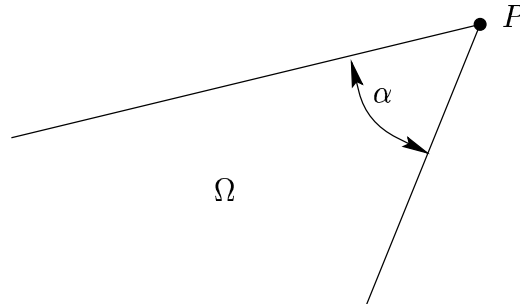
FIGURE 3.4: Illustration of internal angle α.

Thus we get the boundary integral equation.

$$c\left(P\right)u\left(P\right)+\int_{\Gamma}u\frac{\partial\omega}{\partial n}\,d\Gamma=\int_{\Gamma}\frac{\partial u}{\partial n}\omega\,d\Gamma \tag{3.19}$$

where

$$\omega=-\frac{1}{2\pi}\log r$$

$$r=\sqrt{\left(\xi-x\right)^{2}+\left(\eta-y\right)^{2}}$$

$$c\left(P\right)=\begin{cases}1 & \text{if }P\in\Omega\\\frac{1}{2} & \text{if }P\in\Gamma\text{ and }\Gamma\text{ smooth at }P\\\dfrac{\text{internal angle}}{2\pi} & \text{if }P\in\Gamma\text{ and }\Gamma\text{ not smooth at }P\end{cases}$$

For three-dimensional problems, the boundary integral equation expression above is the same, with

$$\omega=\frac{1}{4\pi r}$$

$$r=\sqrt{\left(\xi-x\right)^{2}+\left(\eta-y\right)^{2}+\left(\gamma-z\right)^{2}}$$

$$c\left(P\right)=\begin{cases}1 & \text{if }P\in\Omega\\\frac{1}{2} & \text{if }P\in\Gamma\text{ and }\Gamma\text{ smooth at }P\\\dfrac{\text{inner solid angle}}{4\pi} & \text{if }P\in\Gamma\text{ and }\Gamma\text{ not smooth at }P\end{cases}$$

Equation (3.19) involves only the surface distributions of u and $\frac{\partial u}{\partial n}$ and the value of u at a point P. Once the surface distributions of u and $\frac{\partial u}{\partial n}$ are known, the value of u at any point P inside Ω can be found since all surface integrals in Equation (3.19) are then known. The procedure is thus to use Equation (3.19) to find the surface distributions of u and $\frac{\partial u}{\partial n}$ and then (if required) use Equation (3.19) to find the solution at any point $P\in\Omega$. Thus we solve for the boundary data first, and find the volume data as a separate step.

Since Equation (3.19) only involves surface integrals, as opposed to volume integrals in a finite element formulation, the overall size of the problem has been reduced by one dimension (from volumes to surfaces). This can result in huge savings for problems with large volume to surface ratios (*i.e.,* problems with large domains). Also the effort required to produce a volume mesh of a complex three-dimensional object is far greater than that required to produce a mesh of the surface. Thus the boundary element method offers some distinct advantages over the finite element method in certain situations. It also has some disadvantages when compared to the finite element method and these will be discussed in Section 3.6. We now turn our attention to solving the boundary integral equation given in Equation (3.19).

3.4 Numerical Solution Procedures for the Boundary Integral Equation

The first step is to discretise the surface Γ into some set of elements (hence the name boundary elements).

$$\Gamma = \bigcup_{j=1}^{N} \Gamma_j \tag{3.20}$$
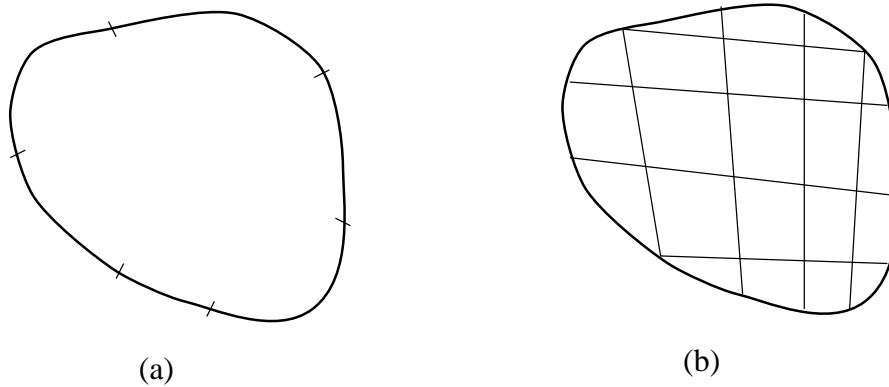
FIGURE 3.5: Schematic illustration of a boundary element mesh (a) and a finite element mesh (b).

Then Equation (3.19) becomes

$$c\left(P\right)u\left(P\right) + \sum_{j=1}^{N} \int_{\Gamma_j} u\frac{\partial \omega}{\partial n}\, d\Gamma = \sum_{j=1}^{N} \int_{\Gamma_j} \frac{\partial u}{\partial n}\omega\, d\Gamma \tag{3.21}$$

Over each element Γ_j we introduce standard (finite element) basis functions

$$u_j = \sum_{\alpha} \varphi_\alpha u_{j\alpha} \quad \text{and} \quad q_j \equiv \frac{\partial u_j}{\partial n} = \sum_{\alpha} \varphi_\alpha q_{j\alpha} \tag{3.22}$$

where u_j, q_j are values of u and q on element Γ_j and $u_{j\alpha}, q_{j\alpha}$ are values of u and q at node α on element Γ_j.

These basis functions for u and q can be any of the standard one-dimensional finite element basis functions (although we are dealing with a two-dimensional problem, we only have to interpolate the functions over a one-dimensional element). In general the basis functions used for u and q do not have to be the same (typically they are) and these basis functions can even be different to the basis functions used for the geometry, but are generally taken to be the same (this is termed an isoparametric formulation).

This gives

$$c\left(P\right)u\left(P\right) + \sum_{j=1}^{N}\sum_{\alpha}u_{j\alpha}\int_{\Gamma_j}\varphi_\alpha\frac{\partial\omega}{\partial n}\,d\Gamma = \sum_{j=1}^{N}\sum_{\alpha}q_{j\alpha}\int_{\Gamma_j}\varphi_\alpha\omega\,d\Gamma \qquad (3.23)$$

This equation holds for any point P on the surface Γ. We now generate one equation per node by putting the point P to be at each node in turn. If P is at node i, say, then we have

$$c_i u_i + \sum_{j=1}^{N}\sum_{\alpha}u_{j\alpha}\int_{\Gamma_j}\varphi_\alpha\frac{\partial\omega_i}{\partial n}\,d\Gamma = \sum_{j=1}^{N}\sum_{\alpha}q_{j\alpha}\int_{\Gamma_j}\varphi_\alpha\omega_i\,d\Gamma \qquad (3.24)$$

where ω_i is the fundamental solution with the singularity at node i (recall ω is $-\dfrac{1}{2\pi}\log r$, where r is the distance from the singularity point). We can write Equation (3.24) in a more abbreviated form as

$$c_i u_i + \sum_{j=1}^{N}\sum_{\alpha}u_{j\alpha}a_{ij}^{\alpha} = \sum_{j=1}^{N}\sum_{\alpha}q_{j\alpha}b_{ij}^{\alpha} \qquad (3.25)$$

where

$$a_{ij}^{\alpha} = \int_{\Gamma_j}\varphi_\alpha\frac{\partial\omega_i}{\partial n}\,d\Gamma \quad\text{and}\quad b_{ij}^{\alpha} = \int_{\Gamma_j}\varphi_\alpha\omega_i\,d\Gamma \qquad (3.26)$$

Equation (3.25) is for node i and if we have L nodes, then we can generate L equations.

We can assemble these equations into the matrix system

$$\boldsymbol{Au} = \boldsymbol{Bq} \qquad (3.27)$$

(compare to the global finite element equations $\boldsymbol{Ku} = \boldsymbol{f}$) where the vectors $\boldsymbol{u}$ and $\boldsymbol{q}$ are the vectors of nodal values of u and q. Note that the ij^{th} component of the $\boldsymbol{A}$ matrix in general is *not* a_{ij}^{α} and similarly for $\boldsymbol{B}$.

At each node, we must specify either a value of u or q (or some combination of these) to have a well-defined problem. We therefore have L equations (the number of nodes) and have L unknowns to find. We need to rearrange the above system of equations to get

$$\boldsymbol{Cx} = \boldsymbol{f} \qquad (3.28)$$

where $\boldsymbol{x}$ is the vector of unknowns. This can be solved using standard linear equation solvers, although specialist solvers are required if the problem is large (refer **[todo : Section ???]**).

The matrices $\boldsymbol{A}$ and $\boldsymbol{B}$ (and hence $\boldsymbol{C}$) are fully populated and not symmetric (compare to the finite element formulation where the global stiffness matrix $\boldsymbol{K}$ is sparse and symmetric). The size of the $\boldsymbol{A}$ and $\boldsymbol{B}$ matrices are dependent on the number of surface nodes, while the matrix $\boldsymbol{K}$ is dependent on the number of finite element nodes (which include nodes in the domain). As

mentioned earlier, it depends on the surface to volume ratio as to which method will generate the smallest and quickest solution.

The use of the fundamental solution as a weight function ensures that the $\boldsymbol{A}$ and $\boldsymbol{B}$ matrices are generally well conditioned (see Section 3.5 for more on this). In fact the $\boldsymbol{A}$ matrix is diagonally dominant (at least for Laplace's equation). The matrix $\boldsymbol{C}$ is therefore also well conditioned and Equation (3.28) can be solved reasonably easily.

The vector $\boldsymbol{x}$ contains the unknown values of $\boldsymbol{u}$ and $\boldsymbol{q}$ on the boundary. Once this has been found, all boundary values of $\boldsymbol{u}$ and $\boldsymbol{q}$ are known. If a solution is then required at a point inside the domain, then we can use Equation (3.25) with the singular point P located at the required solution point *i.e.,*

$$u\left(P\right) = \sum_{j=1}^{N}\sum_{\alpha} q_{j\alpha} b_{Pj}^{\alpha} - \sum_{j=1}^{N}\sum_{\alpha} u_{j\alpha} a_{Pj}^{\alpha} \tag{3.29}$$

The right hand side of Equation (3.29) contains no unknowns and only involves evaluating the surface integrals using the fundamental solution with the singular point located at P.

3.5 Numerical Evaluation of Coefficient Integrals

We consider in detail here how one evaluates the a_{ij}^{α} and b_{ij}^{α} integrals for two-dimensional problems. These integrals typically must be evaluated numerically, and require far more work and effort than the analogous finite element integrals.

Recall that

$$a_{ij}^{\alpha} = \int_{\Gamma_j} \varphi_\alpha \frac{\partial \omega_i}{\partial n} \, d\Gamma \quad \text{and} \quad b_{ij}^{\alpha} = \int_{\Gamma_j} \varphi_\alpha \omega_i \, d\Gamma$$

where

$$\omega_i = -\frac{1}{2\pi} \log r_i$$
$$r_i = \text{distance measured from node } i$$

In terms of a local ξ coordinate we have

$$b_{ij}^{\alpha} = \int_0^1 \varphi_\alpha\left(\xi\right) \omega_i\left(\xi\right) \left|J\left(\xi\right)\right| \, d\xi \tag{3.30}$$

$$a_{ij}^{\alpha} = \int_{\Gamma_j} \varphi_\alpha\left(\xi\right) \frac{\partial \omega_i\left(\xi\right)}{\partial n} \left|J\left(\xi\right)\right| \, d\xi = \int_0^1 \varphi_\alpha\left(\xi\right) \frac{\partial \omega_i}{\partial r_i}\left(\xi\right) \frac{dr_i}{dn} \left|J\left(\xi\right)\right| \, d\xi \tag{3.31}$$

The Jacobian $J(\xi)$ can be found by

$$J(\xi) = \frac{d\Gamma}{d\xi} = \frac{ds}{d\xi} = \sqrt{\left(\frac{dx}{d\xi}\right)^2 + \left(\frac{dy}{d\xi}\right)^2} \tag{3.32}$$

where s represents the arclength and $\frac{dx}{d\xi}$ and $\frac{dy}{d\xi}$ can be found by straight differentiation of the interpolation expression for $x(\xi)$ and $y(\xi)$.

The fundamental solution is

$$\omega_i = -\frac{1}{2\pi} \log(r_i(\xi))$$

$$r_i(\xi) = \sqrt{(x(\xi) - x_i)^2 + (y(\xi) - y_i)^2}$$

where (x_i, y_i) are the coordinates of node i.

To find $\frac{dr_i}{dn}$ we note that

$$\frac{dr_i}{dn} = \nabla r_i \cdot \hat{\boldsymbol{n}} \tag{3.33}$$

where $\hat{\boldsymbol{n}}$ is a unit outward normal vector. To find a unit normal vector, we simply rotate the tangent vector (given by $(x'(\xi), y'(\xi))$) by $\frac{\pi}{2}$ in the appropriate direction and then normalise.

Thus every expression in the integrands of the a_{ij}^α and b_{ij}^α integrals can be found at any value of ξ, and the integrals can therefore be evaluated numerically using some suitable quadrature schemes.

If node i is well removed from element Γ_j then standard Gaussian quadrature can be used to evaluate these integrals. However, if node i is in Γ_j (or close to it) we see that r_i approaches 0 and the fundamental solution ω_i tends to ∞. The integral still exists, but the integrand becomes singular. In such cases special care must be taken - either by using special quadrature schemes, large numbers of Gauss points or other special treatment.

The integrals for which node i lies in element Γ_j are in general the largest in magnitude and lead to the diagonally dominant matrix equation. It is therefore important to ensure that these integrals are calculated as accurately as possible since these terms will have most influence on the solution. This is one of the disadvantages of the BEM - the fact that singular integrands must be accurately integrated.

A relatively straightforward way to evaluate all the integrals is simply to use Gaussian quadrature with varying number of quadrature points, depending on how close or far the singular point is from the current element. This is not very elegant or efficient, but has the benefit that it is relatively easy to implement. For the case when node i is contained in the current element one can use special quadrature schemes which are designed to integrate log-type functions. These are to be preferred when one is dealing with Laplace's equation. However, these special log-type schemes cannot be so readily used on other types of fundamental solution so for a general purpose implementation, Gaussian quadrature is still the norm. It is possible to incorporate adaptive integration schemes that keep adding more quadrature points until some error estimate is small enough, or also to subdivide the current element into two or more smaller elements and evaluate the integral over each
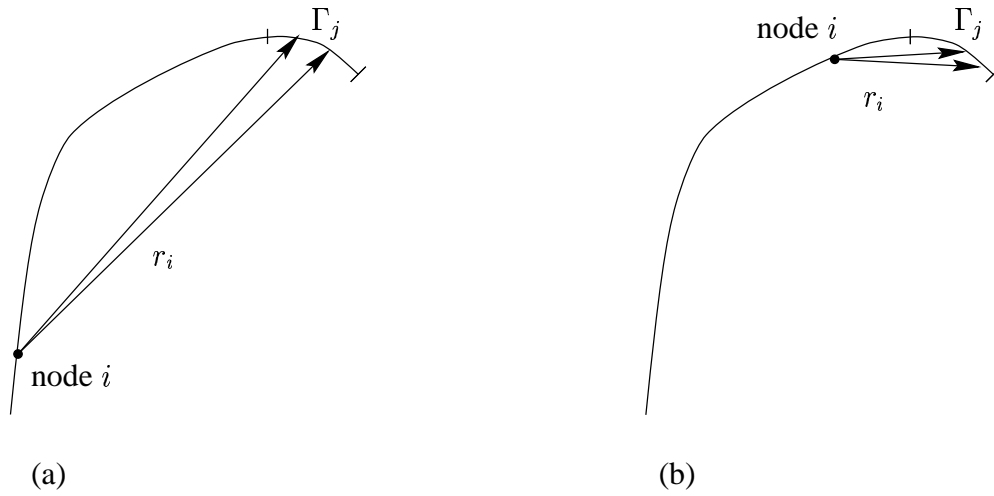
FIGURE 3.6: Illustration of the decrease in r_i as node i approaches element Γ_j.

subelement. It is also possible to evaluate the "worst" integrals by using simple solutions to the governing equation, and this technique is the norm for elasticity problems (Section 4.8). Details on each of these methods is given in Section 3.8. It should be noted that research still continues in an attempt to find more efficient ways of evaluating the boundary element integrals.

3.6   The Three-Dimensional Boundary Element Method

The three-dimensional boundary element method is very similar to the two-dimensional boundary element method discussed above. As noted above, the three-dimensional boundary integral equation is the same as the two-dimensional equation (3.19), with ω and $c(P)$ being defined as in Section 3.3. The numerical solution procedure also parallels that given in Section 3.4, and the expressions given for a_{ij}^{α} and b_{ij}^{α} apply equally well to the three-dimensional case. The only real difference between the two procedures is how to numerically evaluate the terms in each integrand of these coefficient integrals.

As in Section 3.5 we illustrate how to evaluate each of the terms in the integrand of a_{ij}^{α} and b_{ij}^{α}.

The relevant expressions are

$$
a_{ij}^\alpha = \int\limits_{\Gamma_j} \varphi_\alpha \frac{\partial \omega_i}{\partial n} \, d\Gamma
$$

$$
= \int\limits_0^1 \int\limits_0^1 \varphi_\alpha \left(\xi_1, \xi_2\right) \frac{\partial \omega_i}{\partial r_i} \left(\xi_1, \xi_2\right) \frac{dr_i}{dn} \left| J\left(\xi_1, \xi_2\right)\right| \, d\xi_1 \, d\xi_2 \tag{3.34}
$$

$$
b_{ij}^\alpha = \int\limits_{\Gamma_j} \varphi_\alpha \omega_i \, d\Gamma
$$

$$
= \int\limits_0^1 \int\limits_0^1 \varphi_\alpha \left(\xi_1, \xi_2\right) \omega_i \left(\xi_1, \xi_2\right) \left| J\left(\xi_1, \xi_2\right)\right| \, d\xi_1 \, d\xi_2 \tag{3.35}
$$

The fundamental solution is

$$
\omega_i \left(\xi_1, \xi_2\right) = \frac{1}{4\pi r_i \left(\xi_1, \xi_2\right)}
$$

$$
\text{where } r_i \left(\xi_1, \xi_2\right) = \sqrt{\left(x\left(\xi_1, \xi_2\right) - x_i\right)^2 + \left(y\left(\xi_1, \xi_2\right) - y_i\right)^2 + \left(z\left(\xi_1, \xi_2\right) - z_i\right)^2}
$$

where (x_i, y_i, z_i) are the coordinates of node i. As before we use $\dfrac{dr_i}{dn} = \nabla r_i \cdot \hat{n}$ to find $\dfrac{dr_i}{dn}$. The unit outward normal $\hat{n}$ is found by normalising the cross product of the two tangent vectors $\boldsymbol{t}_1 = \left(\dfrac{\partial x}{\partial \xi_1}, \dfrac{\partial y}{\partial \xi_1}, \dfrac{\partial z}{\partial \xi_1}\right)$ and $\boldsymbol{t}_2 = \left(\dfrac{\partial x}{\partial \xi_2}, \dfrac{\partial y}{\partial \xi_2}, \dfrac{\partial z}{\partial \xi_2}\right)$ (it relies on the user of any BEM code to ensure that the elements have been defined with a consistent set of element coordinates ξ_1 and ξ_2).

The Jacobian $J\left(\xi_1, \xi_2\right)$ is given by $\|\boldsymbol{t}_1 \times \boldsymbol{t}_2\|$ (where $\boldsymbol{t}_1$ and $\boldsymbol{t}_2$ are the two tangent vectors). Note that this is different for the determinant in a two-dimensional finite element code - in that case we are dealing with a two-dimensional surface in two-dimensional space, whereas here we have a (possibly curved) two-dimensional surface in three-dimensional space.

The integrals are evaluated numerically using some suitable quadrature schemes (see Section 3.8) (typically a Gauss-type scheme in both the ξ_1 and ξ_2 directions).

3.7 A Comparison of the FE and BE Methods

We comment here on some of the major differences between the two methods. Depending on the application some of these differences can either be considered as advantageous or disadvantageous to a particular scheme.

1. **FEM**: An entire domain mesh is required.
   BEM: A mesh of the boundary only is required.
   Comment: Because of the reduction in size of the mesh, one often hears of people saying that the problem size has been reduced by one dimension. This is one of the major pluses of

the BEM - construction of meshes for complicated objects, particularly in 3D, is a very time consuming exercise.

2. **FEM**: Entire domain solution is calculated as part of the solution.
   BEM: Solution on the boundary is calculated first, and then the solution at domain points (if required) are found as a separate step.
   Comment: There are many problems where the details of interest occur on the boundary, or are localised to a particular part of the domain, and hence an entire domain solution is not required.

3. **FEM**: Reactions on the boundary typically less accurate than the dependent variables.
   BEM: Both u and q of the same accuracy.

4. **FEM**: Differential Equation is being approximated.
   BEM: Only boundary conditions are being approximated.
   Comment: The use of the Green-Gauss theorem and a fundamental solution in the formulation means that the BEM involves no approximations of the differential Equation in the domain - only in its approximations of the boundary conditions.

5. **FEM**: Sparse symmetric matrix generated.
   BEM: Fully populated nonsymmetric matrices generated.
   Comment: The matrices are generally of different sizes due to the differences in size of the domain mesh compared to the surface mesh. There are problems where either method can give rise to the smaller system and quickest solution - it depends partly on the volume to surface ratio. For problems involving infinite or semi-infinite domains, BEM is to be favoured.

6. **FEM**: Element integrals easy to evaluate.
   BEM: Integrals are more difficult to evaluate, and some contain integrands that become singular.
   Comment: BEM integrals are far harder to evaluate. Also the integrals that are the most difficult (those containing singular integrands) have a significant effect on the accuracy of the solution, so these integrals need to be evaluated accurately.

7. **FEM**: Widely applicable. Handles nonlinear problems well.
   BEM: Cannot even handle all linear problems.
   Comment: A fundamental solution must be found (or at least an approximate one) before the BEM can be applied. There are many linear problems (*e.g.,* virtually any nonhomogeneous equation) for which fundamental solutions are not known. There are certain areas in which the BEM is clearly superior, but it can be rather restrictive in its applicability.

8. **FEM**: Relatively easy to implement.
   BEM: Much more difficult to implement.
   Comment: The need to evaluate integrals involving singular integrands makes the BEM at least an order of magnitude more difficult to implement than a corresponding finite element procedure.

3.8 More on Numerical Integration

The BEM involves integrals whose integrands in generally become singular when the source point is contained in the element of integration. If one uses constant or linear interpolation for the geometry and dependent variable, then it is possible to obtain analytic expressions to most (if not all) of the integrals that will appear in the BEM (at least for two-dimensional problems). The expressions can become quite lengthy to write down and evaluate, but benefit from the fact that they will be exact. However, when one begins to use general curved elements and/or solve three-dimensional problems then the integrals will not be available as analytic expressions. The basic tool for evaluation of these integrals is quadrature. As discussed in Section 2.8 a one-dimensional integral is approximated by a sum in which the integrand is evaluated at certain discrete points or abscissa

$$\int_0^1 f(\xi) \, d\xi \approx \sum_{i=1}^N f(\xi_i) \, w_i$$

where w_i are the weights and ξ_i are the abscissa.

The weights and abscissa for the Gaussian quadrature scheme of order N are chosen so that the above expression will exactly integrate any polynomial of degree $2N - 1$ or less. For the numerical evaluation of two or three-dimensional integrals, a Gaussian scheme can be used of each variable of integration if the region of integration is rectangular. This is generally not the optimal choice for the weights and abscissae but it allows easy extension to higher order integration.

3.8.1 Logarithmic quadrature and other special schemes

Low order Gaussian schemes are generally sufficient for all FEM integrals, but that is not the case for BEM. For a two-dimensional BEM solution of Laplace's equation, integrals of the form $\int_0^1 \log(\xi) f(\xi) \, d\xi$ will be required. It is relatively common to use logarithmic schemes for this. These are obtained by approximating the integral as

$$\int_0^1 \log(\xi) f(\xi) \, d\xi \approx \sum_{i=1}^N f(\xi_i) \, w_i$$

i.e., the log function has been factored out.

In the same way as Gaussian quadrature schemes were developed in Section 2.8, log quadrature schemes can be developed which will exactly integrate polynomial functions $f(\xi)$. Tables of these are given below

It is possible to develop similar quadrature schemes for use in the BEM solution of other PDEs, which use different fundamental solutions to the log function. The problem with this approach is the lack of generality - each new equation to be used requires its own special quadrature scheme.

Abscissas = r_i					Weight Factors = w_i		
n	ξ_i	$-w_i$	n	ξ_i	$-w_i$	n	ξ_i	$-w_i$
2	0.112009	0.718539	3	0.063891	0.513405	4	0.041448	0.383464
	0.602277	0.281461		0.368997	0.391980		0.245275	0.386875
				0.766880	0.094615		0.556165	0.190435
							0.848982	0.039225

TABLE 3.1: Abscissas and weight factors for Gaussian integration for integrands with a logarithmic singularity.

3.8.2 Special solutions

Another approach, particularly useful if Cauchy principal values are to be found (see Section 4.8) is to use special solutions of the governing equation to find one or more of the more difficult integrals.

For example $u = x$ is a solution to Laplaces' equation (assuming the boundary conditions are set correctly). Thus if one sets both u and q in Equation (3.27) at every node according to the solution $u = x$, one can then use this to solve for some entry in either the A or B matrix (typically the diagonal entry since this is the most important and difficult to find). Further solutions to Laplaces equation (*e.g.,* $u = x^2 - y^2$) can be used to find the other matrix entries (or just used to check the accuracy of the matrices).

3.9 The Boundary Element Method Applied to other Elliptic PDEs

Helmholtz, modified Helmholtz (CMISS example) Poisson Equation (domain integral and MRM, DRM, Monte-carlo integration.

3.10 Solution of Matrix Equations

The standard BEM approach results in a system of equations of the form $Cx = f$ (refer (3.28)). As mentioned above the matrix C is generally well conditioned, fully populated and nonsymmetric. For small problems, direct solution methods, based on LU factorisations, can be used. As the problem size increases, the time taken for the matrix solution begins to dominate the matrix assembly stage. This usually occurs when there is between 500 and 1000 degrees of freedom, although it is very dependent on the implementation of the BE method. The current technique of favour in the BE community for solution of large BEM matrix equations is a preconditioned Conjugate Gradient solver. Preconditioners are generally problem dependent - what works well for one problem may not be so good for another problem. The conjugate gradient technique is generally regarded as a solution technique for (sparse) symmetric matrix equations.
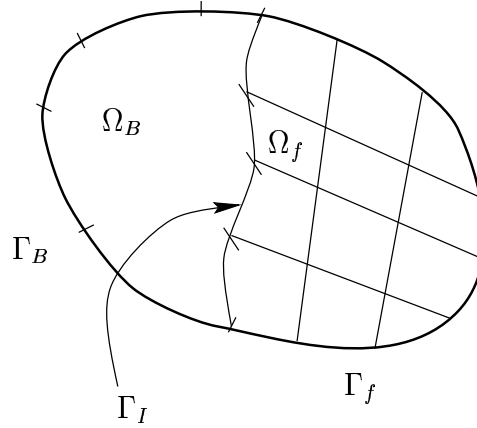
FIGURE 3.7: Coupled finite element/boundary element solution domain.

3.11   Coupling the FE and BE techniques

There are undoubtably situations which favour FEM over BEM and vice versa. Often one problem can give rise to a model favouring one method in one region and the other method in another region, *e.g.,* in a detailed analysis of stresses around a foundation one needs FEM close to the foundation to handle nonlinearities, but to handle the semi-infinite domain (well removed from the foundation), BEM is better. There has been a lot of research on coupling FE and BE procedures - we will only talk about the basic ideas and use Laplace's Equation to illustrate this. There are at least two possible methods.

1. Treat the BEM region as a finite element and combine with FEM

2. Treat the FEM region as an equivalent boundary element and combine with BEM

Note that these are essentially equivalent - the use of one or the other depends on the problem, in the sense of which part is more dominant FEM or BEM)

Consider the region shown in Figure 3.7, where

$$\Omega_f = \text{FEM region}$$
$$\Omega_B = \text{BEM region}$$
$$\Gamma_f = \text{FEM boundary}$$
$$\Gamma_B = \text{BEM boundary}$$
$$\Gamma_I = \text{interface boundary}$$

The BEM matrices for Ω_B can be written as

$$\boldsymbol{Au} = \boldsymbol{Bq} \tag{3.36}$$

where $\boldsymbol{u}$ is a vector of the nodal values of u and $\boldsymbol{q}$ is a vector of the nodal values of $\dfrac{\partial u}{\partial n}$

The FEM matrices for Ω_F can be written as

$$\boldsymbol{Ku} = \boldsymbol{f} \tag{3.37}$$

where $\boldsymbol{K}$ is the stiffness matrix and $\boldsymbol{f}$ is the load vector.

To apply method 1 (*i.e.,* treating BEM as an equivalent FEM region) we get (from Equation (3.36))

$$\boldsymbol{B}^{-1}\boldsymbol{A}\boldsymbol{u} = \boldsymbol{q} \qquad (3.38)$$

If we recall what the elements of $\boldsymbol{f}$ in Equation (3.37) contained, then we can convert $\boldsymbol{q}$ in Equation (3.38) to an equivalent load vector by weighting the nodal values of $\boldsymbol{q}$ by the appropriate basis functions, producing a matrix $\boldsymbol{M}$ *i.e.,* $\boldsymbol{f}_B = \boldsymbol{M}\boldsymbol{q}$

Therefore Equation (3.38) becomes

$$\boldsymbol{M}\left(\boldsymbol{B}^{-1}\boldsymbol{A}\right)\boldsymbol{u} = \boldsymbol{M}\boldsymbol{q} = \boldsymbol{f}_B$$

i.e.,

$$\boldsymbol{K}_B\boldsymbol{u} = \boldsymbol{f}_B$$
$$\text{where} \quad \boldsymbol{K}_B = \boldsymbol{M}\boldsymbol{B}^{-1}\boldsymbol{A}$$

an equivalent stiffness matrix obtain from BEM.

Therefore we can assemble this together with original FEM matrix to produce an FEM-type system for the entire region Ω_B.

Notes:

1. $\boldsymbol{K}_B$ is in general not symmetric and not sparse. This means that different matrix equation solvers must be used for solving the new combined FEM-type system (most solvers in FEM codes assume sparse and symmetric). Attempts have been made to "symmetricise" the $\boldsymbol{K}_B$ matrix - of doubtful quality. (*e.g.,* replace $\boldsymbol{K}_B$ by $\frac{1}{2}\left(\boldsymbol{K}_B - \boldsymbol{K}_B^T\right)$ - often yields inaccurate results).

2. On Γ_I nodal values of $\boldsymbol{u}$ and $\boldsymbol{q}$ are unknown. One must make use of the following

$$\boldsymbol{u}_B^I = \boldsymbol{u}_F^I \qquad (\boldsymbol{u} \text{ is continuous})$$
$$\frac{\partial \boldsymbol{u}_B^I}{\partial \boldsymbol{n}_B} = -\frac{\partial \boldsymbol{u}_F^I}{\partial \boldsymbol{n}_F}(\boldsymbol{q} \text{ is continuous, but } \Gamma_B = -\Gamma_F)$$

To apply method 2 (*i.e.,* to treat the FEM region as an equivalent BEM region) we firstly note that, as before, $\boldsymbol{f} = \boldsymbol{M}\boldsymbol{q}$. Applying this to (3.37) yields $\boldsymbol{K}\boldsymbol{u} = \boldsymbol{M}\boldsymbol{q}$ an equivalent BEM system. This can be assembled into the existing BEM system (using compatability conditions) and use existing BEM matrix solvers.

Notes:

1. This approach does not require any matrix inversion and is hence easier (cheaper) to implement

2. Existing BEM solvers will not assume symmetric or sparse matrices therefore no new matrix solvers to be implemented

3.12   Other BEM techniques

What we have mentioned to date is the so-called singular (direct) BEM. Given a BIE there are other ways of solving the Equation although these are not so widely used.

3.12.1   Trefftz method

Trefftz was the first person to perform a BEM calculation (in 1917 - calculated the value (numerical) of the contraction coefficient of a round jet issuing from an infinite tank - a nonlinear free surface problem). This method basically uses a "complete" set of solutions instead of a Fundamental Solution. *e.g.,* Consider Laplaces Equation in a (bounded) domain Ω

$$\text{weighted residuals} \Rightarrow \int\limits_{\partial\Omega} \omega \frac{\partial u}{\partial n} \, d\Gamma = \int\limits_{\partial\Omega} u \frac{\partial \omega}{\partial n} \, d\Gamma \quad \text{if } \nabla^2 \omega = 0$$

The procedure is to express u as a series of (complete) functions satisfying Laplace's equation with coefficients which need to be numerically determined through utilisation of the boundary conditions.

Notes:

1. Doesn't introduce singular functions so integrals are easy to evaluate

2. Must find a (complete) set of functions (If you just use usual approximations for u matrix system is not diagonally dominant so not so good)

3. Method is not so popular - Green's functions more widely available that complete systems

3.12.2   Regular BEM

Consider the BIE for Laplace's equation

$$c\left(P\right) u\left(P\right) + \int\limits_{\partial\Omega} u \frac{\partial \omega}{\partial n} \, d\Gamma = \int\limits_{\partial\Omega} \frac{\partial u}{\partial n} \omega \, d\Gamma$$

$$\text{with} \quad \omega = -\frac{1}{2\pi} \log r$$

The usual procedure is to put point P at each solution variable node - creating an equation for each node. This leads to singular integrands.

Another possibility is to put point P outside of the domain Ω - this yields

$$\int\limits_{\partial\Omega} u \frac{\partial \omega_p}{\partial n} \, d\Gamma = \int\limits_{\partial\Omega} \frac{\partial u}{\partial n_p} \, d\Gamma$$

Following discretisation as before gives

$$\sum_{j=1}^{N} \sum_{\alpha} u_{j\alpha} \int_{\Gamma_j} \varphi_\alpha \frac{\partial \omega_p}{\partial n} d\Gamma = \sum_{j=1}^{N} \sum_{\alpha} q_{j\alpha} \int_{\Gamma_j} \varphi_\alpha \omega_p \, d\Gamma$$

- an equation involving u and q at each surface node.

By placing the point P (the singular point) at other distinct points outside Ω one can generate as many equations as there are unknowns (or more if required).

Notes:

1. This method does not involve singular integrands, so that integrals are inexpensive to calculate.

2. There is considerable choice for the location of the point P. Often the set of Equations generated are ill-conditioned unless P chosen carefully. In practise P is chosen along the unit outward normal of the surface at each solution variable node. The distance along each node is often found by experimentation - various research papers suggesting "ideal" distances (Patterson & Shiekh).

3. This method is not very popular.

4. The idea of placing the singularity point P away from the solution variable node is often of use in other situations *e.g., Exterior Acoustic Problems*. For an acoustic problem (governed by Helmholtz Equation $\nabla^2 u + k^2 u = 0$) in an unbounded region the system of Equations produced by the usual (singular) BEM approach is singular for certain "fictitious" frequencies (*i.e.,* certain values of k). To overcome this further equations are generated (by placing the singular point P at various locations outside Ω). The system of equations are then overdetermined and are solved in a least squares sense.

3.13 Symmetry

Consider the problem given in Figure 3.8 (the domain is *outside* the circle). Both the boundary conditions and the governing Equation exhibit symmetry about the vertical axis. *i.e.,* putting x to $-x$ makes no difference to the problem formulation. Thus the solution $H(x, z)$ has the property that $H(x, z) = H(-x, z) \, \forall x$. This behaviour can be found in many problems and we can make use of this as follows. The Boundary Element Equation is (with $N = 2M$ (*i.e.,* N is even) *constant* elements)

$$\frac{1}{2} u_i + \sum_{j=1}^{N} u_j \int_{\Gamma_j} \frac{\partial \omega_i}{\partial n} d\Gamma = \sum_{j=1}^{N} q_j \int_{\Gamma_j} \omega_i \, d\Gamma \qquad i = 1, \dots, N \tag{3.39}$$
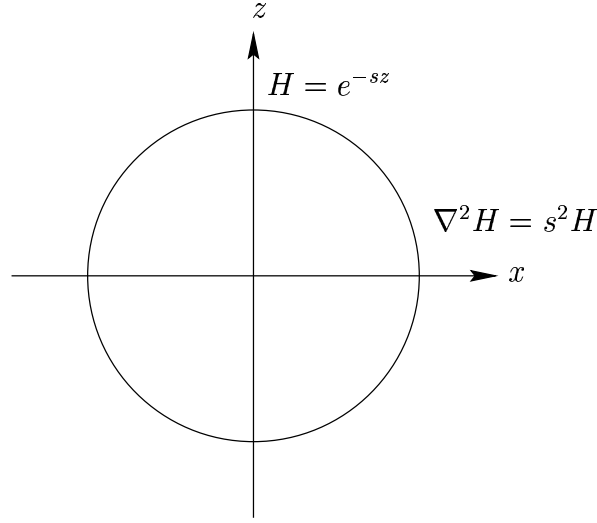
FIGURE 3.8: A problem exhibiting symmetry.

We have N Equations and N unknowns (allowing for the boundary conditions). From symmetry we know that (refer to Figure 3.9).

$$u_i = u_{n+1-i} \qquad i = 1, \dots, M \tag{3.40}$$

So we can write

$$\frac{1}{2}u_i + \sum_{j=1}^{M} u_j \left\{ \int_{\Gamma_j} \frac{\partial \omega_i}{\partial n} \, d\Gamma + \int_{\Gamma_{N+1-j}} \frac{\partial \omega_i}{\partial n} \, d\Gamma \right\} = \sum_{j=1}^{M} q_j \left\{ \int_{\Gamma_j} \omega_i \, d\Gamma + \int_{\Gamma_{N+1-j}} \omega_i \, d\Gamma \right\} \tag{3.41}$$

for nodes $i = 1, \dots, M$. (The Equations for nodes $i = M+1, \dots, N$ are the same as the Equations for nodes $i = 1, \dots, M$). The above M Equations have only M unknowns.

If we define

$$a_{ij} = \int_{\Gamma_j} \frac{\partial \omega_i}{\partial n} \, d\Gamma + \int_{\Gamma_{N+1-j}} \frac{\partial \omega_i}{\partial n} \, d\Gamma \tag{3.42}$$

$$b_{ij} = \int_{\Gamma_j} \omega_i \, d\Gamma + \int_{\Gamma_{N+1-j}} \omega_i^* \, d\Gamma \tag{3.43}$$

then we can write Equation (3.41) as

$$\frac{1}{2}u_i + \sum_{j=1}^{M} a_{ij} u_j = \sum_{j=1}^{M} b_{ij} q_j \quad i = 1, \dots, M \tag{3.44}$$

and solve as before. (This procedure has halved the number of unknowns.)
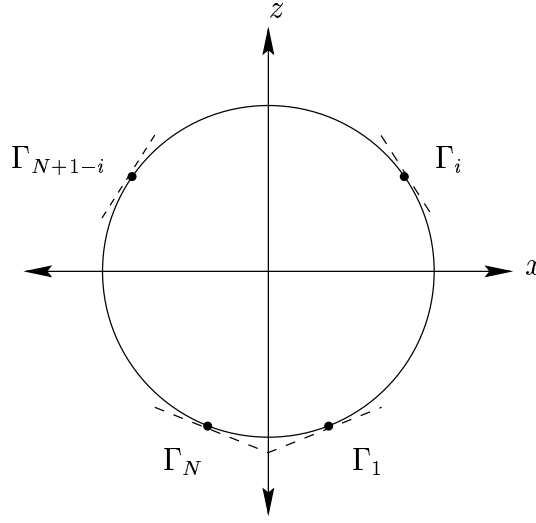
FIGURE 3.9: Illustration of a symmetric mesh.

Note: Since $i = 1, \ldots, M$ this means that the integrals over the elements Γ_{M+1} to Γ_N will never contain a singularity arising from the fundamental solution, except possibly on the axis of symmetry if linear or higher order elements are used.

An alternative approach to the method above arises from the implied no flux across the z axis. This approach ignores the negative x axis and considers the half plane problem shown.

However now the surface to be discretised extends to infinity in the positive and negative z directions and the resulting systems of equations produced is much larger.

Further examples of how symmetry can be used (*e.g.,* radial symmetry) are given in the next section.

3.14 Axisymmetric Problems

If a three-dimensional problem exhibits radial or axial symmetry (*i.e.,* $u\left(r, \theta_1, z\right) = u\left(r, \theta_2, z\right)$) it is possible to reduce the two-dimensional integrals appearing in the standard boundary Equation to one-dimensional line integrals and thus substantially reduce the amount of computer time that would otherwise be required to solve the fully three-dimensional problem. The first step in such a procedure is to write the standard boundary integral equation in terms of cylindrical polars (r, θ, z) *i.e.,*

$$c\left(P\right)u\left(P\right) + \int_{\overline{\Gamma}} u \left(\int_0^{2\pi} \frac{\partial \omega_p}{\partial n}\, d\theta_q \right) r_q\, d\overline{\Gamma} = \int_{\overline{\Gamma}} q \left(\int_0^{2\pi} \omega_p\, d\theta_q \right) r_q\, d\overline{\Gamma} \qquad (3.45)$$

where $\left(r_p, \theta_p, z_p\right)$ and $\left(r_q, \theta_q, z_q\right)$ are the polar coordinates of P and Q respectively, and $\overline{\Gamma}$ is the intersection of Γ and $\theta = 0$ semi-plane (Refer Figure 3.10). (*n.b.* Q is a point on the surface being integrated over.)
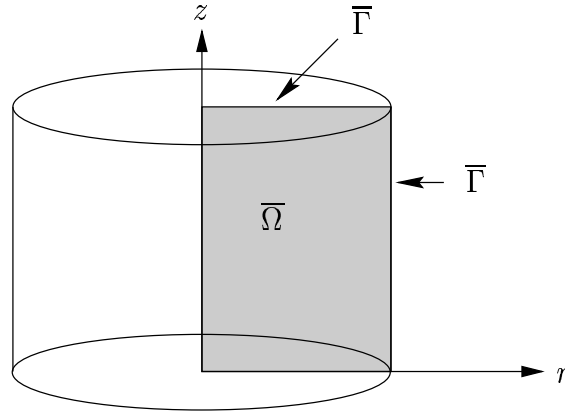
FIGURE 3.10: Illustration of surface $\overline{\Gamma}$ for an axisymmetric problem.
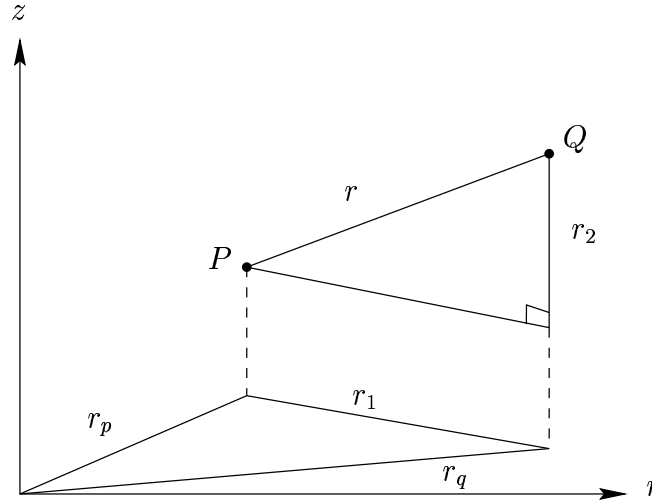
FIGURE 3.11: The distance from the source point (P) to the point of interest (Q) in terms of cylindrical polar coordinates.

For three-dimensional problems governed by Laplace's equation

$$\omega_p = \frac{1}{4\pi r}$$

where r_p is the distance from P to Q. From Figure 3.11

$$r_1^2 = r_p^2 + r_q^2 - 2r_p r_q \cos\left(\theta_p - \theta_q\right)$$
$$r^2 = \sqrt{r_1^2 + r_2^2}$$
$$r = \sqrt{r_p^2 + r_q^2 - 2r_p r_q \cos\left(\theta_p - \theta_q\right) + \left(z_p - z_q\right)^2}$$
$$= \sqrt{a - b \cos\left(\theta_p - \theta_q\right) + \left(z_p - z_q\right)^2} \tag{3.46}$$

We define

$$\overline{\omega}_p = \frac{1}{4\pi} \int\limits_0^{2\pi} \omega_p \, d\theta_q \equiv \frac{K(m)}{\pi\sqrt{a+b}} \quad \text{where } m = \frac{2b}{a+b} \tag{3.47}$$

and $K(m)$ is the complete elliptic integral of the first kind.

$\overline{\omega}_p$ is called the axisymmetric fundamental solution and is the Green's function for a ring source as opposed to a point source. *i.e.,* $\overline{\omega}_p$ is a solution of

$$\nabla^2 \omega + \delta(r - r_p) = 0 \tag{3.48}$$

instead of

$$\nabla^2 \omega + \delta_p = 0 \tag{3.49}$$

where δ_p is the dirac delta centered at the point P and $\delta(r - r_P)$ is the dirac delta centered on the ring $r = r_p$.

Unlike the two- and three-dimensional cases, the axisymmetric fundamental solution cannot be written as simply a function of the distance between two points P and Q, but it also depends upon the distance of these points to the axis of revolution.

We also define

$$\overline{q}_p^* = \frac{1}{4\pi} \int\limits_0^{2\pi} \frac{\partial \omega_p}{\partial n} \, d\theta_q \equiv \frac{\partial \overline{\omega}_p}{\partial n} \tag{3.50}$$

For Laplace's equation Equation (3.50) becomes

$$\overline{q}_p^* = \frac{1}{\pi\sqrt{a+b}} \left[\frac{1}{2r_q} \left\{ \frac{r_p^2 - r_q^2 + (z_p - z_q)}{a - b} E(m) - K(m) \right\} n_r(Q) + \frac{z_p - z_q}{a - b} E(m) \, n_z(Q) \right] \tag{3.51}$$

where $E(m)$ is the complete elliptic integral of the second kind.

Using Equation (3.47) and Equation (3.50) we can write Equation (3.45) as

$$c(P) u(P) + \int\limits_{\overline{\Gamma}} u \frac{\partial \overline{\omega}_p}{\partial n} \, d\overline{\Gamma} = \int\limits_{\overline{\Gamma}} q \overline{\omega}_p \, d\overline{\Gamma} \tag{3.52}$$

and the solution procedure for this Equation follows the same lines as the solution procedure given previously for the two-dimensional version of boundary element method.

3.15   Infinite Regions

The boundary integral equations we have been using have been derived assuming the domain Ω is bounded (although this was never stated). However all concepts presented thus far are also
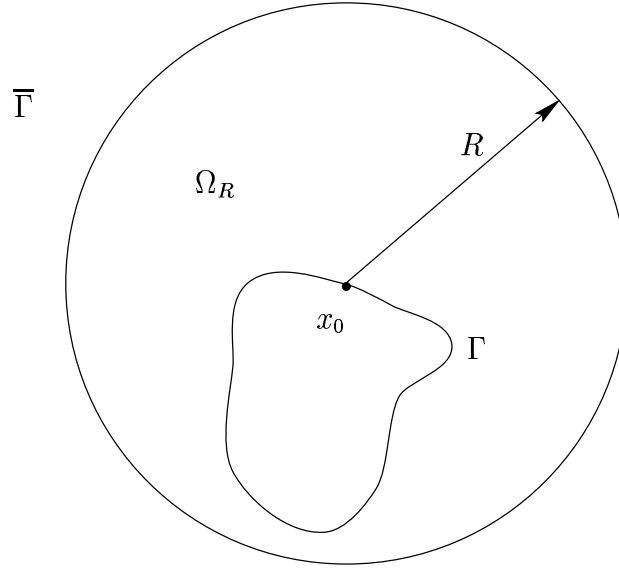
FIGURE 3.12: Derivation of infinite domain boundary integral equations.

valid for infinite regular (*i.e.*, nice) regions provided the solution and its normal derivative behave appropriately as $\Gamma \to \infty$.

Consider the problem of solving $\nabla^2 u = 0$ outside some surface Γ.

$\overline{\Gamma}$ is the centre of a circle (or sphere in three dimensions) of radius centred at some point x_0 on Γ and surrounding Γ (see Figure 3.12). The boundary integral equations for the bounded domain Ω_R can be written as

$$c\left(P\right)u\left(P\right) + \int\limits_{\Gamma} u\frac{\partial \omega_P}{\partial n}\, d\Gamma + \int\limits_{\overline{\Gamma}} u\frac{\partial \omega_P}{\partial n}\, d\Gamma = \int\limits_{\Gamma} q\omega_P\, d\Gamma + \int\limits_{\overline{\Gamma}} q\omega_P\, d\Gamma \tag{3.53}$$

If we let the radius $R \to \infty$ Equation (3.53) will only be valid for the points on Γ if

$$\lim_{R\to\infty} \int\limits_{\overline{\Gamma}} \left(u\frac{\partial \omega_P}{\partial n} - q\omega_P\right)\, d\Gamma = 0 \tag{3.54}$$

If this is satisfied, the boundary integral Equation for Ω will be as expected *i.e.*,

$$c\left(P\right)u\left(P\right) + \int\limits_{\Gamma} u\frac{\partial \omega_P}{\partial n}\, d\Gamma = \int\limits_{\Gamma} q\omega_P\, d\Gamma \tag{3.55}$$

For three-dimensional problems with $\omega^* = \dfrac{1}{4\pi r}$

$$d\Gamma = |J| \, d\theta d\phi \qquad \text{where } |J| = \mathrm{O}\left(R^2\right)$$
$$\omega^* = \mathrm{O}\left(R^{-1}\right)$$
$$\frac{\partial \omega^*}{\partial n} = \mathrm{O}\left(R^{-2}\right)$$

where $|J|$ is the Jacobian and $\mathrm{O}\,()$ represents the asymptotic behaviour of the function as $R \to \infty$. In this case Equation (3.53) will be satisfied if u behaves at most as $\mathrm{O}\left(R^{-1}\right)$ so that $q = \mathrm{O}\left(R^{-2}\right)$. These are the regularity conditions at infinity and these ensure that each term in the integral Equation (3.53) behaves at most as $\mathrm{O}\left(R^{-1}\right)$ (*i.e.,* each term will $\to 0$ as $R \to \infty$)

For two-dimensional problems with $\omega^* = \mathrm{O}\left(\log\left(R\right)\right)$ we require u to behave as $\log\left(R\right)$ so that $q = \mathrm{O}\left(R^{-1}\right)$. For almost all well posed infinite domain problems the solution behaves appropriately at infinity.

3.16 Appendix: Common Fundamental Solutions

3.16.1 Two-Dimensional equations

Here $r = \sqrt{(x_1^2 + x_2^2)}$.

Laplace   Equation $\dfrac{\partial^2 u^*}{\partial x_1{}^2} + \dfrac{\partial^2 u^*}{\partial x_2{}^2} + \delta_0 = 0$

             Solution $u^* = \dfrac{1}{2\pi} \log\left(\dfrac{1}{r}\right)$

Helmholtz   Equation $\dfrac{\partial^2 u^*}{\partial x_1{}^2} + \dfrac{\partial^2 u^*}{\partial x_2{}^2} + \lambda^2 u^* + \delta_0 = 0$

             Solution $u^* = \dfrac{1}{4i} H_0^{(2)}(\lambda r)$

                      where H is the Hankel funtion.

Wave   Equation $c^2\left(\dfrac{\partial^2 u^*}{\partial x_1{}^2} + \dfrac{\partial^2 u^*}{\partial x_2{}^2}\right) - \dfrac{\partial^2 u^*}{\partial t^2} + \delta_0\left(t\right) = 0$

                      where c is the wave speed.

             Solution $u^* = -\dfrac{H\left(ct - r\right)}{2\pi c\left(c^2 t^2 - r^2\right)}$

Diffusion   Equation $\dfrac{\partial^2 u^*}{\partial x_1{}^2} + \dfrac{\partial^2 u^*}{\partial x_2{}^2} - \dfrac{1}{k}\dfrac{\partial u^*}{\partial t} = 0$

                      where k is the diffusivity.

             Solution $u^* = -\dfrac{1}{(4\pi kt)^{\frac{3}{2}}} exp\left(-\dfrac{r^2}{4kt}\right)$

Navier's   Equation $\dfrac{\partial \sigma_{jk}^*}{\partial x_j} + \delta_l = 0$ for a point load in direction l.

             Solution $p_i^* = p_{ji}^* e_j$

                      $p_{ji}^* = -\dfrac{1}{8\pi\left(1 - \nu^2\right) r^2}$

                      $\left(\dfrac{\partial r}{\partial n}\left[\left(1 - 2\nu\right)\delta_{ij} + 3r_{,i} r_{,j}\right] + \left(1 - 2\nu\right)\left(n_j r_{,i} - n_i r_{,j}\right)\right) e_j$

                      for a traction in direction k where ν is Poisson's ratio.

3.16.2 Three-Dimensional equations

Here $r = \sqrt{(x_1^2 + x_2^2 + x_3^2)}$.

Laplace   Equation $\dfrac{\partial^2 u^*}{\partial x_1{}^2} + \dfrac{\partial^2 u^*}{\partial x_2{}^2} + \dfrac{\partial^2 u^*}{\partial x_3{}^2} + \delta_0 = 0$

                Solution $u^* = \dfrac{1}{4\pi r}$

Helmholtz   Equation $\dfrac{\partial^2 u^*}{\partial x_1{}^2} + \dfrac{\partial^2 u^*}{\partial x_2{}^2} + \dfrac{\partial^2 u^*}{\partial x_3{}^2} + \lambda^2 u^* + \delta_0 = 0$

                Solution $u^* = \dfrac{1}{4\pi r} \exp\left(-i\lambda r\right)$

Wave   Equation $c^2 \left(\dfrac{\partial^2 u^*}{\partial x_1{}^2} + \dfrac{\partial^2 u^*}{\partial x_2{}^2} + \dfrac{\partial^2 u^*}{\partial x_3{}^2} \right) - \dfrac{\partial^2 u^*}{\partial t^2} + \delta_t = 0$

                where c is the wave speed.

                Solution $u^* = \dfrac{\delta\left(t - \dfrac{r}{c}\right)}{4\pi r}$

Navier's   Equation $\dfrac{\partial \sigma^*_{jk}}{\partial x_j} + \delta_l = 0$ for a isotropic homogenenous Kelvin
                solution for a point load in direction l.

                Solution $u^*_k = u^*_{lk} e_l$

                              $u^*_{lk} = \dfrac{1}{16\pi G\left(1-\nu\right)}\left(\dfrac{3-4\nu}{r}\delta_{lk} + \dfrac{\partial r}{\partial x_1}\dfrac{\partial r}{\partial x_2}\right)$
                for a displacement in direction k where ν is Poisson's
                ratio and G is the shear modulus.

3.16.3   Axisymmetric problems

Laplace   For u^* see Equation (3.47) and for q^* see Equation (3.51)

3.17   CMISS Examples

1. 2D steady-state heat conduction inside an annulus To determine the steady-state heat conduction inside an annulus run the CMISS example 324.

2. 3D steady-state heat conduction inside a sphere. To determine the steady-state heat conduction inside a sphere run the CMISS example 328.

3. CMISS comparison of 2-D FEM and BEM calculations To determine the CMISS comparison of 2-D FEM and BEM calculations run examples 324 and 312.

4. CMISS biopotential problems C4 and C5.

Chapter 4

Linear Elasticity

4.1 Introduction

To analyse the stress in various elastic bodies we calculate the strain energy of the body in terms of nodal displacements and then minimize the strain energy with respect to these parameters - a technique known as the Rayleigh-Ritz. In fact, as we will show later, this leads to the same algebraic equations as would be obtained by the Galerkin method (now equivalent to virtual work) but the physical assumptions made (in neglecting certain strain energy terms) are exposed more clearly in the Rayleigh-Ritz method. We will first consider one-dimensional truss and beam elements, then two-dimensional plane stress and plane strain elements, and finally three-dimensional elasticity.

In all cases the steps are:

1. Evaluate the components of strain in terms of nodal displacements,

2. Evaluate the components of stress from strain using the elastic material constants,

3. Evaluate the strain energy for each element by integrating the products of stress and strain components over the element volume,

4. Evaluate the potential energy from the sum of total strain energy for all elements together with the work done by applied boundary forces,

5. Apply the boundary conditions, *e.g.,* by fixing nodal displacements,

6. Minimize the potential energy with respect to the unconstrained nodal displacements,

7. Solve the resulting system of equations for the unconstrained nodal displacements,

8. Evaluate the stresses and strains using the nodal displacements and element basis functions,

9. Evaluate the boundary reaction forces (or moments) at the nodes where displacement is constrained.

4.2   Truss Elements

Consider the one-dimensional truss of undeformed length L in Figure 3.1 with end points $(0, 0)$ and (x, y) and making an angle θ with the x-axis. Under the action of forces in the x- and y-directions the right hand end of the truss displaces by u in the x-direction and v in the y-direction, relative to the left hand end.
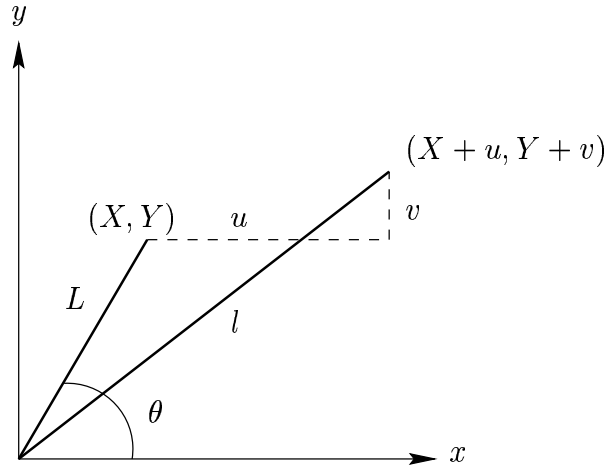
FIGURE 4.1: A truss of initial length L is stretched to a new length l. Displacements of the right hand end relative to the left hand end are u and v in the x- and y- directions, respectively.

The new length is l with axial strain

$$
\begin{aligned}
e = \frac{l}{L} - 1 &= \frac{\sqrt{(X + u)^2 + (Y + v)^2}}{\sqrt{X^2 + Y^2}} - 1 \\
&= \frac{\sqrt{L^2 + 2(Xu + Yv) + u^2 + v^2}}{L} - 1 \\
&= \sqrt{1 + 2\left(\cos\theta.\frac{u}{L} + \sin\theta.\frac{v}{L}\right) + \frac{u^2 + v^2}{L^2}} - 1
\end{aligned}
$$

using $\dfrac{X}{L} = \cos\theta$ and $\dfrac{Y}{L} = \sin\theta$, where θ is defined to be positive in the anticlockwise direction. Neglecting second order terms in the binomial expansion $\sqrt{(1 + \varepsilon)} = 1 + \dfrac{1}{2}\varepsilon + \mathrm{O}\left(\varepsilon^2\right)$, the strain for small displacements u and v is

$$
e \cong \cos\theta.\frac{u}{L} + \sin\theta.\frac{v}{L} \tag{4.1}
$$

The strain energy associated with this uniaxial stretch is

$$\text{SE} = \frac{1}{2}\int \sigma e \, dV = \frac{1}{2}A\int_0^L \sigma e \, dx = \frac{1}{2}\int_0^L EAe^2 \, dx = \frac{1}{2}ALEe^2 \qquad (4.2)$$

where $\sigma = Ee$ is the stress in the truss (of cross-sectional area A), linearly related to the strain e via Young's modulus E. We now substitute for e from Equation (4.1) into Equation (4.2) and put $u = u_2 - u_1$ and $v = v_2 - v_1$, where (u_1, v_1) and (u_2, v_2) are the nodal displacements of the two ends of the truss

$$\text{SE} = \frac{1}{2}ALE\left(\cos\theta . \frac{u_2 - u_1}{L} + \sin\theta . \frac{v_2 - v_1}{L}\right)^2 \qquad (4.3)$$

The potential energy is the combined strain energy from all trusses in the structure minus the work done on the structure by external forces. The Rayleigh-Ritz approach is to minimize this potential energy with respect to the nodal displacements once all displacement boundary conditions have been applied.

For example, consider the system of three trusses shown in Figure 4.2. A force of 100 kN is applied in the x-direction at node 1. Node 2 is a sliding joint and has zero displacement in the y-direction only. Node 3 is a pivot and therefore has zero displacement in both x- and y- directions. The problem is to find all nodal displacements and the stress in the three trusses.
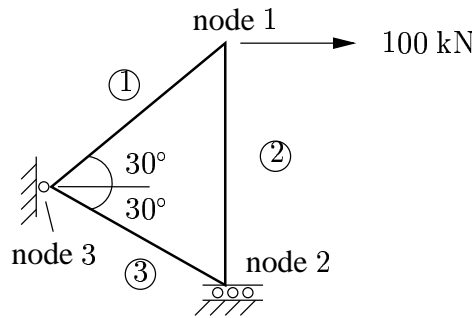
FIGURE 4.2: A system of three trusses.

The strain in truss 1 (joining nodes 1 and 3) is

$$\frac{u_1}{L}\cos 30 + \frac{v_1}{L}\sin 30 = \frac{\sqrt{3}}{2}\frac{u_1}{L} + \frac{1}{2}\frac{v_1}{L}$$

The strain in truss 2 (joining nodes 1 and 2) is

$$\frac{(u_1 - u_2)}{L}\cos 90 + \frac{v_1}{L}\sin 90 = \frac{v_1}{L}$$

The strain in truss 3 (joining nodes 2 and 3) is

$$\frac{u_2}{L}\cos(-30) = \frac{\sqrt{3}}{2}\frac{u_2}{L}$$

Since a force of 100 kN acts at node 1 in the x-direction, the potential energy is

$$\text{PE} = \sum_{\text{trusses}} \frac{1}{2}ALEe^2 - 100u_1 = \frac{1}{2}\frac{AE}{L}\left[\left(\frac{\sqrt{3}}{2}u_1 + \frac{1}{2}v_1\right)^2 + \left(\frac{\sqrt{3}}{2}u_2\right)^2 + (v_1)^2\right] - 100u_1$$

[Note that if the force was applied in the negative x-direction, the final term would be $+100u_1$]

Minimizing the potential energy with respect to the three unknowns u_1, v_1 and u_2 gives

$$\frac{\partial \text{PE}}{\partial u_1} = \frac{AE}{L}\left(\frac{\sqrt{3}}{2}u_1 + \frac{1}{2}v_1\right)\frac{\sqrt{3}}{2} - 100 = 0 \tag{4.4}$$

$$\frac{\partial \text{PE}}{\partial v_1} = \frac{AE}{L}\left[\left(\frac{\sqrt{3}}{2}u_1 + \frac{1}{2}v_1\right)\frac{1}{2} + v_1\right] = 0 \tag{4.5}$$

$$\frac{\partial \text{PE}}{\partial u_2} = \frac{AE}{L}\left(\frac{\sqrt{3}}{2}u_2\right)\frac{\sqrt{3}}{2} = 0 \tag{4.6}$$

If we choose $A = 5 \times 10^{-3}$ m^2, $E = 10$ GPa and $L = 1$ m (*e.g.*, 100 mm $\times$ 50 mm timber truss) then $\frac{AE}{L} = 5 \times 10^{-3}$ m^2 $\times 10^7$ kPa/m $= 5 \times 10^4$ kN m^{-1}.

Equation (4.6) gives

$$u_2 = 0$$

Equation (4.4) gives

$$3u_1 + \sqrt{3}v_1 = 4 \times 10^2 / \left(5 \times 10^4\right)$$

Equation (4.5) gives for two dimensions

$$v_1 = -\frac{\sqrt{3}}{5}u_1$$

Solving these last two equations gives $u_1 = 3.34$ mm and $v_1 = -1.15$ mm. Thus the strain in truss 1 is $(\frac{\sqrt{3}}{2}3.34 - \frac{1}{2}1.15) \times 10^{-3} = 0.232\%$, in truss 2 is -0.115% and in truss 3 is zero.

The tension in truss 1 is $A\sigma = AEe = 5 \times 10^{-3}$ m$^2 10^7$ kPa $\times 0.232 \times 10^{-2} = 116$ kN (tensile), in truss 2 is -57.5 kN (compressive) and in truss 3 is zero. The nodal reaction forces are shown in Figure 4.3.
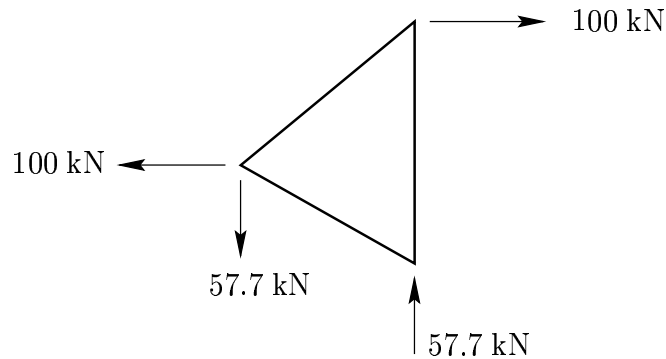
FIGURE 4.3: Reaction forces for the truss system of Figure 4.2.

4.3 Beam Elements

Simple beam theory ignores all but axial strain e_x and stress $\sigma_x = E e_x$ (E = Young's modulus) along the beam (assumed here to be in the x-direction). The axial strain is given by $e_x = \dfrac{z}{R}$, where z is the lateral distance from the neutral axis in the plane of the bending and R is the radius of curvature in that plane. The bending moment is given by $M = \displaystyle\int \sigma_x z \, dA$, where A is the beam crosssectional area. Thus

$$\sigma_x = E e_x = E \frac{z}{R} \tag{4.7}$$

$$M = \int \sigma_x z \, dA = \frac{E}{R} \int z^2 \, dA = \frac{EI}{R} \tag{4.8}$$

where $I = \displaystyle\int z^2 \, dA$ is the second moment of area of the beam cross-section. Thus, $\dfrac{E}{R} = \dfrac{M}{I}$ and Equation (4.7) becomes

$$\sigma_x = \frac{Mz}{I} \tag{4.9}$$

The slope of the beam is $\dfrac{dw}{dx} = \theta$ and the rate of change of slope is the curvature

$$K = \frac{d\theta}{dx} = \frac{d^2 w}{dx^2} = \frac{1}{R} \tag{4.10}$$

Thus the bending moment is

$$M = EI\frac{d^2 w}{dx^2} = EIw'' \tag{4.11}$$

and a force balance gives the shear force

$$V = -\frac{dM}{dx} = -\frac{d}{dx}\left(EIw''\right) \tag{4.12}$$

and the normal force (per unit length of beam)

$$p = \frac{dV}{dx} = -\frac{d^2}{dx^2}\left(EIw''\right) \tag{4.13}$$

This last equation is the equilibrium equation for the beam, balancing the loading forces p with the axial stresses associated with beam flexure

$$-\frac{d^2}{dx^2}\left(EI\frac{d^2 w}{dx^2}\right) = p \tag{4.14}$$

The elastic strain energy stored in a bent beam is the sum of flexural strain energy and shear strain energy, but this latter is ignored in the simple beam theory considered here. Thus, the (flexural) strain energy is

$$\begin{aligned}
\text{SE} &= \frac{1}{2}\int_{x=0}^{L}\int_{A}\sigma_x e_x\, dA\, dx = \frac{1}{2}\int_{x=0}^{L} E\int_{A} e_x^2\, dA\, dx \\
&= \frac{1}{2}\int_{x=0}^{L} E\int_{A}\left(\frac{z}{R}\right)^2\, dA\, dx = \frac{1}{2}\int_{x=0}^{L} EI\left(w''\right)^2\, dx
\end{aligned}$$

where x is taken along the beam and A is the cross-sectional area of the beam.

The external work associated with forces p acting normal to the beam and moving through a transverse displacement w is $\int_{0}^{L} pw\, dx$. The potential energy is therefore

$$\text{PE} = \frac{1}{2}\int_{0}^{L} EI\left(w''\right)^2\, dx - \int_{0}^{L} pw\, dx. \tag{4.15}$$

The finite element approximation for the transverse displacement w must be able to represent the second derivative w''. A linear basis function has a zero second derivative and therefore cannot represent the flexural strain. The natural choice of basis function for beam deflection is in fact cubic Hermite because the inter-element slope continuity of this basis ensures transmission of bending moment as well as shear force across element boundaries.

The boundary conditions associated with the 4th order equilibrium Equation (4.14) or the equa-

tions arising from minimum potential energy Equation (4.15) (which contain the square of 2nd derivative terms) are more complex than the simple temperature or flux boundary conditions for the (second order) heat equation. Three possible combinations of boundary condition with their associated reactions are

		Boundary conditions	*Reactions*
(i)	Simply supported	zero displacement $w = 0$	shear force V
		zero moment $M = EIw'' = 0$	slope $\theta(= w')$
(ii)	Cantilever	zero displacement $w = 0$	shear force V
		zero slope $\theta = w' = 0$	moment M
(iii)	Free end	zero shear force $V = -\dfrac{d}{dx}(EIw'') = 0$	displacement w
		zero moment $M = EI'' = 0$	slope θ

4.4 Plane Stress Elements

For two-dimensional problems, we define the displacement vector $\boldsymbol{u} = \begin{bmatrix} u \\ v \end{bmatrix}$, strain vector $\boldsymbol{e} = \begin{bmatrix} e_x \\ e_y \\ e_{xy} \end{bmatrix}$ and stress vector $\boldsymbol{\sigma} = \begin{bmatrix} \sigma_x \\ \sigma_y \\ \sigma_{xy} \end{bmatrix}$. The stress-strain relation for two-dimensional plane stress:

$$\sigma_x = \frac{E}{1 - \nu^2}(e_x + \nu e_y)$$
$$\sigma_y = \frac{E}{1 - \nu^2}(e_y + \nu e_x) \qquad (4.16)$$
$$\sigma_{xy} = \frac{E}{1 + \nu}(e_{xy})$$

can be written in matrix form

$$\boldsymbol{\sigma} = \boldsymbol{E}\boldsymbol{e}$$

where $\boldsymbol{E} = \dfrac{E}{1 - \nu^2}\begin{bmatrix} 1 & \nu & 0 \\ \nu & 1 & 0 \\ 0 & 0 & 1 - \nu \end{bmatrix}$. The strain components are given in terms of displacement gradients by

$$\begin{aligned} e_x &= \frac{\partial u}{\partial x} \\ e_y &= \frac{\partial v}{\partial y} \\ e_{xy} &= \frac{1}{2}\left(\frac{\partial u}{\partial y} + \frac{\partial v}{\partial x}\right) \end{aligned} \qquad (4.17)$$

The strain energy is

$$\text{SE} = \frac{1}{2}\int_V \boldsymbol{\sigma}^T \boldsymbol{e}\, dV = \frac{1}{2}\int_V \left(e_x\sigma_x + e_y\sigma_y + e_{xy}\sigma_{xy}\right)\, dV$$

$$= \frac{1}{2}\int_V \boldsymbol{e}^T \boldsymbol{E}\boldsymbol{e}\, dV = \frac{1}{2}\int_V \frac{E}{1-\nu^2}\left[e_x^2 + e_y^2 + 2\nu e_x e_y + (1-\nu)\,e_{xy}^2\right]\, dV$$

The potential energy is

$$\text{PE} = \text{SE} - \text{ external work } = \frac{1}{2}\int_V \boldsymbol{e}^T \boldsymbol{E}\boldsymbol{e}\, dV - \int_A \boldsymbol{u}^T l\, dA \tag{4.18}$$

where l represents the external loads (forces) acting on the elastic body.

Following the steps outlined in Section 4.1 we approximate the displacement field $\boldsymbol{u}$ with a finite element basis $u = \varphi_n u_n$, $v = \varphi_n v_n$ and calculate the strains

$$\begin{aligned}
e_x &= \frac{\partial u}{\partial x} = \frac{\partial \varphi_n}{\partial x}u_n \\
e_y &= \frac{\partial v}{\partial y} = \frac{\partial \varphi_n}{\partial y}v_n \\
e_{xy} &= \frac{1}{2}\left(\frac{\partial u}{\partial y} + \frac{\partial v}{\partial x}\right) = \frac{1}{2}\left(\frac{\partial \varphi_n}{\partial y}u_n + \frac{\partial \varphi_n}{\partial x}v_n\right)
\end{aligned} \tag{4.19}$$

or

$$\boldsymbol{e} = \begin{bmatrix} e_x \\ e_y \\ e_{xy} \end{bmatrix} = \begin{bmatrix} \dfrac{\partial \varphi_n}{\partial x} & 0 \\ 0 & \dfrac{\partial \varphi_n}{\partial y} \\ \dfrac{1}{2}\dfrac{\partial \varphi_n}{\partial y} & \dfrac{1}{2}\dfrac{\partial \varphi_n}{\partial x} \end{bmatrix} \begin{bmatrix} u_n \\ v_n \end{bmatrix} = \boldsymbol{B}\boldsymbol{u} \tag{4.20}$$

From Equation (4.18) the potential energy is therefore

$$\text{PE} = \frac{1}{2}\int_V (\boldsymbol{B}\boldsymbol{u})^T \boldsymbol{E}\,(\boldsymbol{B}\boldsymbol{u})\, dV - \int_A \boldsymbol{u}^T l\, dA$$

$$= \frac{1}{2}\boldsymbol{u}^T \int_V \boldsymbol{B}^T \boldsymbol{E}\boldsymbol{B}\, dV.\boldsymbol{u} - \int_A \boldsymbol{u}^T l\, dA$$

$$= \frac{1}{2}\boldsymbol{u}^T \boldsymbol{K}\boldsymbol{u} - \int_A \boldsymbol{u}^T l\, dA$$

where $\boldsymbol{K} = \displaystyle\int_V \boldsymbol{B}^T \boldsymbol{E} \boldsymbol{B} \, dV$ is the element stiffness matrix.

We next minimize the potential energy with respect to the nodal parameters u_n and v_n giving

$$\boldsymbol{K u} = \boldsymbol{f} \tag{4.21}$$

where $\boldsymbol{f} = \displaystyle\int_A \boldsymbol{l} \, dA$ is a vector of nodal forces.

4.4.1 Notes on calculating nodal loads

If a known stress acts normal to a given surface (*e.g.,* a surface pressure), it may be applied by calculating equivalent nodal forces. For example, consider a uniform load p kN m^{-1} applied to the edge of the plane stress element in Figure 4.4a.

The nodal load vector $\boldsymbol{f}$ in Equation (4.21) has components

$$f_n = \int_x p\varphi_n \, dx = pL \int_0^1 \varphi_n \, d\xi \tag{4.22}$$

where ξ is the normalized element coordinate along the side of length L loaded by the constant stress p kN m^{-1}. If the element side has a linear basis, Equation (4.22) gives

$$f_1 = pL \int_0^1 \varphi_1 \, d\xi = pL \int_0^1 (1 - \xi) \, d\xi = \frac{1}{2}pL$$

$$f_2 = pL \int_0^1 \varphi_2 \, d\xi = pL \int_0^1 \xi \, d\xi = \frac{1}{2}pL$$

as shown in Figure 4.4b. If the element side has a quadratic basis, Equation (4.22) gives

$$f_1 = pL \int_0^1 \varphi_1 \, d\xi = pL \int_0^1 2 \left(\frac{1}{2} - \xi \right) (1 - \xi) \, d\xi = \frac{1}{6}pL$$

$$f_2 = pL \int_0^1 \varphi_2 \, d\xi = pL \int_0^1 4\xi (1 - \xi) \, d\xi = \frac{2}{3}pL$$

$$f_3 = pL \int_0^1 \varphi_3 \, d\xi = pL \int_0^1 2\xi \left(\xi - \frac{1}{2} \right) \, d\xi = \frac{1}{6}pL$$

as shown in Figure 4.4c. A node common to two elements will receive contributions from both elements, as shown in Figure 4.4d.
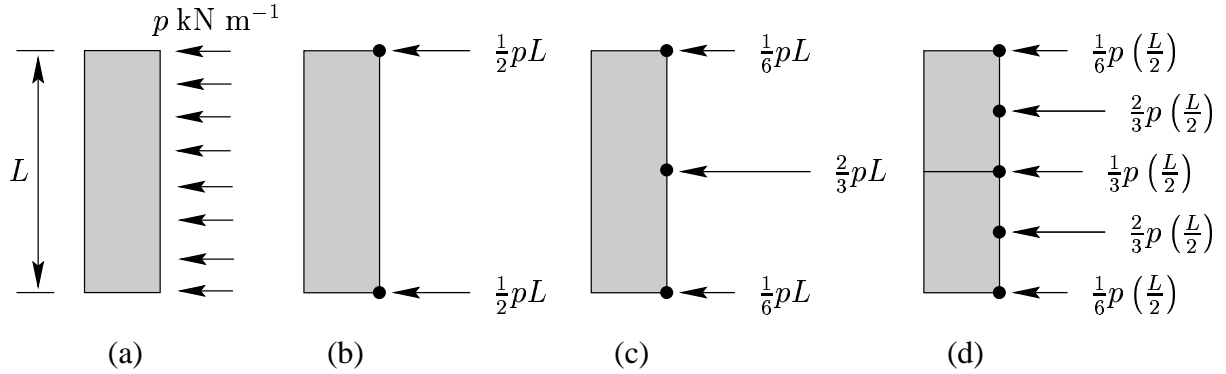
FIGURE 4.4: A uniform boundary stress applied to the element side in (a) is equivalent to nodal loads of $\frac{1}{2}pL$ and $\frac{1}{2}pL$ for the linear basis used in (b) and to $\frac{1}{6}pL$, $\frac{2}{3}pL$ and $\frac{1}{6}pL$ for the quadratic basis used in (c). Two adjacent quadratic elements both contribute to a common node in (d), where the element length is now $\frac{L}{2}$.

4.5   Three-Dimensional Elasticity

Consider a surface Γ enclosing a volume Ω of material of mass density ρ. Conservation of linear momentum over the domain Ω results in the governing equilibrium equations

$$\sigma_{ij,j} + b_i = 0 \qquad i,j = 1,2,3 \tag{4.23}$$

where σ_{ij} are the components of the stress tensor (σ_{ij} is the component of the traction or stress vector in the ith direction which is acting on the face of a rectangle whose normal is in the jth direction), and b_i is the body force/unit volume (*e.g.,* $\boldsymbol{b} = \rho\boldsymbol{g}$). Note that the notation $\sigma_{ij,j} = \dfrac{\partial \sigma_{ij}}{\partial x_j}$ has been introduced to represent the derivative.

Recall that the components of the linear (or small) strain tensor are

$$e_{ij} = \frac{1}{2}\left(u_{i,j} + u_{j,i}\right) \qquad i,j = 1,2,3 \tag{4.24}$$

where $\boldsymbol{u}$ is the displacement vector (*i.e.,* $\boldsymbol{u}$ is the difference between the final and initial positions of a material point in question). Note: we are assuming here that the displacement gradients are small compared to unity, which is appropriate for many materials in solid mechanics. However, for soft materials, such as rubber or biological tissue, then we need to use the exact finite strain tensor.

The object of solving an elasticity problem is to find the distributions of stress and displacement in an elastic body, subject to a known set of body forces and prescribed stresses or displacements at the boundaries. In the general three-dimensional case, this means finding 6 stress components σ_{ij} ($= \sigma_{ji}$ which arises from the conservation of angular momentum) and 3 displacements u_i each as a function of position in the body. Currently we have 15 unknowns (6 stresses, 6 strains and 3 displacements), but only 9 equations (3 equilibrium equations and 6 strain-displacement relations).

To progress, we require an equation of state, *i.e.,* a stress-strain relation or constitutive law. For a linear elastic material we may propose that the components of stress σ_{ij} depend linearly on e_{ij}.

i.e.,

$$\sigma_{ij} = c_{ijkl}e_{kl}$$

where c_{ijkl} are the 81 components of a 4th order tensor, although symmetry of the strain and stress tensors reduces the number of independent components to 21.

If the material is assumed to be isotropic (*i.e.,* the material response is independent of orientation of the material element), then we end up with the generalized Hooke's Law.

$$\sigma_{ij} = \lambda e_{kk}\delta_{ij} + 2\mu e_{ij} \tag{4.25}$$

or inversely

$$e_{ij} = \frac{1}{2\mu}\sigma_{ij} - \frac{\lambda}{2\mu\left(3\lambda + 2\mu\right)}\sigma_{kk}\delta_{ij}$$

where λ, μ are Lamés constants.

Note: λ, μ are related to Young's modules E and Poisson's ratio ν by

$$E = \frac{\mu\left(3\lambda + 2\mu\right)}{\lambda + \mu}$$

$$\nu = \frac{\lambda}{2\left(\lambda + \mu\right)}$$

Providing that the displacements are continuous functions of position, then Equation (4.23), Equation (4.24) and Equation (4.25) are sufficient to determine the 15 unknown quantities. This can often work with some smaller grouping or simplification of these equations, *e.g.,* if all boundary conditions are expressed in terms of displacements, substituting Equation (4.24) into Equation (4.25) then into Equation (4.23) yields Navier's equation of motion.

$$\mu u_{i,kk} + \left(\lambda + \mu\right)u_{k,ki} + b_i = 0 \qquad i, k = 1, 2, 3$$

These 3 equations can be solved for the unknown displacements. Then Equation (4.24) can be used to determine the strains and Equation (4.25) to calculate the stresses.

4.5.1 Weighted Residual Integral Equation

Using weighted residuals as before we can write

$$\int\limits_{\Omega} \left(\sigma_{ij,j} + b_i\right)u_i^* \, d\Omega = 0 \tag{4.26}$$

where $\boldsymbol{u}^* = (u_i^*)$ is a (vector) weighting field. The u_i^* are usually interpreted as a consistent set of virtual displacements (hence we use the notation u instead of w).

By the chain-rule

$$\left(\sigma_{ij}u_i^*\right)_{,j} = \sigma_{ij,j}u_i^* + \sigma_{ij}u_{i,j}^*$$

Therefore, the first term in the integrand of Equation (4.26) can be re-written

$$\int_\Omega \sigma_{ij,j}u_i^* \, d\Omega = \int_\Omega \left(\sigma_{ij}u_i^*\right)_{,j} \, d\Omega - \int_\Omega \sigma_{ij}u_{i,j}^* \, d\Omega$$

$$= \int_\Omega \nabla \cdot \left(\sigma_{ij}u_i^*\right) \, d\Omega - \int_\Omega \sigma_{ij}u_{i,j}^* \, d\Omega$$

$$= \int_{\partial\Omega} \sigma_{ij}u_i^* n_j \, d\Gamma - \int_\Omega \sigma_{ij}u_{i,j}^* \, d\Omega \qquad (4.27)$$

where the domain integral involving "$\nabla \cdot \ = \dfrac{\partial}{\partial x_j}$" has been transformed into a surface integral using the divergence theorem

$$\int_\Omega \nabla \cdot \boldsymbol{g} \, d\Omega = \int_{\partial\Omega} \boldsymbol{g} \cdot \boldsymbol{n} \, d\Gamma \qquad \text{or} \qquad \int_\Omega g_{j,j} \, d\Omega = \int_{\partial\Omega} g_j n_j \, d\Gamma$$

where $\boldsymbol{n} = n_j \boldsymbol{i}_j$ is the outward normal vector to the surface Γ.

Thus, combining Equation (4.26) and Equation (4.27) we have

$$\int_\Omega \sigma_{ij}u_{i,j}^* \, d\Omega = \int_\Omega b_i u_i^* \, d\Omega + \int_{\partial\Omega} \sigma_{ij}n_j u_i^* \, d\Gamma$$

$$= \int_\Omega b_i u_i^* \, d\Omega + \int_{\partial\Omega} t_i u_i^* \, d\Gamma \qquad (4.28)$$

where t_i are the components of the internal stress vector ($\boldsymbol{t}$) and are related to the components of the stress tensor (σ_{ij}) by Cauchy's formula

$$\boldsymbol{t} = \sigma_{ij}n_j \boldsymbol{i}_i \qquad (4.29)$$

To arrive at this point, we have used weighted residuals to tie in with Chapter 2, however Equation (4.28) is more usually derived using the principle of virtual work (below). Note that the weighted integral Equation (4.28) is independent of the constitutive law of the material.

4.5.2 The Principle of Virtual Work

The governing equations for elastostatics can also be derived from a physically appealing argument. Let $\boldsymbol{s}$ be the external traction vector (*i.e.,* force per unit surface area). For equilibrium, the work done by the external surface forces $\boldsymbol{s} = s_i \boldsymbol{i}_i$, in moving through a virtual displacement $\boldsymbol{u}^* = u_i^* \boldsymbol{i}_i$

is equal to the work done by the stress vector $\boldsymbol{t} = t_i \boldsymbol{i}_i$ in moving through a compatible set of virtual displacements $\boldsymbol{u}^*$. In mathematical terms, the principle of virtual work can be written

$$\int\limits_{\partial\Omega} s_i u_i^* \, d\Gamma = \int\limits_{\partial\Omega} t_i u_i^* \, d\Gamma = \int\limits_{\partial\Omega} \sigma_{ij} n_j u_i^* \, d\Gamma \tag{4.30}$$

using Cauchy's formula (Equation (4.29)).

The Green-Gauss theorem (Equation (2.15)) is now used to replace the right hand surface integral in Equation (4.30) by a volume integral, giving

$$\int\limits_{\partial\Omega} s_i u_i^* \, d\Gamma = \int\limits_{\Omega} \left(\sigma_{ij,j} u_i^* + \sigma_{ij} u_{i,j}^* \right) \, d\Omega \tag{4.31}$$

Substituting the equilibrium relation (Equation (4.23)) into the first integrand on the right hand side, yields the *virtual work* equation

$$\int\limits_{\Omega} \sigma_{ij} u_{i,j}^* \, d\Omega = \int\limits_{\Omega} b_i u_i^* \, d\Omega + \int\limits_{\partial\Omega} s_i u_i^* \, d\Gamma \tag{4.32}$$

where the internal work done due to the stress field is equated to the work due to internal body forces and external surface forces. Note that Equation (4.32) is equivalent to Equation (4.28) via Equation (4.30). In practice, Equation (4.32) is in a more useful form than Equation (4.28), because the right hand side integrals can be expressed in terms of the known body forces and the applied boundary conditions (surface traction forces or stresses).

4.5.3   The Finite Element Approximation

Let $\Omega = \bigcup \Omega_e$ and interpolate the virtual displacements u_i^* from their nodal values. *i.e.,*

$$
\begin{aligned}
u_i^* &= \varphi_m (u_i^m)^* \\
\text{so} \quad u_{i,j}^* &= \frac{\partial \varphi_m}{\partial x_j} (u_i^m)^* \\
&= \varphi_{m,k} \frac{\partial \xi_k}{\partial x_j} (u_i^m)^*
\end{aligned}
\tag{4.33}
$$

where $(u_i^m)^* = (U_i^{\triangle(m,e)})^*$, $\triangle(m,e)$ is the global node number of local node m on element e, and the shorthand $\varphi_{m,k} = \dfrac{\partial \varphi_m}{\partial \xi_k}$ has been introduced.

Substituting this into Equation (4.32) gives

$$\sum_e \left(\int\limits_{\Omega_e} \sigma_{ij} \varphi_{m,k} \frac{\partial \xi_k}{\partial x_j} \, d\Omega \right) \left(U_i^{\triangle(m,e)} \right)^* = \sum_e \left(\int\limits_{\Omega_e} b_i \varphi_m \, d\Omega + \int\limits_{\partial\Omega_e} s_i \varphi_m \, d\Gamma \right) \left(U_i^{\triangle(m,e)} \right)^*$$

and since the virtual displacements are arbitrary we get

$$\sum_e \int_{\Omega_e} \sigma_{ij} \varphi_{m,k} \frac{\partial \xi_k}{\partial x_j} \, d\Omega = \sum_e \left(\int_{\Omega_e} b_i \varphi_m \, d\Omega + \int_{\partial \Omega_e} s_i \varphi_m \, d\Gamma \right) \tag{4.34}$$

The next step is to express the stress components σ_{ij} in terms of the virtual displacements and their finite element approximation by substituting Equation (4.33) into Equation (4.24) (the strain-displacement relation) and in turn into Equation (4.25) (the generalized Hooke's law).

We first introduce the finite element approximation for the displacement field $u_j = \varphi_n u_j^n$ which gives

$$e_{ij} = \frac{1}{2} \left(\frac{\partial}{\partial x_j} \left(\varphi_n u_i^n \right) + \frac{\partial}{\partial x_i} \left(\varphi_n u_j^n \right) \right) = \frac{1}{2} \left(\frac{\partial \varphi_n}{\partial \xi_l} \frac{\partial \xi_l}{\partial x_j} u_i^n + \frac{\partial \varphi_n}{\partial \xi_l} \frac{\partial \xi_l}{\partial x_i} u_j^n \right) \tag{4.35}$$

and

$$e_{kk} = u_{k,k} = \frac{\partial \varphi_n}{\partial \xi_l} \frac{\partial \xi_l}{\partial x_k} u_k^n$$

Thus

$$\sigma_{ij} = \lambda \delta_{ij} \frac{\partial \varphi_n}{\partial \xi_l} \frac{\partial \xi_l}{\partial x_k} u_k^n + 2\mu \left(\frac{1}{2} \frac{\partial \varphi_n}{\partial \xi_l} \frac{\partial \xi_l}{\partial x_j} u_i^n + \frac{1}{2} \frac{\partial \varphi_n}{\partial \xi_l} \frac{\partial \xi_l}{\partial x_i} u_j^n \right)$$

which, due to symmetry of the stress tensor, simplifies to

$$\sigma_{ij} = \lambda \delta_{ij} \frac{\partial \varphi_n}{\partial \xi_l} \frac{\partial \xi_l}{\partial x_k} u_k^n + 2\mu \frac{\partial \varphi_n}{\partial \xi_l} \frac{\partial \xi_l}{\partial x_i} u_j^n$$
$$= \left(\lambda \delta_{i(j)} \varphi_{n,l} \frac{\partial \xi_l}{\partial x_j} + 2\mu \varphi_{n,l} \frac{\partial \xi_l}{\partial x_i} \right) u_j^n \tag{4.36}$$

where the summation index k has been replaced with j, but the parenthesis in $\delta_{i(j)}$ implies that there is no sum with respect to that particular index.

Substituting this expression into Equation (4.34) and simplifying, we get for each element

$$u_j^n \int_{\Omega_e} \left(\lambda \varphi_{n,l} \frac{\partial \xi_l}{\partial x_j} \varphi_{m,k} \frac{\partial \xi_k}{\partial x_i} + 2\mu \varphi_{n,l} \frac{\partial \xi_l}{\partial x_i} \varphi_{m,k} \frac{\partial \xi_k}{\partial x_j} \right) d\Omega = f_{im} \tag{4.37}$$

where f_{im} denotes the right hand side terms in Equation (4.34). (Note that there has been some careful manipulation of summation indices with the substitution of Equation (4.36) to arrive at Equation (4.37).)

So for each element

$$E_{imjn} u_j^n = f_{im}$$

where

$$
E_{imjn} = \iiint\limits_{0}^{1} \left(\lambda \frac{\partial \xi_l}{\partial x_j} \frac{\partial \xi_k}{\partial x_i} + 2\mu \frac{\partial \xi_l}{\partial x_i} \frac{\partial \xi_k}{\partial x_j} \right) \varphi_{n,l} \varphi_{m,k} J(\xi_1, \xi_2, \xi_3) d\xi_1 d\xi_2 d\xi_3
$$

$$
f_{im} = \iiint\limits_{0}^{1} b_i \varphi_m J(\xi_1, \xi_2, \xi_3) d\xi_1 d\xi_2 d\xi_3 + \iint\limits_{0}^{1} s_i \varphi_m J_{2D}(\xi_1, \xi_2) d\xi_1 d\xi_2
$$

(4.38)

where the Jacobians $J(\xi_1, \xi_2, \xi_3)$ and $J_{2D}(\xi_1, \xi_2)$ have been used to transform volume and surface integrals so that they can be can be calculated using ξ-coordinates. (Note: without loss of generality, the above definition of f_{im} assumes that (ξ_1, ξ_2) are defined to lie in the surface Γ.)

So in summary, the finite element approximation leads to element stiffness matrix components that can be calculated from the known material parameters, the chosen interpolation functions, and the geometry of the material (note that the element stiffness components are independent of the unknown displacement parameters). Element stiffness components are then assembled into the global stiffness matrix in the usual manner (as described previously). Note that this is implicitly a Galerkin formulation, since the unknown displacement fields are interpolated using the same basis functions as those used to weight the integral equations.

4.6   Linear Elasticity with Boundary Elements

Equation (4.28) is the starting point for the general finite element formulation (Section 4.5). In the above derivation, we have essentially used the Green-Gauss theorem once to move from Equation (4.26) to Equation (4.28) (as was done for the derivation of the FEM equation for Laplace's equation). To continue, we firstly note that

$$
\begin{aligned}
\sigma_{ij} e^*_{ij} &= \frac{1}{2}\sigma_{ij} u^*_{i,j} + \frac{1}{2}\sigma_{ij} u^*_{j,i} \\
&= \frac{1}{2}\sigma_{ij} u^*_{i,j} + \frac{1}{2}\sigma_{ji} u^*_{j,i} \\
&= \frac{1}{2}\sigma_{ij} u^*_{i,j} + \frac{1}{2}\sigma_{ij} u^*_{i,j} \\
&= \sigma_{ij} u^*_{i,j}
\end{aligned}
$$

where e^*_{ij} are the virtual strains corresponding to the virtual displacements.

Using the constitutive law for linearly elastic materials (Equation (4.25)) we have

$$\int_{\Omega} \sigma_{ij} u_{i,j}^* \, d\Omega = \int_{\Omega} \sigma_{ij} e_{ij}^* \, d\Omega$$

$$= \lambda \int_{\Omega} e_{kk} e_{ij}^* \delta_{ij} \, d\Omega + 2\mu \int_{\Omega} e_{ij} e_{ij}^* \, d\Omega$$

$$= \lambda \int_{\Omega} e_{kk} e_{kk}^* \, d\Omega + 2\mu \int_{\Omega} e_{ij} e_{ij}^* \, d\Omega$$

$$= \int_{\Omega} e_{ij} \sigma_{ij}^* \, d\Omega$$

due to symmetry.

Thus from the virtual work statement, Equation (4.28) and the above symmetry we have

$$\int_{\Omega} b_i u_i^* \, d\Omega + \int_{\partial\Omega} t_i u_i^* \, d\Gamma = \int_{\Omega} b_i^* u_i \, d\Omega + \int_{\partial\Omega} t_i^* u_i \, d\Gamma \qquad (4.39)$$

This is known as Betti's second reciprical work theorem or the Maxwell-Betti reciprocity relationship between two different elastic problems (the starred and unstarred variables) established on the same domain.

Note that $b_i^* = -\sigma_{ij,j}^*$ (*i.e.*, $\sigma_{ij,j}^* + b_i^* = 0$). Therefore Equation (4.39) can be written as

$$\int_{\Omega} \left(\sigma_{ij,j}^* \right) u_i \, d\Omega + \int_{\Omega} b_i u_i^* \, d\Omega = \int_{\partial\Omega} t_i^* u_i \, d\Gamma - \int_{\partial\Omega} t_i u_i^* \, d\Gamma \qquad (4.40)$$

($\sigma_{ij}^*, e_{ij}^*, t_i^*$ represents the equilibrium state corresponding to the virtual displacements u_i^*).

Note: What we have essentially done is use integration of parts to get Equation (4.28), then use it again to get Equation (4.39) above (after noting the reciprocity between σ_{ij} and e_{ij}).

Since the body forces, b_i, are known functions, the second domain integral on the left hand side of Equation (4.40) does not introduce any unknowns into the problem (more about this later). The first domain integral contains unknown displacements in Ω and it is this integral we wish to remove.

We choose the virtual displacements such that

$$\sigma_{ij,j}^* + e_i \delta = 0 \qquad (4.41)$$

(or equivalently $-b_i^* + e_i \delta = 0$), where e_i is the ith component of a unit vector in the ith direction and $e_i \delta = e_i \delta \left(\boldsymbol{x} - P \right)$. We can interpret this as the body force components which correspond to a positive unit point load applied at a point $P \in \Omega$ in each of the three orthogonal directions.

Therefore

$$\int_\Omega \sigma^*_{ij,j} u_i \, d\Omega = -\int_\Omega \delta\left(\boldsymbol{x} - P\right) e_i u_i \, d\Omega = -u_i(P)e_i$$

i.e., the volume integral is replaced with a point value (as for Laplace's equation).
Therefore, Equation (4.40) becomes

$$u_i\left(P\right) e_i = \int_{\partial\Omega} t_j u^*_j \, d\Gamma - \int_{\partial\Omega} t^*_j u_j \, d\Gamma + \int_\Omega b_j u^*_j \, d\Omega \qquad P \in \Omega \tag{4.42}$$

If each point load is taken to be independent then u^*_j and t^*_j can be written as

$$u^*_j = u^*_{ij}\left(P, x\right) e_i \tag{4.43}$$
$$t^*_j = t^*_{ij}\left(P, x\right) e_i \tag{4.44}$$

where $u^*_{ij}\left(P, x\right)$ and $t^*_{ij}\left(P, x\right)$ represent the displacements and tractions in the jth direction at x corresponding to a unit point force acting in the ith direction (e_i) applied at P. Substituting these into Equation (4.42) (and equating components in each e_i direction) yields

$$u_i\left(P\right) = \int_{\partial\Omega} u^*_{ij}\left(P, x\right) t_j\left(x\right) \, d\Gamma\left(x\right) - \int_{\partial\Omega} t^*_{ij}\left(P, x\right) u_j\left(x\right) \, d\Gamma\left(x\right)$$
$$+ \int_\Omega u^*_{ij}\left(P, x\right) b_j\left(x\right) \, d\Omega\left(x\right) \tag{4.45}$$

where $P \in \Omega$ (see later for $P \in \partial\Omega$).
This is known as Somigliana's [1] identity for displacement.

4.7 Fundamental Solutions

Recall from Equation (4.41) that σ^*_{ij} satisfied

$$\sigma^*_{ij,j} + \delta\left(\boldsymbol{x} - P\right) e_i = 0 \tag{4.46}$$

or equivalently

$$b^*_i = e_i \delta\left(\boldsymbol{x} - P\right)$$

Navier's equation for the displacements u^*_i is

$$G \, u^*_{i,kk} + \frac{G}{1 - 2\nu} u^*_{k,ki} + b^*_i = 0$$

---

[1]Somigliana was an Italian Mathematician who published this result around 1894-1902.

where G = shear Modulus.

Thus u_i^* satisfy

$$G\, u_{i,kk}^* + \frac{G}{1-2\nu} u_{k,ki}^* + \delta\left(\boldsymbol{x} - P\right) e_i = 0 \tag{4.47}$$

The solutions to the above equation in either two or three dimensions are known as Kelvin [2]'s fundamental solutions and are given by

$$u_{ij}^*\left(P, \boldsymbol{x}\right) = \frac{1}{16\pi\left(1-\nu\right)Gr}\left\{\left(3-4\nu\right)\delta_{ij} + r_{,i}r_{,j}\right\} \tag{4.48}$$

for three-dimensions and for two-dimensional plane strain problems,

$$u_{ij}^*\left(P, \boldsymbol{x}\right) = \frac{-1}{8\pi\left(1-\nu\right)G}\left\{\left(3-4\nu\right)\delta_{ij}\log r - r_{,i}r_{,j}\right\} \tag{4.49}$$

and

$$t_{ij}^*\left(P, \boldsymbol{x}\right) = \frac{-1}{4\alpha\pi\left(1-\nu\right)r^{\alpha}}\left\{\left(\left(1-2\nu\right)\delta_{ij} + \beta r_{,i}r_{,j}\right)\frac{\partial r}{\partial n} - \left(1-2\nu\right)\left(r_{,i}n_j - r_{,j}n_i\right)\right\} \tag{4.50}$$

where $\alpha = 1, 2;\ \beta = 2, 3$ for two-dimensional plane strain and three-dimensional problems respectively.

Here $r \equiv r\left(P, \boldsymbol{x}\right)$, the distance between load point (P) and field point $(\boldsymbol{x})$, $r_i = x_i\left(\boldsymbol{x}\right) - x_i\left(P\right)$ and $r_{,i} = \dfrac{\partial r}{\partial x_i\left(\boldsymbol{x}\right)} = \dfrac{r_i}{r}$.

In addition the strains at an point $\boldsymbol{x}$ due to a unit point load applied at P in the ith direction are given by

$$e_{jki}^*\left(P, \boldsymbol{x}\right) = \frac{-1}{8\alpha\pi\left(1-\nu\right)Gr^{\alpha}}\left\{\left(1-2\nu\right)\left(r_{,k}\delta_{ij} + r_{,j}\delta_{ik}\right) - r_{,i}\delta_{jk} + \beta r_{,i}r_{,j}r_{,k}\right\}$$

and the stresses are given by

$$\sigma_{ijk}^*\left(P, \boldsymbol{x}\right) = \frac{-1}{4\alpha\pi\left(1-\nu\right)r^{\alpha}}\left\{\left(1-2\nu\right)\left(r_{,k}\delta_{ij} + r_{,j}\delta_{ki} - r_{,i}\delta_{jk}\right) + \beta r_{,i}r_{,j}r_{,k}\right\}$$

where α and β are defined above.

The plane strain expressions are valid for plane stress if ν is replaced by $\overline{\nu} = \dfrac{\nu}{1+\nu}$ (This is a mathematical equivalence of plane stress and plane strain - there are obviously physical differences. What the mathematical equivalence allows us to do is to use one program to solve both types of problems - all we have to do is modify the values of the elastic constants).

Note that in three dimensions

$$u_{ij}^* = \mathrm{O}\left(\frac{1}{r}\right) \qquad t_{ij}^* = \mathrm{O}\left(\frac{1}{r^2}\right)$$

---

[2]Lord Kelvin (1824-1907) Scottish physicist who made great contributions to the science of thermodynamics

and for two dimensions

$$u_{ij}^* = \mathrm{O}\left(\log r\right) \qquad t_{ij}^* = \mathrm{O}\left(\frac{1}{r}\right).$$

Somigliana's identity (Equation (4.45)) is a continuous representation of displacements at any point $P \in \Omega$. Consequently, one can find the stress at any $P \in \Omega$ firstly by combining derivatives of (4.45) to produce the strains and then substituting into Hooke's law. Details can be found in Brebbia, Telles & Wrobel (1984b) pp 190–191, 255–258.

This yields

$$\sigma_{ij}\left(P\right) = \int_{\Gamma} u_{ijk}^*\left(P, \boldsymbol{x}\right) t_k\left(\boldsymbol{x}\right)\, d\Gamma\left(\boldsymbol{x}\right) - \int_{\Gamma} t_{ijk}^*\left(P, \boldsymbol{x}\right) u_k\left(\boldsymbol{x}\right)\, d\Gamma\left(\boldsymbol{x}\right)$$

$$+ \int_{\Omega} u_{ijk}^*\left(P, \boldsymbol{x}\right) b_k\left(\boldsymbol{x}\right)\, d\Omega\left(\boldsymbol{x}\right)$$

Note: One can find internal stress via numerical differentiation as in FE/FD but these are not as accurate as the above expressions.

Expressions for the new tensors u_{ijk}^* and t_{ijk}^* are on page 191 in (Brebbia et al. 1984b).

4.8 Boundary Integral Equation

Just as we did for Laplace's equation we need to consider the limiting case of Equation (4.45) as P is moved to $\partial\Omega$. (*i.e.,* we need to find the equivalent of $c\left(P\right)$ (in section 3) - called here $c_{ij}\left(P\right)$.) We use the same procedure as for Laplace's equation but here things are not so easy.

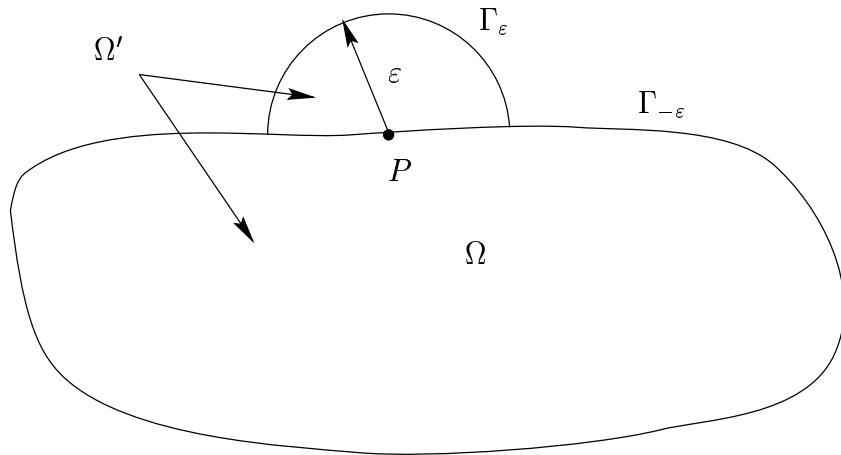If $P \in \partial\Omega$ we enlarge Ω to Ω' as shown.

FIGURE 4.5: Illustration of enlarged domain when singular point is on the boundary.

Then Equation (4.45) can be written as

$$u_i\left(P\right) = \int\limits_{\Gamma_{-\varepsilon}+\Gamma_\varepsilon} u_{ij}^*\left(P, \boldsymbol{x}\right) t_j\left(\boldsymbol{x}\right) d\Gamma\left(\boldsymbol{x}\right) - \int\limits_{\Gamma_{-\varepsilon}+\Gamma_\varepsilon} t_{ij}^*\left(P, \boldsymbol{x}\right) u_j\left(\boldsymbol{x}\right) d\Gamma\left(\boldsymbol{x}\right)$$

$$+ \int\limits_{\Omega'} u_{ij}^*\left(P, \boldsymbol{x}\right) b_j\left(\boldsymbol{x}\right) d\Omega\left(\boldsymbol{x}\right) \quad (4.51)$$

We need to look at each integral in turn as $\varepsilon \!\downarrow\! 0$ (*i.e.*, $\varepsilon \to 0$ from above). The only integral that presents a problem is the second integral. This can be written as

$$\int\limits_{\Gamma_{-\varepsilon}+\Gamma_\varepsilon} t_{ij}^*\left(P, \boldsymbol{x}\right) u_j\left(\boldsymbol{x}\right) d\Gamma\left(\boldsymbol{x}\right) = \int\limits_{\Gamma_\varepsilon} t_{ij}^*\left(P, \boldsymbol{x}\right) u_j\left(\boldsymbol{x}\right) d\Gamma\left(\boldsymbol{x}\right)$$

$$+ \int\limits_{\Gamma_{-\varepsilon}} t_{ij}^*\left(P, \boldsymbol{x}\right) u_j\left(\boldsymbol{x}\right) d\Gamma\left(\boldsymbol{x}\right) \quad (4.52)$$

The first integral on the right hand side can be written as

$$\int\limits_{\Gamma_\varepsilon} t_{ij}^*\left(P, \boldsymbol{x}\right) u_j\left(\boldsymbol{x}\right) d\Gamma\left(\boldsymbol{x}\right) = \underbrace{\int\limits_{\Gamma_\varepsilon} t_{ij}^*\left(P, \boldsymbol{x}\right) \left[u_j\left(\boldsymbol{x}\right) - u_j\left(P\right)\right] d\Gamma(x)}_{0 \text{ by continuity of } u_j\left(x\right)}$$

$$+ u_j\left(P\right) \int\limits_{\Gamma_\varepsilon} t_{ij}^*\left(P, \boldsymbol{x}\right) d\Gamma\left(\boldsymbol{x}\right) \quad (4.53)$$

Let

$$c_{ij}\left(P\right) = \delta_{ij} + \lim_{\varepsilon\downarrow 0} \int\limits_{\Gamma_\varepsilon} t_{ij}^*\left(P, \boldsymbol{x}\right) d\Gamma\left(\boldsymbol{x}\right) \quad (4.54)$$

As $\varepsilon \!\downarrow\! 0$, $\Gamma_{-\varepsilon} \to \Gamma$ and we write the second integral of Equation (4.52) as $\int\limits_{\Gamma} t_{ij}^*\left(P, \boldsymbol{x}\right) u_j\left(\boldsymbol{x}\right) d\Gamma\left(\boldsymbol{x}\right)$ where we interpret this in the Cauchy Principal Value[3] sense.

---

[3]What is a Cauchy Principle Value?

Consider $f\left(x\right) = \dfrac{1}{x}$ on $\Gamma_{-\varepsilon} = [-2, -\varepsilon) \cup (\varepsilon, 2]$

Thus as $\varepsilon \downarrow 0$ we get the boundary integral equation

$$c_{ij}(P) u_j(P) + \int_{\Gamma} t_{ij}^*(P, \boldsymbol{x}) u_j(\boldsymbol{x}) \, d\Gamma(\boldsymbol{x})$$

$$= \int_{\Gamma} u_{ij}^*(P, \boldsymbol{x}) t_j(\boldsymbol{x}) \, d\Gamma(\boldsymbol{x}) + \int_{\Omega} u_{ij}^*(P, \boldsymbol{x}) b_j(\boldsymbol{x}) \, d\Omega \quad (4.55)$$

(or, in brief (no body force), $c_{ij} u_j + \int_{\Gamma} t_{ij}^* u_j \, d\Gamma = \int_{\Gamma} u_{ij}^* t_j \, d\Gamma$) where the integral on the left hand side is interpreted in the Cauchy Principal sense. In practical applications c_{ij} and the principal value integral can be found indirectly from using Equation (4.55) to represent rigid-body movements.

The numerical implementation of Equation (4.55) is similar to the numerical implementation of an elliptic equation (*e.g.,* Laplace's Equation). However, whereas with Laplace's equation the unknowns were u and $\dfrac{\partial u}{\partial n}$ (scalar quantities) here the unknowns are vector quantities. Thus it is more convenient to work with matrices instead of indicial notation.
i.e., use

$$\boldsymbol{u} = \begin{bmatrix} u_1 \\ u_2 \\ u_3 \end{bmatrix}, \qquad \boldsymbol{t} = \begin{bmatrix} t_1 \\ t_2 \\ t_3 \end{bmatrix}$$

$$\boldsymbol{u}^* = \begin{bmatrix} u_{11}^* & u_{12}^* & u_{13}^* \\ u_{21}^* & u_{22}^* & u_{23}^* \\ u_{31}^* & u_{32}^* & u_{33}^* \end{bmatrix}, \qquad \boldsymbol{t}^* = \begin{bmatrix} t_{11}^* & t_{12}^* & t_{13}^* \\ t_{21}^* & t_{22}^* & t_{23}^* \\ t_{31}^* & t_{32}^* & t_{33}^* \end{bmatrix}$$

Then

$$\int_{\Gamma_{-\varepsilon}} f(x) \, dx = \int_{-2}^{-\varepsilon} \frac{1}{x} \, dx + \int_{\varepsilon}^{2} \frac{1}{x} \, dx = \ln|x| \big|_{-2}^{-\varepsilon} + \ln|x| \big|_{\varepsilon}^{2}$$

$$= \ln \varepsilon - \ln 2 + \ln 2 - \ln \varepsilon = 0 \;\; \forall \varepsilon > 0$$

$$\Rightarrow \lim_{\varepsilon \to 0} \int_{\Gamma_{-\varepsilon}} f(x) \, dx = 0 \qquad\qquad \text{This is the Cauchy Principle Value of } \int_{\Gamma} f(x) \, dx$$

But if we replace $\Gamma_{-\varepsilon}$ by $\lim_{\varepsilon \to 0} \Gamma_{-\varepsilon} = [-2, 2] = \Gamma$ then

$$\int_{\Gamma} \frac{1}{x} \, dx = \int_{-2}^{2} \frac{1}{x} \, dx = \left(\lim_{\varepsilon_1 \to 0} \int_{-2}^{\varepsilon_1} \frac{1}{x} \, dx \right) + \left(\lim_{\varepsilon_2 \to 0} \int_{-\varepsilon_2}^{2} \frac{1}{x} \, dx \right) \text{(by definition of improper integration)}$$

which does NOT exist. *i.e.,* the integral does not exist in the proper sense, but it does in the Cauchy Principal Value sense. However, if an integral exists in the proper sense, then it exists in the Cauchy Principal Value sense and the two values are the same.

Then (in absence of a body force) we can write Equation (4.55) as

$$\boldsymbol{cu} + \int_\Gamma \boldsymbol{t^*u}\, d\Gamma = \int_\Gamma \boldsymbol{u^*t}\, d\Gamma \tag{4.56}$$

We can discretise the boundary as before and put P, the singular point, at each node (each node has 6 unknowns - 3 displacements and 3 tractions - we get 3 equations per node). The overall matrix equation

$$\boldsymbol{Au} = \boldsymbol{Bt} \tag{4.57}$$

where $\boldsymbol{u} = \begin{bmatrix} \boldsymbol{u}_1 \\ \boldsymbol{u}_2 \\ \vdots \\ \boldsymbol{u}_n \end{bmatrix}$ and $\boldsymbol{t} = \begin{bmatrix} \boldsymbol{t}_1 \\ \boldsymbol{t}_2 \\ \vdots \\ \boldsymbol{t}_n \end{bmatrix}$ where n is the number nodes.

The diagonal elements of the $\boldsymbol{A}$ matrix in Equation (4.57) (for three-dimensions, a 3 x 3 matrix) contains principal value components. If we have a rigid-body displacement of a *finite* body in any one direction then we get

$$\boldsymbol{Ai}_l = \boldsymbol{0}$$

($\boldsymbol{i}_l$ = vector defining a rigid body displacement in direction l)

$$\Rightarrow a_{ii} = -\sum_{i \neq j} a_{ij} \qquad \text{(no sum on } i\text{)}$$

i.e., the diagonal entries of $\boldsymbol{A}$ (the c_{ij}'s) do not need to be determined explicitly. There is a similar result for an infinite body.

4.9   Body Forces (and Domain Integrals in General)

The body force gives rise to a domain integral although it does not give rise to any further unknowns in the system of equations. (This is because the body force is known - the fundamental solution was chosen so that it removed all unknowns appearing in domain integrals).

Thus Equation (4.55) is still classed as a Boundary Integral Equation. Integrals over the domain containing known functions (eg body force integral) appear in many situations *e.g.,* the Poisson equation $\nabla^2 u = f$ yields a domain integral involving f.

The question is how do we evaluate domain integrals such as those appearing in the boundary integral forumalation of such equations? Since the functions are known a *coarse* domain mesh may work.(*n.b.* Since the integral also contains the fundamental solution and Ω may not be a "nice" region it is unlikely that it can be evaluated analytically). However, a domain mesh nullifies one of the advantages of BEM - that of having to prepare only a boundary mesh.

In some cases domain integrals must be used but there are techniques developing to avoid many of them. In some standard situations a domain integral can be transformed to a boundary integral.

e.g., a body force arising from a constant gravitational load, or a centrifugal load due to rotation about a fixed axis or the effect of a steady state thermal load can all be transformed to a boundary integral.

Firstly, let G_{ij}^* (the Galerkin tension) be related to u_{ij}^* by

$$u_{ij}^* = G_{ij,kk}^* - \frac{1}{2\,(1-\nu)} G_{ik,kj}^*$$

$$\Rightarrow G_{ij} = \begin{cases} \dfrac{1}{8\pi G} r \delta_{ij} & \text{(3D)} \\[2mm] \dfrac{1}{8\pi G} r^2 \log\left(\dfrac{1}{r}\right) \delta_{ij} & \text{(2D)} \end{cases}$$

Then

$$B_i = \int\limits_\Omega u_{ij}^* b_j \, d\Omega = \int\limits_\Omega \left(G_{ij,kk}^* - \frac{1}{2\,(1-\nu)} G_{ik,kj}^* \right) b_j \, d\Omega$$

Under a constant gravitational load $\boldsymbol{g} = (g_j)$

$$b_j = \rho g_j$$

$$\Rightarrow B_i = \rho g_j \int\limits_\Omega \left(G_{ik,j}^* - \frac{1}{2\,(1-\nu)} G_{ik,kj}^* \right) d\Omega$$

$$= \rho g_j \int\limits_\Gamma \left\{ G_{ij,k}^* - \frac{1}{2\,(1-\nu\})\,G_{ik,j}^*} \right\} n_k \, d\Gamma$$

which is a boundary integral.

Unless the domain integrand is "nice" the above simple application of Green's theorem won't work in general. There has been a considerable amount of research on domain integrals in BEM which has produced techniques for overcoming some domain methods. The two integrals of note are the DRM, dual reciprocity method, developed around 1982 and the MRM, multiple reciprocity method, developed around 1988.

4.10   CMISS Examples

1. To solve a truss system run CMISS example 411 This solves the simple three truss system shown in Figure 4.2.

2. To solve stresses in a bicycle frame modelled with truss elements run CMISS example 412.
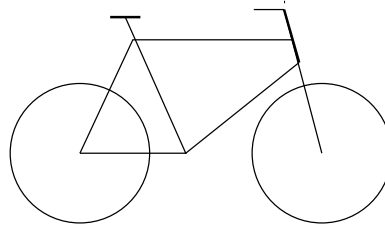
Chapter 5

Transient Heat Conduction

5.1 Introduction

In the previous discussion of steady state boundary value problems the principal advantage of the finite element method over the finite difference method has been the greater ease with which complex boundary shapes can be modelled. In time-dependent problems the solution proceeds from an initial solution at $t = 0$ and it is almost always convenient to calculate each new solution at a constant time ($t > 0$) throughout the entire spatial domain Ω. There is, therefore, no need to use the greater flexibility (and cost) of finite elements to subdivide the time domain: finite difference approximations of the time derivatives are usually preferred. Finite difference techniques are introduced in Section 5.2 to solve the transient one dimensional heat equation. A combination of finite elements for the spatial domain and finite differences for the time domain is used in Section 5.3 to solve the transient advection-diffusion equation - a slight generalization of the heat equation.

5.2 Finite Differences

5.2.1 Explicit Transient Finite Differences

Consider the transient one-dimensional heat equation

$$\frac{\partial u}{\partial t} = D \frac{\partial^2 u}{\partial x^2}, \qquad (0 < x < L, t > 0) \tag{5.1}$$

where D is the conductivity and $u = u(x,t)$ is the temperature, subject to the boundary conditions $u(0,t) = u_0$ and $u(L,t) = u_1$ and the initial conditions $u(x,0) = 0$. A finite difference approximation of this equation is obtained by defining a grid with spacing Δx in the x-domain and Δt in the time domain, as shown in Figure 5.1.

Grid points are labelled by the indices $i = 0, 1, \ldots, I$ (for the x-direction) and $n = 0, 1, \ldots, N$ (for the t-direction). The temperature at the grid point (i, n) is therefore labelled as

$$u(x,t) = u(i\Delta x, n\Delta t) = u_i^n. \tag{5.2}$$

Finite difference equations are derived by writing Taylor Series expansions for $u_{i+1}^n, u_{i-1}^n u_i^{n+1}$

about the grid point (i, n)

$$u_{i+1}^n = u_i^n + \Delta x. \left(\frac{\partial u}{\partial x}\right)_i^n + \frac{1}{2}\Delta x^2. \left(\frac{\partial^2 u}{\partial x^2}\right)_i^n + \frac{1}{6}\Delta x^3. \left(\frac{\partial^3 u}{\partial x^3}\right)_i^n + \mathrm{O}\left(\Delta x^4\right) \qquad (5.3)$$

$$u_{i-1}^n = u_i^n - \Delta x. \left(\frac{\partial u}{\partial x}\right)_i^n + \frac{1}{2}\Delta x^2. \left(\frac{\partial^2 u}{\partial x^2}\right)_i^n - \frac{1}{6}\Delta x^3. \left(\frac{\partial^3 u}{\partial x^3}\right)_i^n + \mathrm{O}\left(\Delta x^4\right) \qquad (5.4)$$

$$u_i^{n+1} = u_i^n + \Delta t. \left(\frac{\partial u}{\partial t}\right)_i^n + \mathrm{O}\left(\Delta t^2\right) \qquad (5.5)$$

where $\mathrm{O}\left(\Delta x^4\right)$ and $\mathrm{O}\left(\Delta t^2\right)$ represent all the remaining terms in the Taylor Series expansions.

Adding Equations (5.3) and (5.4) gives

$$u_{i+1}^n + u_{i-1}^n = 2u_i^n + \Delta x^2. \left(\frac{\partial^2 u}{\partial x^2}\right)_i^n + \mathrm{O}\left(\Delta x^4\right)$$

or

$$\left(\frac{\partial^2 u}{\partial x^2}\right)_i^n = \frac{u_{i+1}^n - 2u_i^n + u_{i-1}^n}{\Delta x^2} + \mathrm{O}\left(\Delta x^2\right), \qquad (5.6)$$

which is a "central difference" approximation of the second order spatial derivative.

Rearranging Equation (5.5) gives a "difference" approximation of the first order time derivative

$$\left(\frac{\partial u}{\partial t}\right)_i^n = \frac{u_i^{n+1} - u_i^n}{\Delta t} + \mathrm{O}\left(\Delta t\right). \qquad (5.7)$$

Substituting Equation (5.6) and Equation (5.7) into the transient heat equation Equation (5.1) gives the finite difference approximation

$$\frac{u_i^{n+1} - u_i^n}{\Delta t} + \mathrm{O}\left(\Delta t\right) = D\frac{u_{i+1}^n - 2u_i^n + u_{i-1}^n}{\Delta x^2} + \mathrm{O}\left(\Delta x^2\right)$$

which is rearranged to give an expression for u_i^{n+1} in terms of the values of u at the nth time step

$$u_i^{n+1} = u_i^n + D\frac{\Delta t}{\Delta x^2}\left(u_{i+1}^n - 2u_i^n + u_{i-1}^n\right) + \mathrm{O}\left(\Delta t^2, \Delta x^2\right). \qquad (5.8)$$

Given the initial values of u_i^n at $n = 0$ (*i.e.,* $t = 0$), the values of u_i^{n+1} for the next time step are found from Equation (5.8) with $i = 1, 2, \ldots, I$. Applying Equation (5.8) iteratively for time steps $n = 1, 2, \ldots$ *etc.* yields the time dependent temperatures at the grid points (see Figure 5.1). This is an *explicit* finite difference formula because the value of u_i^n depends only on the values of u_i^n $(i = 1, 2, \ldots, I)$ at the previous time step and not on the neighbouring terms u_{i+1}^{n+1} and u_{i-1}^{n+1} at the latest time step. The accuracy of the solution depends on the chosen values of Δx and Δt and in fact the stability of the scheme depends on these satisfying the *Courant* condition:

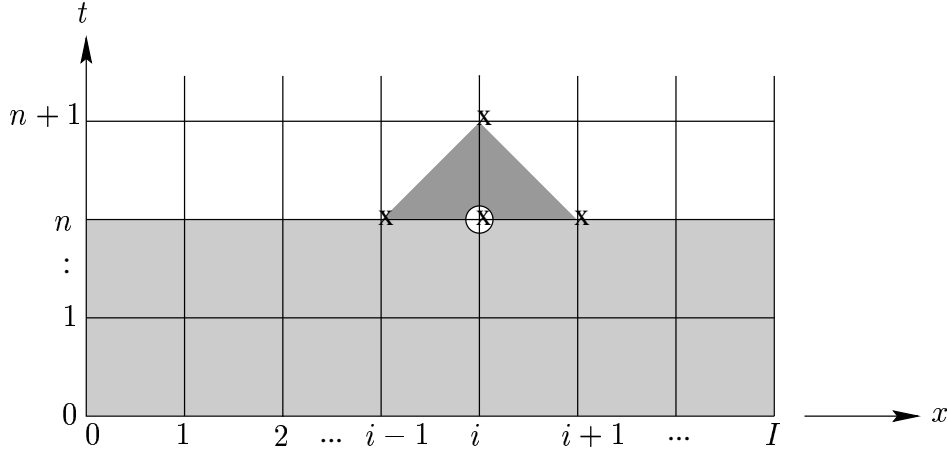$$D\frac{\Delta t}{\Delta x^2} \leq \frac{1}{2}. \qquad (5.9)$$

FIGURE 5.1: A finite difference grid for the solution of the transient 1D heat equation. The equation is centred at grid point (i, n) shown by the **O**. The lightly shaded region shows where the solution is known at time step n. With central differences in x and a forward difference in t an explicit finite difference formula gives the solution at time step $n + 1$ explicitly in terms of the solution at the three points below it at step n, as indicated by the dark shading.

5.2.2 Von Neumann Stability Analysis

The concept behind the Von Neumann analysis is that all Fourier components decay as time advances or as they are processed by an iterative solver. Considering Equation (5.8), we can rearrange this to be of the form,

$$u_i^{n+1} = \Upsilon u_{i+1}^n + (1 - 2\Upsilon)u_i^n + \Upsilon u_{i-1}^n \tag{5.10}$$

where $\Upsilon = D\dfrac{\Delta t}{\Delta x^2}$. By substituting the general Fourier component $u_j^n = A_k^n e^{i\left(\frac{\pi k j \Delta x}{L}\right)}$, we obtain,

$$A_k^{n+1} e^{i\left(\frac{\pi k j \Delta x}{L}\right)} = A_k^n \left[\Upsilon e^{i\left(\frac{\pi k (j+1) \Delta x}{L}\right)} + (1 - 2\Upsilon) e^{i\left(\frac{\pi k j \Delta x}{L}\right)} + \Upsilon e^{i\left(\frac{\pi k (j-1) \Delta x}{L}\right)} \right] \tag{5.11}$$

If divide Equation (5.11) by, $A_k^n e^{i\left(\frac{\pi k j \Delta x}{L}\right)}$ we obtain (no sum on k),

$$
\begin{aligned}
\frac{A_k^{n+1}}{A_k^n} &= (1 - 2\Upsilon) + \Upsilon e^{i\left(\frac{\pi k \Delta x}{L}\right)} + \Upsilon e^{-i\left(\frac{\pi k \Delta x}{L}\right)} \\[2mm]
&= 1 - 2\Upsilon + 2\Upsilon cos\left(\frac{\pi k \Delta x}{L}\right) \qquad \text{using} \qquad cos(x) = \frac{e^{ix} + e^{-ix}}{2} \\[2mm]
&= 1 - 4\Upsilon sin^2\left(\frac{\pi k \Delta x}{2L}\right) \qquad \text{using} \qquad cos(2x) = 1 - 2sin^2(x)
\end{aligned}
\tag{5.12}
$$

Equation (5.12) predicts the growth of any component (specified by k) admitted by the system.

If all components are to decay,

$$\left| \frac{A_k^{n+1}}{A_k^n} \right| \leq 1 \qquad \text{for stability (no sum on } k) \tag{5.13}$$

Since the sin^2 term in Equation (5.12) is always between 0 and 1, we effectively have the stablity criteria that

$$1 - 4\Upsilon \leq 1 \qquad \text{and} \qquad 1 - 4\Upsilon \geq -1 \tag{5.14}$$

The first inequality is trivially satisfied, since $\Upsilon \geq 0$ for positive values of Δt and D, and the second condition will always hold if

$$\Upsilon = D\frac{\Delta t}{\Delta x^2} \leq \frac{1}{2} \tag{5.15}$$

Thus, to ensure stability, the time step should be chosen such that

$$\Delta t \leq \frac{\Delta x^2}{2D} \qquad \text{The } \textit{Courant} \text{ condition} \tag{5.16}$$

5.2.3 Higher Order Approximations

An improvement in accuracy and stability can be obtained by using a higher order approximation for the time derivative. For example, if a central difference approximation is used for $\dfrac{\partial u}{\partial t}$ by centering the equation at $(i\Delta x, \left(n + \frac{1}{2}\right)\Delta t)$ rather than $(i\Delta x, n\Delta t)$ we get

$$\left(\frac{\partial u}{\partial t} \right)_i^{n+\frac{1}{2}} = \frac{u_i^{n+1} - u_i^n}{\Delta t} + \mathrm{O}\left(\Delta t^2\right) \tag{5.17}$$

in place of Equation (5.7) and Equation (5.1) is approximated with the "Crank-Nicolson" formula

$$\frac{u_i^{n+1} - u_i^n}{\Delta t} = D \left\{ \frac{1}{2}\left(\frac{\partial^2 u}{\partial x^2} \right)_i^{n+1} + \frac{1}{2}\left(\frac{\partial^2 u}{\partial x^2} \right)_i^n \right\} \tag{5.18}$$

in which the spatial second derivative term is weighted by $\frac{1}{2}$ at the old time step n and by $\frac{1}{2}$ at the new time step $n + 1$. Notice that the finite difference time derivative has not changed - only the time position at which it is centred. The price paid for the better accuracy (for a given Δt) and unconditional stability (*i.e.,* stable for **any** Δt) is that Equation (5.18) is an *implicit* scheme - the equations for the new time step are now coupled in that u_i^{n+1} depends on the neighbouring terms u_{i+1}^{n+1} and u_{i-1}^{n+1}. Thus each new time step requires the solution of a system of coupled equations.

A generalization of (5.18) is

$$\frac{u_i^{n+1} - u_i^n}{\Delta t} = D \left\{ \theta \left(\frac{\partial^2 u}{\partial x^2}_i \right)^{n+1} + (1 - \theta)\left(\frac{\partial^2 u}{\partial x^2}_i \right)^n \right\} \tag{5.19}$$
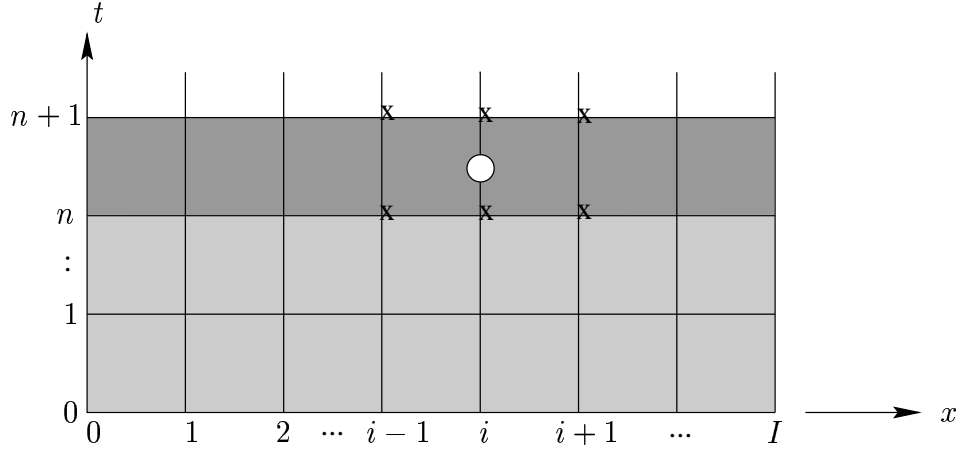
FIGURE 5.2: An implicit finite difference scheme based on central differences in t, as well as x, which tie together the 6 points shown by **x**. The equation is centred at the point $(i, n + \frac{1}{2})$ shown by the **O**. The lightly shaded region shows where the solution is known at time step n. The dark shading shows the region of the coupled equations.

in which the spatial second derivative of Equation (5.1) has been weighted by θ at the new time step and by $(1 - \theta)$ at the old time step. The original explicit forward difference scheme Equation (5.8) is recovered when $\theta = 0$ and the implicit central difference (Crank-Nicolson) scheme (5.19) when $\theta = \frac{1}{2}$. An implicit backward difference scheme is obtained when $\theta = 1$.

In the following section the transient heat equation is approximated for numerical analysis by using finite differences in time and finite elements in space. We also generalize the partial differential equation to include an advection term and a source term.

5.3 The Transient Advection-Diffusion Equation

Consider a linear parabolic equation

$$\frac{\partial u}{\partial t} + \boldsymbol{v} \cdot \nabla u = D\nabla^2 u + f \tag{5.20}$$

where u is a scalar variable (*e.g.,* the advection-diffusion equation, where u is concentration or temperature; $\boldsymbol{v} \cdot \nabla u$ then represents advective transport by a velocity field $\boldsymbol{v}$, D is the diffusivity and f is source term. The ratio of advective to diffusive transport is characterised by the *Peclet number* VL/D where $V = \|\boldsymbol{v}\|_2$ and L is a characteristic length).

Applying the Galerkin weighted residual method to Equation (5.20) with weight $\boldsymbol{\omega}$ gives

$$\int_{\Omega} \left(\frac{\partial u}{\partial t} + \boldsymbol{v} \cdot \nabla u - D\nabla^2 u - f \right) \omega \, d\Omega = 0$$

or

$$\int\limits_{\Omega} \left[\left(\frac{\partial u}{\partial t} + \boldsymbol{v} \cdot \nabla u \right) \omega + D \nabla u \cdot \nabla \omega \right] d\Omega = \int\limits_{\Omega} f \omega \, d\Omega + D \int\limits_{\partial\Omega} \frac{\partial u}{\partial n} \omega \, d\Gamma \qquad (5.21)$$

where $\dfrac{\partial}{\partial n}$ is the normal derivative to the boundary $\partial\Omega$.

Putting $u = \varphi_n u_n$ and $\omega = \varphi_m$ and summing the element contributions to the global equations, Equation (5.21) can be represented by a system of first order ordinary differential equations,

$$\boldsymbol{M}\frac{d\boldsymbol{u}}{dt} + \boldsymbol{K}\boldsymbol{u} = \boldsymbol{K}\boldsymbol{u}_{\infty} \qquad (5.22)$$

where $\boldsymbol{M}$ is the global mass matrix, $\boldsymbol{K}$ the global stiffness matrix and $\boldsymbol{u}$ a vector of global nodal unknowns with steady state values ($t \to \infty$) $\boldsymbol{u}_{\infty}$. The element contributions to $\boldsymbol{M}$ and $\boldsymbol{K}$ are given by

$$M_{mn_e} = \int\limits_0^1 \varphi_m \varphi_n J \, d\xi \qquad (5.23)$$

and

$$K_{mn_e} = \int\limits_0^1 D \frac{\partial\varphi_m}{\partial\xi_i} \frac{\partial\varphi_n}{\partial\xi_j} \cdot \frac{\partial\xi_i}{\partial x_k} \frac{\partial\xi_j}{\partial x_k} J \, d\xi + \int\limits_0^1 v_j \varphi_m \frac{\partial\varphi_n}{\partial\xi_i} \frac{\partial\xi_i}{\partial x_j} J \, d\xi \qquad (5.24)$$

If the time domain is now discretized ($t = n\Delta t, n = 0, 1, 2, \ldots$) Equation (5.22) can be replaced by

$$\boldsymbol{M}\frac{\boldsymbol{u}^{n+1} - \boldsymbol{u}^n}{\Delta t} + \boldsymbol{K}\left[\theta\boldsymbol{u}^{n+1} + (1 - \theta)\boldsymbol{u}^n\right] = \boldsymbol{K}\boldsymbol{u}_{\infty} \qquad 0 \le \theta \le 1 \qquad (5.25)$$

where θ is a weighting factor discussed in Section 5.2. Note that for $\theta = \dfrac{1}{2}$ the method is known as the *Crank-Nicolson-Galerkin* method and errors arising from the time domain discretization are $\mathrm{O}\left(\Delta t^2\right)$. Rearranging Equation (5.25) as

$$\left[\boldsymbol{M} + \theta\Delta t\boldsymbol{K}\right]\boldsymbol{u}^{n+1} = \left[\boldsymbol{M} - (1 - \theta)\Delta t\boldsymbol{K}\right]\boldsymbol{u}^n + \Delta t\boldsymbol{K}\boldsymbol{u}_{\infty} \qquad (5.26)$$

gives a set of linear algebraic equations to solve at the new time step $(n + 1)\Delta t$ from the known solution $\boldsymbol{u}^n$ at the previous time step $n\Delta t$.

The stability of the above scheme can be examined by expanding $\boldsymbol{u}$ (assumed to be smoothly continuous in time) in terms of the eigenvectors $\boldsymbol{s}_i$ (with associated eigenvalues λ_i) of the matrix $\boldsymbol{A} = \boldsymbol{M}^{-1}\boldsymbol{K}$. Writing the initial conditions $\boldsymbol{u}(0) = \sum\limits_i a_i\boldsymbol{s}_i$ and steady state solution $\boldsymbol{u}_{\infty} =$

$\sum_i b_i \boldsymbol{s}_i$, the set of ordinary differential equations Equation (5.22) has solution

$$\boldsymbol{u} = \sum_i \left[b_i + (a_i - b_i) e^{-\lambda_i t} \right] \boldsymbol{s}_i \tag{5.27}$$

The time-difference scheme Equation (5.26) on the other hand, with $\boldsymbol{u}$ now replaced by a set of discrete values $\boldsymbol{u}^n$ at each time step $n\Delta t$, can be written as the recursion formula

$$\left[\boldsymbol{I} + \theta \Delta t \boldsymbol{A} \right] \boldsymbol{u}^{n+1} = \left[\boldsymbol{I} - (1 - \theta) \Delta t \boldsymbol{A} \right] \boldsymbol{u}^n + \Delta t \boldsymbol{A} \boldsymbol{u}_\infty \tag{5.28}$$

with solution

$$\boldsymbol{u} = \sum_i \left\{ b_i + (a_i - b_i) \left[\frac{1 - \Delta t (1 - \theta) \lambda_i}{1 + \Delta t \theta \lambda_i} \right]^n \right\} \boldsymbol{s}_i \tag{5.29}$$

(You can verify that Equation (5.27) and Equation (5.29) are indeed the solutions of Equation (5.22) and Equation (5.25), respectively, by substituting and using $\boldsymbol{A}\boldsymbol{s}_i = \lambda_i \boldsymbol{s}_i$.)

Comparing Equation (5.27) and Equation (5.29) shows that replacing the ordinary differential equations (5.22) by the finite difference approximation Equation (5.25) is equivalent to replacing the exponential $e^{-\lambda_i t}$ in Equation (5.27) by the approximation

$$e^{-\lambda_i t} \sim \left[\frac{1 - \Delta t (1 - \theta) \lambda_i}{1 + \Delta t \theta \lambda_i} \right]^n \tag{5.30}$$

or, with $t = n\Delta t$,

$$e^{-\lambda_i t} \sim \frac{1 - \Delta t (1 - \theta) \lambda_i}{1 + \Delta t \theta \lambda_i} = 1 - \frac{\Delta t \lambda_i}{1 + \Delta t \theta \lambda_i} \tag{5.31}$$

The stability of the numerical time integration scheme can now be investigated by examining the behaviour of this approximation to the exponential. For stability we require

$$-1 \leq 1 - \frac{\Delta t \lambda_i}{1 + \Delta t \theta \lambda_i} \leq 1 \tag{5.32}$$

since this term appears in Equation (5.29) raised to the power n. The right hand inequality in Equation (5.32) is trivially satisfied, since Δt, λ_i and θ are all positive, and the left hand inequality gives

$$\frac{\Delta t \lambda_i}{1 + \Delta t \theta \lambda_i} \leq 2 \qquad \text{or} \quad \Delta t \lambda_i (1 - 2\theta) \leq 2 \tag{5.33}$$

A consequence of Equation (5.33) is that the scheme is *unconditionally stable* if $\frac{1}{2} \leq \theta \leq 1$. For $\theta < \frac{1}{2}$ the *stability criterion* is

$$\Delta t \lambda_i < \frac{2}{1 - 2\theta} \tag{5.34}$$

If the exponential approximation given by Equation (5.31) is negative for any λ_i the solution will contain components which change sign with each time step n. This *oscillatory noise* can be avoided by choosing

$$\Delta t < \frac{1}{(1 - \theta)\, \lambda_{\text{max}}},$$ (5.35)

where λ_{max} is the largest eigenvalue in the matrix $\boldsymbol{A}$, but in practice this imposes a limit which is too severe for Δt and a small amount of oscillatory noise, associated with the high frequency vibration modes of the system, is tolerated. Alternatively the oscillatory noise can be filtered out by averaging.

These theoretical results are explored numerically with a Crank-Nicolson-Galerkin scheme ($\theta = \frac{1}{2}$) in Figure 5.3, where the one-dimensional diffusion equation

$$\frac{\partial u}{\partial t} = D \frac{\partial^2 u}{\partial x^2} \quad \text{on} \quad 0 \leq x \leq 1$$

subject to initial conditions $\quad u(x, 0) = 0$ (5.36)

and boundary conditions $\quad u(0, t) = 0, u(1, t) = 1$

is solved for various time increments (Δt) and element lengths (Δx) for both linear and cubic Hermite elements.

Decreasing Δx from 0.25 to 0.1 with linear elements produces more oscillation because the system has more degrees of freedom and leads to greater oscillation. At a sufficiently small Δt the oscillations are negligible (bottom right, Figure 5.3). With this value of Δt (0.01 s) the numerical results agree well with the exact solution (top, Figure 5.3) given by

$$u(x, t) = x + \frac{2}{\pi} \sum_{n=1}^{\infty} \frac{(-1)^n}{n} e^{-n^2 \pi^2 t} \sin(n\pi x)$$ (5.37)

5.4 Mass lumping

A technique known as *mass lumping* is sometimes used in which the mass matrix $\boldsymbol{M}$ is replaced by a diagonal matrix having diagonal terms equal to the row sums. For example, consider the mass

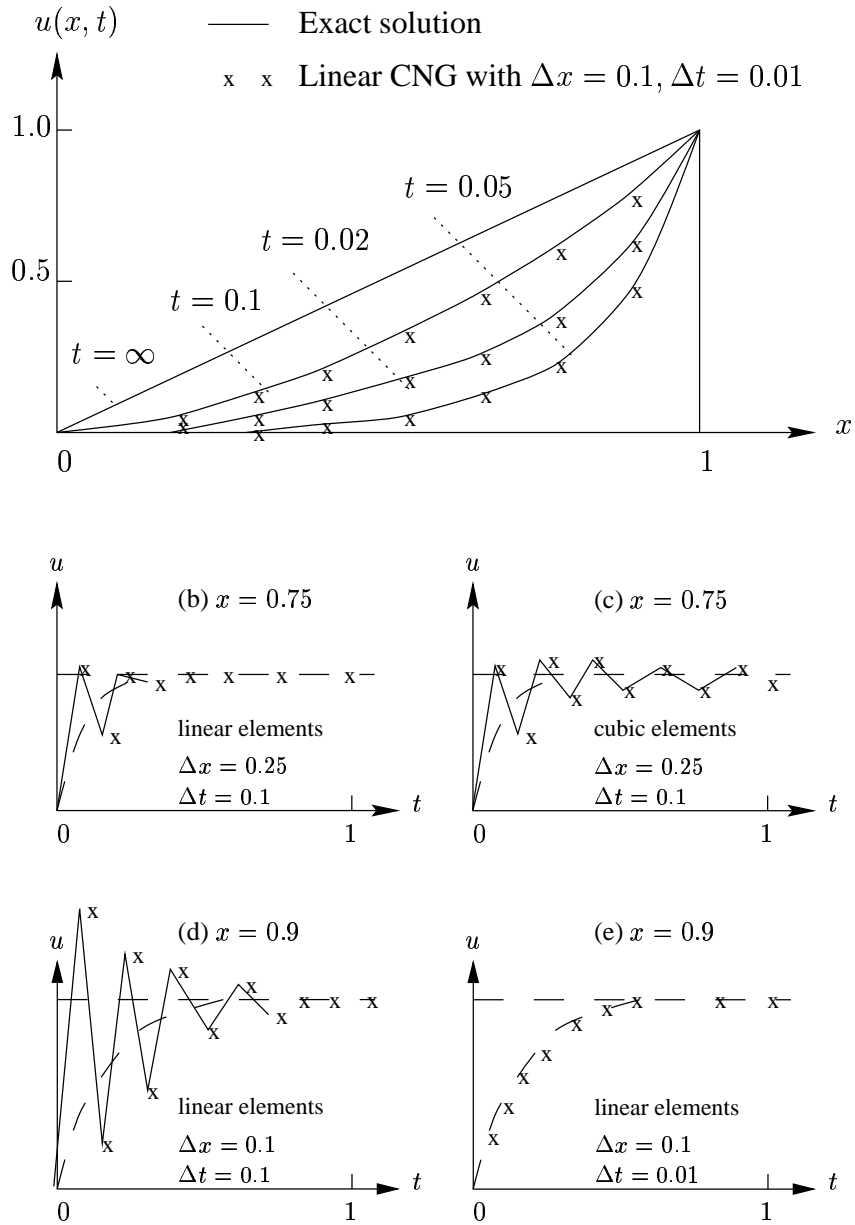FIGURE 5.3: Analytical and numerical solutions of the transient 1D heat equation showing the effects of element size Δx and time step size Δt. The top graph shows the exact and approximate solutions as functions of x at various times. The lower graphs show the solution through time at the specified x positions and with various choices of Δx and Δt as indicated.

matrix ((5.23)) for a bilinear element (see Figure 1.9 and (1.6)).

$$M_{11} = \iint (1-\xi_1)^2 (1-\xi_2)^2 \xi_1 \xi_2 \quad = -\frac{(1-\xi_1)^3}{3}\bigg|_0 1 - \frac{(1-\xi_2)^3}{3}\bigg|_0 1 = \frac{1}{3}\cdot\frac{1}{3} = \frac{1}{9}$$

$$M_{22} = \iint \xi_1^2 (1-\xi_2)^2 \xi_1 \xi_2 \quad = \frac{1}{3}\cdot\frac{1}{3} = \frac{1}{9} \text{ and similarly } M_{33} \text{ and } M_{44}.$$

$$M_{12} = \iint \xi_1 (1-\xi_1)(1-\xi_1)^2 \xi_1 \xi_2 \quad = \left(-\frac{1}{2}-\frac{1}{3}\right)\cdot\frac{1}{3} = \frac{1}{18}$$

$$M_{13} = \iint (1-\xi_1)^2 \xi_2 (1-\xi_2)\xi_1 \xi_2 \quad = \frac{1}{18} \text{ and similarly } M_{34} \text{ and } M_{24}.$$

$$M_{14} = \iint \xi_1 (1-\xi_1)\xi_2 (1-\xi_2)\xi_1 \xi_2 = \frac{1}{36} \text{ and similarly } M_{23}.$$

$$\text{therefore } \boldsymbol{M} = \begin{bmatrix} \frac{1}{9} & \frac{1}{18} & \frac{1}{18} & \frac{1}{36} \\ \frac{1}{18} & \frac{1}{9} & \frac{1}{36} & \frac{1}{18} \\ \frac{1}{18} & \frac{1}{136} & \frac{1}{9} & \frac{1}{18} \\ \frac{1}{36} & \frac{1}{18} & \frac{1}{18} & \frac{1}{9} \end{bmatrix} \overset{\text{mass lumping}}{\longrightarrow} \begin{bmatrix} \frac{1}{4} & 0 & 0 & 0 \\ 0 & \frac{1}{4} & 0 & 0 \\ 0 & 0 & \frac{1}{4} & 0 \\ 0 & 0 & 0 & \frac{1}{4} \end{bmatrix}$$

The element mass is effectively lumped at the element vertices. Such a scheme has computational advantages when $\theta = 0$ in Equation (5.26) because each component of the vector $\boldsymbol{u}^{n+1}$ is obtained directly without the need to solve a set of coupled equations. This *explicit* time integration scheme, however, is only conditionally stable (see (5.34)) and suffers from *phase lag errors* - see below. For evenly spaced elements the finite element scheme with mass lumping is equivalent to finite differences with central spatial differences.

In Figure 5.4, the finite element and finite differences (lumped f.e. mass matrix) solutions of the one-dimensional advection-diffusion equation (5.20) with $V = 5$ m s^{-1}, $D = 0.1$ m^{2}s^{-1}, $f = 0$ are compared for the propagation and dispersion of an initial unit mass pulse at $x = 0$. The length of the solution domain is sufficient to avoid reflected end effects.

The exact solution is a Gaussian distribution whose variance increases with time:

$$u(x,t) = \frac{M}{\sqrt{4\pi\Delta t}} e^{-\frac{(x-Vt)^2}{4Dt}} \tag{5.38}$$

The finite element solution, using the Crank-Nicolson-Galerkin technique, shows excellent amplitude and phase characteristics when compared with the exact solution. The finite difference, or lumped mass, solution also using centered time differences, reproduces the amplitude of the pulse very well but shows a slight phase lag.

5.5 CMISS Examples

1. To solve for the transient heat flow in a plate run CMISS example 331

2. To investigate the stability of time integration schemes run CMISS examples 3321 and 3322.
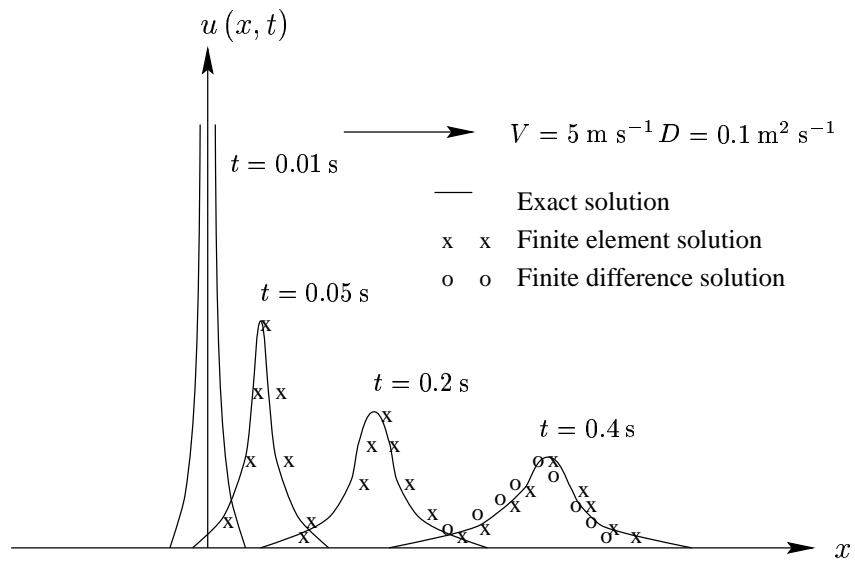
FIGURE 5.4: Advection-diffusion of a unit mass pulse. The finite element solutions (at t=0.01 s, 0.05 s, 0.2 s and 0.4 s) and finite difference solutions (at t=0.4 s only) are compared with the exact solution. Δx= 0.1, $\Delta t = 0.001$ s for 0< t <0.01 s and $\Delta t = 0.01$ for $t \geq 0.01$ s.

Chapter 6

Modal Analysis

6.1 Introduction

The system of ordinary differential equations which results from the application of the Galerkin finite element (or other) discretization of the spatial domain to linear parabolic or hyperbolic equations can either be integrated directly - as in the last section for parabolic equations - or analysed by *mode superposition*. That is, the time-dependent solution is expressed as the superposition of the natural (or resonant) modes of the system. To find these modes requires the solution of an eigenvalue problem.

6.2 Free Vibration Modes

Consider an extension of Equation (5.22) which includes second order time derivatives (*e.g.*, nodal point accelerations)

$$\boldsymbol{M}\ddot{\boldsymbol{u}}\left(t\right)+\boldsymbol{C}\dot{\boldsymbol{u}}\left(t\right)+\boldsymbol{K}\boldsymbol{u}\left(t\right)=\boldsymbol{f}\left(t\right) \tag{6.1}$$

$\boldsymbol{M}, \boldsymbol{C}$ and $\boldsymbol{K}$ are the mass, damping and stiffness matrices, respectively, $\boldsymbol{f}\left(t\right)$ is the external load vector and $\boldsymbol{u}\left(t\right)$ is the vector of n nodal unknowns. In direct time integration methods $\ddot{\boldsymbol{u}}\left(t\right)$ and $\dot{\boldsymbol{u}}\left(t\right)$ are replaced by finite differences and the resulting system of algebraic equations is solved at successive time steps. For a small number of steps this is the most economical method of solution but, if a solution is required over a long time period, or for a large number of different load vectors $\boldsymbol{f}\left(t\right)$, a suitable transformation

$$\boldsymbol{u}\left(t\right)=\boldsymbol{P}\boldsymbol{x}\left(t\right) \tag{6.2}$$

applied to Equation (6.1) can result in the matrices of the transformed system

$$\boldsymbol{P}^{T}\boldsymbol{M}\boldsymbol{P}\ddot{\boldsymbol{x}}\left(t\right)+\boldsymbol{P}^{T}\boldsymbol{C}\boldsymbol{P}\dot{\boldsymbol{x}}\left(t\right)+\boldsymbol{P}^{T}\boldsymbol{K}\boldsymbol{P}\boldsymbol{x}\left(t\right)=\boldsymbol{P}^{T}\boldsymbol{f} \tag{6.3}$$

having a much smaller bandwidth than in the original system and hence being more economical to solve. In fact, if damping is neglected, $\boldsymbol{P}$ can be chosen to diagonalize $\boldsymbol{M}$ and $\boldsymbol{K}$ and thereby uncouple the equations entirely. This transformation (which is still applicable when damping is

included but does not then result in an uncoupled system unless further simplications are made) is found by solving the free vibration problem

$$M\ddot{u}(t) + Ku(t) = 0 \tag{6.4}$$

Proof: Consider a solution to Equation (6.4) of the form

$$u(t) = s \sin \omega (t - t_0), \tag{6.5}$$

where ω and t_0 are constants and s is a vector of order n. Substituting Equation (6.5) into Equation (6.4) gives the *generalized eigenproblem*

$$Ks = \omega^2 Ms \tag{6.6}$$

having n *eigensolutions* $(\omega_1^2 s_1), (\omega_2^2 s_2), \dots, (\omega_n^2 s_n)$. If K is a symmetric matrix (as is the case when the original partial differential operator is self-adjoint) the eigenvectors are orthogonal and can be "*normalized*" such that

$$s_i{}^T M s_j = \begin{cases} 1 & i = j \\ 0 & i \neq j \end{cases} \tag{6.7}$$

(the eigenvectors are said to be M-*orthonormalised*). Combining the n eigenvectors into a matrix $S = [s_1, s_2, \dots, s_n]$ - the *modal matrix* - rewriting Equation (6.7) as

$$S^T M S = I \tag{6.8}$$

where I is the identity matrix, (6.6) becomes

$$KS = MS\Lambda \tag{6.9}$$

where

$$\Lambda = \begin{bmatrix} \omega_1^2 & & & 0 \\ & \omega_2^2 & & \\ & & \ddots & \\ 0 & & & \omega_n^2 \end{bmatrix} \tag{6.10}$$

or

$$S^T K S = S^T M S \Lambda = I \Lambda = \Lambda \tag{6.11}$$

Thus the modal matrix - whose columns are the M-orthonormalised eigenvectors of K (*i.e.,* satisfying Equation (6.6)) - can be used as the transformation matrix P in Equation (6.2) required to reduce the original system of equations (6.1) to the *canonical* form

$$\ddot{x}(t) + S^T C S \dot{x}(t) + \Lambda x(t) = S^T f(t) \tag{6.12}$$

With damping neglected equation Equation (6.12) becomes a system of uncoupled equations

$$\ddot{x}_i(t) + \omega_i^2 x_i(t) = r_i(t) \qquad i = 1, 2, \ldots, n \tag{6.13}$$

where x_i is the ith component of $\boldsymbol{x}$ and r_i is the ith component of the vector $\boldsymbol{S}^T\boldsymbol{f}$. The solution of this system is given by the Duhamel integral

$$x_i(t) = \frac{1}{\omega_i} \int_0^t r_i(\tau) \sin \omega_i(t - \tau) \, d\tau + \alpha_i \sin \omega_i t + \beta_i \cos \omega_i d\tau \tag{6.14}$$

where the constants α_i and β_i are determined from the initial conditions

$$
\begin{aligned}
x_i(0)|_{t=0} &= {s_i}^T \boldsymbol{M} \, \boldsymbol{u}(0)|_{t=0} \\
\dot{x}_i(0)|_{t=0} &= x_i(0)|_{t=0} = {s_i}^T \boldsymbol{M} \, \boldsymbol{u}(0)|_{t=0} \, {s_i}^T \boldsymbol{M} \, \boldsymbol{u}(0)|_{t=0}
\end{aligned}
\tag{6.15}
$$

6.3   An Analytic Example

As an example, consider the equilibrium equations $\boldsymbol{M}\ddot{\boldsymbol{u}} + \boldsymbol{K}\boldsymbol{u} = \boldsymbol{f}$ where

$$\boldsymbol{M} = \begin{bmatrix} 2 & 0 \\ 0 & 1 \end{bmatrix}, \quad \boldsymbol{K} = \begin{bmatrix} 6 & -2 \\ -2 & 4 \end{bmatrix} \quad \text{and} \quad \boldsymbol{f} = \begin{bmatrix} 0 \\ 10 \end{bmatrix}$$

To find the solution by modal analysis we first solve the generalised eigenproblem $\boldsymbol{K}\boldsymbol{s} = \omega^2 \boldsymbol{M}\boldsymbol{s}$ *i.e.*,

$$\begin{bmatrix} 6 - 2\omega^2 & -2 \\ -2 & 4 - \omega^2 \end{bmatrix} \boldsymbol{s} = 0$$

has a solution when $\det\left[\boldsymbol{K} - \omega^2\boldsymbol{M}\right] = 0$ or $\omega^4 - 7\omega^2 + 10 = 0$. This *characteristic polynomial* has solutions $\omega^2 = 2, 5$ with corresponding eigenvectors $\boldsymbol{s}_1^T = a \begin{bmatrix} 1 & 1 \end{bmatrix}, \boldsymbol{s}_1^T = b \begin{bmatrix} -1 & 2 \end{bmatrix}$. To find the magnitude of the eigenvectors we use Equation (6.7), *i.e.*,

$$a^2 \begin{bmatrix} 1 & 1 \end{bmatrix} \begin{bmatrix} 2 & 0 \\ 0 & 1 \end{bmatrix} \begin{bmatrix} 1 \\ 1 \end{bmatrix} = 1 \Rightarrow a = \frac{1}{\sqrt{3}} \qquad b^2 \begin{bmatrix} -1 & 2 \end{bmatrix} \begin{bmatrix} 2 & 0 \\ 0 & 1 \end{bmatrix} \begin{bmatrix} -1 \\ 2 \end{bmatrix} = 1 \Rightarrow b = \frac{1}{\sqrt{3}}$$

(Notice that the orthogonality condition is satisfied: $ab \begin{bmatrix} 1 & 1 \end{bmatrix} \begin{bmatrix} 2 & 0 \\ 0 & 1 \end{bmatrix} \begin{bmatrix} -1 \\ 2 \end{bmatrix} = 0$).

The M-orthognormalised eigenvectors are now $\boldsymbol{s}_1^T = \begin{bmatrix} \dfrac{1}{\sqrt{3}} & \dfrac{1}{\sqrt{3}} \end{bmatrix}$ and $\boldsymbol{s}_2^T = \begin{bmatrix} -\dfrac{1}{\sqrt{6}} & \dfrac{2}{\sqrt{6}} \end{bmatrix}$,

giving the modal matrix $\boldsymbol{S} = \begin{bmatrix} \dfrac{1}{\sqrt{3}} & -\dfrac{1}{\sqrt{6}} \\ \dfrac{1}{\sqrt{3}} & \dfrac{2}{\sqrt{6}} \end{bmatrix}$ which, when used as the transformation matrix,

reduces the stiffness matrix to

$$
\boldsymbol{S}^T \boldsymbol{K} \boldsymbol{S} = \begin{bmatrix} \dfrac{1}{\sqrt{3}} & \dfrac{1}{\sqrt{3}} \\ -\dfrac{1}{\sqrt{6}} & \dfrac{2}{\sqrt{6}} \end{bmatrix} \begin{bmatrix} 6 & -2 \\ -2 & 4 \end{bmatrix} \begin{bmatrix} \dfrac{1}{\sqrt{3}} & -\dfrac{1}{\sqrt{6}} \\ \dfrac{1}{\sqrt{3}} & \dfrac{2}{\sqrt{6}} \end{bmatrix} = \begin{bmatrix} 2 & 0 \\ 0 & 5 \end{bmatrix} = \boldsymbol{\Lambda}
$$

and the mass matrix to

$$
\boldsymbol{S}^T \boldsymbol{M} \boldsymbol{S} = \begin{bmatrix} \dfrac{1}{\sqrt{3}} & \dfrac{1}{\sqrt{3}} \\ -\dfrac{1}{\sqrt{6}} & \dfrac{2}{\sqrt{6}} \end{bmatrix} \begin{bmatrix} 2 & 0 \\ 0 & 1 \end{bmatrix} \begin{bmatrix} \dfrac{1}{\sqrt{3}} & -\dfrac{1}{\sqrt{6}} \\ \dfrac{1}{\sqrt{3}} & \dfrac{2}{\sqrt{6}} \end{bmatrix} = \begin{bmatrix} 1 & 0 \\ 0 & 1 \end{bmatrix} = \boldsymbol{I}
$$

Thus the natural modes of the system are given by

$$
\boldsymbol{u}_1(t) = \begin{bmatrix} \dfrac{1}{\sqrt{3}} \\ \dfrac{1}{\sqrt{3}} \end{bmatrix} \sin \sqrt{2}\,(t - t_0) \quad \text{and} \quad \boldsymbol{u}_2(t) = \begin{bmatrix} -\dfrac{1}{\sqrt{6}} \\ \dfrac{2}{\sqrt{6}} \end{bmatrix} \sin \sqrt{5}\,(t - t_0').
$$

The solution of the non-homogeneous system, subject to given initial conditions, is found by solving the uncoupled equations

$$
\ddot{\boldsymbol{x}}(t) + \begin{bmatrix} 2 & 0 \\ 0 & 5 \end{bmatrix} \boldsymbol{x}(t) = \begin{bmatrix} \dfrac{1}{\sqrt{3}} & \dfrac{1}{\sqrt{3}} \\ -\dfrac{1}{\sqrt{6}} & \dfrac{2}{\sqrt{6}} \end{bmatrix} \begin{bmatrix} 0 \\ 10 \end{bmatrix} = \begin{bmatrix} \dfrac{10}{\sqrt{3}} \\ \dfrac{20}{\sqrt{6}} \end{bmatrix}
$$

by means of the Duhamel integral (6.14) (in this case with $\boldsymbol{r}$ constant) and then, from Equation (6.2) with $\boldsymbol{P} \equiv \boldsymbol{S} = [(\boldsymbol{s}_1, \boldsymbol{s}_2, \ldots, \boldsymbol{s}_n]$

$$
\boldsymbol{u}(t) = \boldsymbol{S}\boldsymbol{x}(t) = \sum_{i=1}^{n} \boldsymbol{s}_i x_i(t) \tag{6.16}
$$

Notice that the solution is expressed in Equation (6.16) as the superposition of the natural modes (eigenvectors) of the homogeneous equations. If the forcing function (load vector) is close to one of these modes the corresponding coefficient x_i will be large and will dominate the response - if it coincides then resonance will occur. Very often it is unnecessary to evaluate all n eigenvectors of the system; the higher frequency modes can be ignored and the solution adequately represented by superposition of the p eigenvectors associated with the p lowest eigenvalues, where $p < n$.

6.4 Proportional Damping

When element damping terms are included in the original dynamic equations (6.1) the transformation to a lower bandwidth system is still based on the model matrix $\boldsymbol{S}$ but Equation (6.12) is then not a system of uncoupled equations. One simplification often made in order to retain the diago-

nal nature of Equation (6.12) is to approximate the overall energy dissipation of the finite element system with *proportional damping*

$$\boldsymbol{s_i}^T \boldsymbol{C} \boldsymbol{s}_j = 2\omega_i \xi_i \delta_{ij},$$ (6.17)

where ξ_i is a modal damping parameter and δ_{ij} is the Kronecker delta. Equation (6.12) now reduces to n equations of the form

$$\ddot{x}_i(t) + 2\omega_i \xi_i \dot{x}_i(t) + \omega_1^2 x_1(t) = r_i(t)$$ (6.18)

with solution (the Duhamel integral)

$$x_i(t) = \frac{1}{\overline{\omega}_i} \int_0^t r_i(\tau) . e^{\xi_i \omega_i (t-\tau)} . \sin \overline{\omega}_i(t-\tau) \ dt + e^{-\xi_i \omega_i t} \{\alpha_i \sin \overline{\omega}_i t + \beta_i \cos \overline{\omega}_i t\}$$ (6.19)

where $\overline{\omega}_i = \omega_i \sqrt{1 - \xi_i^2}$. α_i and β_i are calculated from the initial conditions Equation (6.15). Once the components $x_i(t)$ have been found from Equation (6.19) (or alternative time integration methods applied to (6.18)), the solution $\boldsymbol{u}(t)$ is expressed as a superposition of the mode shapes $\boldsymbol{s}_i$ by Equation (6.16).

6.5 CMISS Examples

1. To analyse a plane stress modal analysis run CMISS example 451

2. To analyse a clamped beam modal analysis run CMISS example 452

3. To analyse a steel-framed building modal analysis run CMISS example 453

Chapter 7

Domain Integrals in the BEM

7.1 Achieving a Boundary Integral Formulation

The principal advantage of the BEM over other numerical methods is the ability to reduce the problem dimension by one. This property is advantagous as it reduces the size of the solution system leading to improved computational efficiency. This reduction of dimension also eases the burden on the engineer as it is only necessary to construct a boundary mesh to implement the BEM.

To achieve this reduction of dimension it is necessary to formulate the governing equation as a boundary integral equation. To achieve a boundary integral formulation it is necessary to find an appropriate reciprocity relationship for the problem and to determine an appropriate fundamental solution. If either of these requirements cannot be satisfied then a boundary integral formulation cannot be achieved. The most common difficulty in applying the BEM is in determining an appropriate fundamental solution.

A linear differential equation can be expressed in operator form as $Lu = \gamma$ where L is a linear operator, γ is an inhomogeneous source term and u is the dependent variable. The fundamental solution for this equation is a solution of

$$L^* \omega\left(\boldsymbol{x}, \boldsymbol{\xi}\right) + \delta\left(\boldsymbol{\xi}\right) = 0 \qquad (7.1)$$

where * indicates the adjoint of the operator L and δ is the Dirac delta function. No specific boundary conditions are prescribed but in some cases regularity conditions at infinity need to be satisfied. The fundamental solution is a Green's function which is not required to satisfy any boundary conditions and is therefore also commonly termed the free-space Green's function.

The mathematical theory required to determine the fundamental solution of a constant coefficient PDE is well-developed and has been used successfully to determine the fundamental solutions for a wide range of constant coefficient equations (Brebbia & Walker 1980) (Clements & Rizzo 1978) (Ortner 1987). Fundamental solutions are known and have been published for many of the most important equations in engineering such as Laplace's equation, the diffusion equation and the wave equation (Brebbia, Telles & Wrobel 1984*a*). However, by no means can it be guaranteed that the fundamental solution to a specific differential equation is known. In particular, PDEs with variable coefficients do not, in general, have known fundamental solutions. If the fundamental solution to an operator cannot be found then domain integrals cannot be completely removed from the integral formulation. Domain integrals will also arise for inhomogeneous equations.

Wu (1985) argued that the BEM has several advantages over other numerical methods which justify its use for many practical problems - even in cases where domain integration is required. He argued that for problems such as flow problems a wide range of phenomena are described by the same governing equations. What distinguishes these phenomena is the boundary conditions of the problem. For this reason accurate description of the boundary conditions is vital for solution accuracy. The BEM generates a formulation involving both the dependent variable u and the flux q. This allows flux boundary conditions to be applied directly which cannot be achieved in either the finite element or finite difference methods.

Another advantage of the BEM over other numerical methods is that it allows an explicit expression for the solution at an internal point. This allows a problem to be subdivided into a number of zones for which the BEM can be applied individually. This zoning approach is suited to problems with significantly different length scales or different properties in different areas.

Domain integration can be simply and accurately performed in the BEM. However, the presence of domain integrals in the BEM formulation negates one of the principal advantages of the BEM in that the problem dimension is no longer reduced by one. Several methods have been developed which allow domain integrals to be expressed as equivalent boundary integrals. In this section these methods will be discussed.

7.2 Removing Domain Integrals due to Inhomogeneous Terms

Inhomogeneous PDEs occur for a large number of physical problems. An inhomogeneous term may arise due to a number of factors including a source term, a body force term, or due to initial conditions in time-dependent problems. An inhomogeneous linear PDE can be expressed in operator form as $Lu = \gamma$ where γ is a known function of position or a non-zero constant. If the fundamental solution is known for the operator L, the resulting BEM formulation will be

$$\boldsymbol{H}\boldsymbol{u} - \boldsymbol{G}\boldsymbol{q} = -\int_{\Omega} \gamma\omega \, d\Omega \tag{7.2}$$

The domain integral in this formulation does not involve any unknowns so domain integration can be used directly to solve this equation. This requires discretising the domain into internal cells in much the same way as for the finite element method. As the domain integral does not involve any unknown values accurate results can generally be achieved using a fairly coarse mesh. This method is simple and has been shown to produce accurate results (Brebbia et al. 1984a). This approach, however, requires a domain discretisation and a numerical domain integration procedure which reduces the attraction of the BEM over domain-based numerical methods.

7.2.1 The Galerkin Vector technique

For some particular forms of the inhomogeneous function γ the domain integral can be transformed directly into boundary integrals.

Consider the Poisson equation $\nabla^2 u = \gamma$. Applying the BEM gives an equation of the form of

Equation (7.2). Using Green's second identity

$$\int_{\Omega} \left(\gamma \nabla^2 v - v \nabla^2 \gamma \right) d\Omega = \int_{\Gamma} \left(\gamma \frac{\partial v}{\partial n} - v \frac{\partial \gamma}{\partial n} \right) d\Gamma \tag{7.3}$$

domain integration can be avoided for certain forms of γ. If a v can be found which satisfies $\nabla^2 v = \omega$, where ω is the fundamental solution of Laplace's equation, then for the specific case of γ being harmonic ($\nabla^2 \gamma = 0$) Green's second identity can be reduced to

$$\int_{\Omega} \gamma \omega \, d\Omega = \int_{\Gamma} \left(\gamma \frac{\partial v}{\partial n} - v \frac{\partial \gamma}{\partial n} \right) d\Gamma \tag{7.4}$$

Therefore if a Galerkin vector can be found and γ is harmonic the domain integral in Equation (7.2) can be expressed as equivalent boundary integrals.

Fairweather, Rizzo, Shippy & Wu (1979) determined the Galerkin vector for the two-dimensional Poisson equation and Monaco & Rangogni (1982) determined the Galerkin vector for the three-dimensional Poisson equation. Danson (1981) showed how this method can be applied successfully for a number of physical problems involving linear isotropic problems with body forces. He considered the practical cases where the body force term arose due to either a constant gravitational load, rotation about a fixed axis or steady-state thermal loading. In each of these cases the domain integral can be expressed as equivalent boundary integrals.

This Galerkin vector approach provides a simple method of expressing domain integrals as equivalent boundary integrals. Unfortunately, it only applies to specific forms of the inhomogeneous term γ (*i.e.*, γ is required to be harmonic).

7.2.2 The Monte Carlo method

Domain discretisation could be avoided by using a Monte Carlo technique. This technique approximates a domain integral as a sum of the integrand at a number of random points. Specifically, in two dimensions, a domain integral I is approximated as

$$I \approx \frac{A}{N} \sum_{i=1}^{N} f(x_i, y_i) \tag{7.5}$$

where $f(x_i, y_i)$ is the value of the integrand at random point (x_i, y_i), N is the number of random points used and A is the area of the region over which the integration is performed. This approximation allows a domain integral to be approximated by a summation over a set of random points so domain integration can be performed without requiring a domain mesh. This method has the secondary advantage of allowing the integration to be performed over a simple geometry enclosing the problem domain - if a random point is not in the problem domain its contribution is ignored.

The method was proposed by Gipson (1987). Gipson has successfully applied this method to a number of Poisson-type problems. Unfortunately this method often proves to be computationally expensive as a large number of integration points are needed for accurate domain integration. Gipson argues however that, as this method removes the burden of preparing a domain mesh,

the extra computational expense is justified.

7.2.3 Complementary Function-Particular Integral method

A more general approach can be developed using particular solutions. Consider the linear problem $Lu = \gamma$. u can be considered as the sum of the complementary function u_c, which is a solution of the homogeneous equation $Lu_c = 0$, and a particular solution u_p which satisfies $Lu_p = \gamma$ but is not required to satisfy the boundary conditions of the problem. Applying BEM to the governing equation using the expansion $u = u_c + u_p$ gives

$$\boldsymbol{H}\boldsymbol{u} - \boldsymbol{G}\boldsymbol{q} = \boldsymbol{H}\boldsymbol{u_p} - \boldsymbol{G}\boldsymbol{q_p} \tag{7.6}$$

If a particular solution u_p can be found, all values on the right-hand-side of Equation (7.6) are known - reducing the problem to

$$\boldsymbol{H}\boldsymbol{u} - \boldsymbol{G}\boldsymbol{q} = \boldsymbol{d} \tag{7.7}$$

where $\boldsymbol{d}$ is a vector of known values. This linear system can be solved by applying boundary conditions.

This approach can be applied in a situation where an analytic expression for a particular solution can be found. Unfortunately particular solutions are generally only known for simple operators and for simple forms of γ. Alternatively an approximate particular solution could be calculated numerically. Zheng, Coleman & Phan-Thien (1991) proposed a method where a particular solution is determined by approximating the inhomogeneous source term using a global interpolation function. This approach is a special case of a more general method known as the dual reciprocity boundary element method.

7.3 Domain Integrals Involving the Dependent Variable

Consider the linear homogeneous PDE $Lu = 0$. For many operators the fundamental solution to the operator L may be unobtainable or may be in an unusable form. This is especially likely if L involves variable coefficients for which case it has been shown that it is particularly difficult to find a fundamental solution. Instead, a BEM formulation can be derived based on a related operator $\hat{L}$ with known fundamental solution. A BEM formulation for $Lu = 0$ based on the operator $\hat{L}$ will be of the form

$$\boldsymbol{H}\boldsymbol{u} - \boldsymbol{G}\boldsymbol{q} = -\int_{\Omega} \left(\hat{L} - L\right) u\omega \, d\Omega \tag{7.8}$$

where ω is the fundamental solution corresponding to the operator $\hat{L}$. This integral equation is similar to Equation (7.2). However in this case the domain integral term involves the dependent variable u. This problem could be solved using domain integration where the internal nodes are treated as formal problem unknowns.

7.3.1 The Perturbation Boundary Element Method

Rangogni (1986) proposed solving variable coefficient PDEs by coupling the boundary element method with a perturbation method. He considered the two-dimensional generalised Laplace equation

$$\nabla \cdot (\kappa (x, y) \nabla V (x, y)) = 0 \tag{7.9}$$

Using the substitution $V (x, y) = \kappa^{-\frac{1}{2}} u (x, y)$ Equation (7.9) can be recast as a heterogeneous Helmholtz equation

$$\nabla^2 u + f (x, y) u = 0 \tag{7.10}$$

where f is a known function of position.

Rangogni treated this equation as a perturbation about Laplace's equation. He considered the class of equations

$$\nabla^2 u + \varepsilon f (x, y) u = 0 \qquad \text{where } 0 \leq \varepsilon \leq 1 \tag{7.11}$$

for which he sought a solution of the form

$$u = u_0 + \varepsilon u_1 + \varepsilon^2 u_2 + \ldots = \sum_{j=0}^{\infty} u_j \varepsilon^j \tag{7.12}$$

Substituting Equation (7.12) into Equation (7.11) and grouping powers of ε gives

$$\nabla^2 u_0 + \varepsilon \left(\nabla^2 u_1 + f u_0 \right) + \varepsilon^2 \left(\nabla^2 u_2 + f u_1 \right) + \ldots = 0 \tag{7.13}$$

A solution will only exist for all values of ε if the terms at each power of ε equal zero. This allows Equation (7.13) to be treated as an infinite series of distinct problems which can be solved using the boundary element method. u_0 can be found by solving $\nabla^2 u_0 = 0$ which Rangogni assumes will satisfy the boundary conditions of the original problem. Each successive u_j can then be found by solving a Poisson equation with homogeneous boundary conditions as u_{j-1} has been previously determined. Rangogni used a domain discretisation to solve these Poisson problems.

Equation (7.10) is a particular member of this family of equations for which $\varepsilon = 1$. The solution to Equation (7.10) is therefore given by $\sum_{j=0}^{\infty} u_j$. Rangogni reported that in practice this series converged rapidly and in his numerical examples he achieved accurate results using only u_0 and u_1.

Rangogni (1991) extended this coupled perturbation - boundary element method to the general second-order variable coefficient PDE

$$\nabla^2 u + f (x, y) \frac{\partial u}{\partial x} + g (x, y) \frac{\partial u}{\partial y} = h (x, y) \tag{7.14}$$

He considered the family of equations

$$\nabla^2 u + \varepsilon \left[f\left(x,y\right) \frac{\partial u}{\partial x} + g\left(x,y\right) \frac{\partial u}{\partial y} \right] = h\left(x,y\right) \quad \left(0 \leq \varepsilon \leq 1\right) \tag{7.15}$$

Applying the perturbation method to this family of equations allows Equation (7.15) to be expressed as an infinite series of distinct Poisson equations which can be solved using the boundary element method. Again Rangogni used an domain mesh to solve these Poisson equations. Rangogni found that in practice convergence was rapid and accurate results were produced.

Gipson, Reible & Savant (1987) considered a class of hyperbolic and elliptic problems which can be transformed into an inhomogeneous Helmholtz equation. They used the perturbation method to recast this as an infinite sequence of Poisson equations. They avoided domain discretisation by using a Monte Carlo integration technique (Gipson 1987) to evaluate the required domain integrals.

Lafe & Cheng (1987) used the perturbation method to solve steady-state groundwater flow problems in heterogeneous aquifers. They showed the method produced accurate results for simply varying hydraulic conductivities with convergence after two or three terms. Lafe & Cheng investigated the convergence of the perturbation method. They found that for rapidly varying hydraulic conductivity convergence is not guaranteed. From this investigation they concluded that accurate results can be obtained so long as the hydraulic conductivity does not vary by more than one order of magnitude within the solution domain. If the hydraulic conductivity variation is more significant they recommend using the perturbation method in conjunction with a subregion technique so that the variation of conductivity within each subregion satisfies their requirements. This process could become computationally expensive, particularly if convergence is not rapid, as the solution of multiple subproblems will be required within each subregion.

7.3.2   The Multiple Reciprocity Method

The multiple reciprocity method (MRM) was initially proposed by Nowak (1987) for the solution of transient heat conduction problems. Since then the method has been successfully applied to a wide range of problems. The MRM can be viewed as a generalisation of the Galerkin vector approach. Instead of using one higher-order fundamental solution, the Galerkin vector, to convert the remaining domain integrals to equivalent boundary integrals a series of higher-order fundamental solutions is used.

Consider the Poisson equation

$$\nabla^2 u = b_0 \tag{7.16}$$

where $b_0 = b_0\left(\boldsymbol{x}\right)$ is a known function of position. Applying BEM to this equation, using the fundamental solution to the Laplace operator, gives

$$c\left(\boldsymbol{\xi}\right) u\left(\boldsymbol{\xi}\right) + \int_\Gamma u \frac{\partial \omega_0}{\partial n}\, d\Gamma + \int_\Omega b_0 \omega_0\, d\Omega = \int_\Gamma \omega_0 \frac{\partial u}{\partial n}\, d\Gamma \tag{7.17}$$

where ω_0 is the known fundamental solution to Laplace's equation applied at point $\boldsymbol{\xi}$. To avoid domain discretisation the domain integral in Equation (7.17) needs to be expressed as equivalent

boundary integrals. Using MRM this is achieved by defining a higher-order fundamental solution ω_1 such that

$$\nabla^2 \omega_1 = \omega_0 \tag{7.18}$$

Using this higher-order fundamental solution the domain integral in Equation (7.17) can be written as

$$\int_\Omega b_0 \omega_0 \, d\Omega = \int_\Omega b_0 \nabla^2 \omega_1 \, d\Omega \tag{7.19}$$

or

$$\int_\Omega b_0 \omega_0 \, d\Omega = \int_\Gamma \left(u \frac{\partial \omega_1}{\partial n} - \omega_1 \frac{\partial u}{\partial n} \right) d\Gamma + \int_\Omega \omega_1 \nabla^2 b_0 \, d\Omega \tag{7.20}$$

This formulation has generated a new domain integral. b_0 is a known function so we can introduce a new function b_1 which can be determined analytically from the relationship

$$b_1 = \nabla^2 b_0 \tag{7.21}$$

giving

$$\int_\Omega \omega_1 \nabla^2 b_0 \, d\Omega = \int_\Omega \omega_1 b_1 \, d\Omega \tag{7.22}$$

This process can be repeated by introducing a new higher-order fundamental solution ω_2 such that

$$\nabla^2 \omega_2 = \omega_1 \tag{7.23}$$

and continuing until convergence is reached.

This procedure is based on the recurrence relationships

$$b_{j+1} = \nabla^2 b_j \qquad \text{for } j = 0, 1, 2, \ldots \tag{7.24}$$

$$\nabla^2 \omega_{j+1} = \omega_j \qquad \text{for } j = 0, 1, 2, \ldots \tag{7.25}$$

Using these recurrence relationships gives the boundary integral formulation

$$c\left(\boldsymbol{\xi}\right) u\left(\boldsymbol{\xi}\right) + \int_\Gamma \left(u \frac{\partial \omega_0}{\partial n} - \omega_0 \frac{\partial u}{\partial n} \right) d\Gamma + \sum_{j=0}^{\infty} \int_\Gamma \left(b_j \frac{\partial \omega_{j+1}}{\partial n} - \omega_{j+1} \frac{\partial b_j}{\partial n} \right) d\Gamma = 0 \tag{7.26}$$

which is an exact formulation if the infinite series converges. Errors are only introduced at the stage of boundary discretisation.

Introducing interpolattion functions and discretising the boundary gives the matrix system

$$\boldsymbol{H_0 u} - \boldsymbol{G_0 q} = \sum_{j=0}^{\infty} \left(\boldsymbol{H_{J+1} p_j} - \boldsymbol{G_{J+1} r_j} \right) \tag{7.27}$$

where $\boldsymbol{H_{J+1}}$ and $\boldsymbol{G_{J+1}}$ are influence coefficient matrices corresponding to the higher-order fundamental solutions and $\boldsymbol{p_j}$ and $\boldsymbol{r_j}$ contain the nodal values of b_j and its normal derivative.

The MRM can be applied based on operators other than the Laplace operator. This approach relies on knowledge of the higher-order fundamental solutions necessary for application of the method. These solutions have been determined and successfully used for the Laplace operator in both two and three dimensions but the extension of the method to other equation types needs further research. Itagaki & Brebbia (1993) have determined the higher order fundamental solutions for the two-dimensional modified Helmholtz equation.

The MRM can be extended to other equations by allowing the forcing function b_0 to be a general function such that $b_0 = b_0\left(\boldsymbol{x}, u, t\right)$. The MRM will be restricted to cases where the recurrence relationships - Equations (7.24) and (7.25) - can be employed. Brebbia & Nowak (1989) have applied the MRM to the Helmholtz equation $\nabla^2 u + \kappa^2 u = 0$ where $b_0 = -\kappa^2 u$ and the recurrence relationship defined by Equation (7.24) becomes simply

$$u_{j+1} = \nabla^2 u_j = -\kappa^{2j} u \tag{7.28}$$

In this case the boundary integral formulation will be

$$c\left(\boldsymbol{\xi}\right) u\left(\boldsymbol{\xi}\right) + \sum_{j=0}^{\infty} \int_{\Gamma} \kappa^{2j} \left(u \frac{\partial \omega_j}{\partial n} - \omega_j \frac{\partial u}{\partial n} \right) d\Gamma = 0 \tag{7.29}$$

7.3.3   The Dual Reciprocity Boundary Element Method

Equation Derivation

The dual reciprocity boundary element method (DR-BEM) was developed to avoid the need for domain integration in cases where the fundamental solution of the governing differential equation is unknown or is impractical to apply. Instead the DR-BEM is applied using an appropriate related operator with known fundamental solution. The most common choice is the Laplace operator (Partridge, Brebbia & Wrobel 1992) and in this chapter the DR-BEM will be illustrated for this choice.

Consider a second-order PDE which can be expressed in the form

$$\nabla^2 u = b \tag{7.30}$$

The forcing function b can be completely general. If $b = b\left(\boldsymbol{x}\right)$ then b is a known function of position and the differential equation described is simply the Poisson equation. For potential problems $b = b\left(\boldsymbol{x}, u\right)$ and for transient problems $b = b\left(\boldsymbol{x}, u, t\right)$. Applying the BEM to Equation (7.30) will

give

$$\boldsymbol{Hu} - \boldsymbol{Gq} = -\int\limits_{\Omega} b\omega\, d\Omega \tag{7.31}$$

where ω is the known fundamental solution to Laplace's equation. The aim of the DR-BEM is to express the domain integral due to the forcing function b as equivalent boundary integrals.

The DR-BEM uses the idea of approximating b using interpolation functions. A global approximation to b of the form

$$b = \sum_{j=1}^{M} \alpha_j f_j \tag{7.32}$$

is proposed. α_j are unknown coefficients and f_j are approximating functions used in the interpolation and are generally chosen to be functions of the source point and the field point of the fundamental solution. The approximating functions f_j are applied at M different collocation points - called poles - generally most, but not all, of which are located on the boundary of the problem domain.

As discussed in the previous chapter the solution to a linear PDE $Lu = \gamma$ can be constructed as the sum of a complimentary function u_c (which satisfies the homogeneous equation $Lu_c = 0$) and a particular solution u_p to the equation $Lu_p = \gamma$. Instead of using a single particular solution, which may be difficult to determine, the DR-BEM employs a series of particular solutions $\hat{u}_j$ which are related to the approximating functions f_j as shown in Equation (7.33).

$$\nabla^2 \hat{u}_j = f_j \quad j = 1, \dots, M \tag{7.33}$$

By substituting Equations (7.32) and (7.33) into Equation (7.30) the forcing function b is approximated by a weighted summation of particular solutions to the Poisson equation.

$$\nabla^2 u = \sum_{j=1}^{M} \alpha_j \nabla^2 \hat{u}_j \tag{7.34}$$

The DR-BEM essentially constructs an approximate particular solution to the governing PDE as a summation of localised particular solutions.

With the governing equation rewritten in the form of Equation (7.34) the standard boundary element approach can be applied. Equation (7.34) is multiplied by a weighting function ω and integrated over the domain. Green's theorem is applied twice and the fundamental solution of the Laplacian is used to remove the remaining domain integrals. The name dual reciprocity BEM is derived from the application of reciprocity relationships to both sides of Equation (7.34). After applying these steps Equation (7.35) is obtained, where the fundamental solution pole is applied at

point $\boldsymbol{\xi}$.

$$c\left(\boldsymbol{\xi}\right)u\left(\boldsymbol{\xi}\right)+\int\limits_{\Gamma}\left(u\frac{\partial\omega}{\partial n}-\omega\frac{\partial u}{\partial n}\right)d\Gamma$$

$$=\sum_{j=1}^{M}\alpha_{j}\left(c\left(\boldsymbol{\xi}\right)u_{j}\left(\boldsymbol{\xi}\right)+\int\limits_{\Gamma}\left(\hat{u}_{j}\frac{\partial\omega}{\partial n}-\omega\frac{\partial hat u_{j}}{\partial n}\right)d\Gamma\right) \quad (7.35)$$

In implementing a numerical solution of this equation similar steps are taken as for the standard BEM. The boundary is discretised into elements and interpolation functions are introduced to approximate the dependent variable within each element.

The form of each $\hat{u}_j$ is known from Equation (7.33) once the approximating functions f_j have been defined. It is not necessary to use interpolation functions to approximate each $\hat{u}_j$. However by using the same interpolation functions to approximate u and $\hat{u}_j$ the numerical implementation will generate the same matrices $\boldsymbol{H}$ and $\boldsymbol{G}$ on both sides of Equation (7.35). The error generated by approximating each $\hat{u}_j$ in this manner has been found to be small and can be justified by the improved computational efficiency of the method (Partridge et al. 1992).

The application of this method results in the system

$$\boldsymbol{Hu}-\boldsymbol{Gq}=\sum_{j=1}^{N+I}\alpha_{j}\left(\boldsymbol{H\hat{u}_{j}}-\boldsymbol{G\hat{q}_{j}}\right) \quad (7.36)$$

where the M poles were chosen to be the N boundary nodes plus I internal points so that $M = N + I$. Although it is not generally necessary to include poles at internal points it has been found that in general improved accuracy is achieved by doing so (Nowak & Partridge 1992). It has been shown that for many problems (Partridge et al. 1992) (Huang & Cruse 1993) using boundary points only in this procedure is insufficient to define the problem. In general using internal points is likely to improve the solution accuracy as it increases the number of degrees of freedom. No theory has been developed of how many internal collocation points should be used for optimal accuracy, or where these points should be positioned within the problem domain. Using internal poles in this interpolation does not require domain discretisation - it is only necessary to specify the coordinates of the internal collocation points. The internal points can be chosen to be locations where the solution is of interest.

The $\hat{u}_j$ and $\hat{q}_j$ vectors can be treated as columns of the matrices $\hat{\boldsymbol{U}}$ and $\hat{\boldsymbol{Q}}$ respectively. This allows Equation (7.36) to be rewritten as

$$\boldsymbol{Hu}-\boldsymbol{Gq}=\left(\boldsymbol{H\hat{U}}-\boldsymbol{G\hat{Q}}\right)\boldsymbol{\alpha} \quad (7.37)$$

where $\boldsymbol{\alpha}$ is a vector containing the nodal values of α. To solve this system it is necessary to evaluate $\boldsymbol{\alpha}$. $\boldsymbol{\alpha}$ is defined by Equation (7.32) which, for the nodal values, can be expressed in matrix form as $\boldsymbol{b}=\boldsymbol{F\alpha}$. If the $\boldsymbol{F}$ matrix is nonsingular this expression can be rearranged to give Equation (7.38) which provides an explicit expression for $\boldsymbol{\alpha}$.

$$\boldsymbol{\alpha}=\boldsymbol{F}^{-1}\boldsymbol{b} \quad (7.38)$$

Including this explicit expression for $\boldsymbol{\alpha}$ in Equation (7.37) gives

$$\boldsymbol{Hu} - \boldsymbol{Gq} = \left(\boldsymbol{H\hat{U}} - \boldsymbol{G\hat{Q}} \right) \boldsymbol{F}^{-1} \boldsymbol{b} \tag{7.39}$$

The approach taken to solve this equation will depend on the form of b.

The Approximating Function f

The accuracy of the DR-BEM hinges on the accuracy of the global approximation to the forcing function b (defined by Equation (7.32)). Therefore the choice of the approximating functions f_j is a key consideration when implementing the DR-BEM. The only requirement so far prescribed on the form of the approximating functions f_j is that the $\boldsymbol{F}$ matrix generated should be nonsingular and that the related particular solutions $\hat{u}_j$ can be determined and can be expressed in a practical closed form. Some work has been conducted into investigating what form of f_j should be used in a given situation to provide the highest accuracy and computational efficiency.

Usually a form of f_j is defined and this can be used, applying Equation (7.33), to specify $\hat{u}$ and $\hat{q}$. The fundamental solution of Laplace's equation is $\omega(\boldsymbol{x}, \boldsymbol{\xi}) = -\dfrac{1}{2\pi} \ln r$ in two-dimensional space and $\omega(\boldsymbol{x}, \boldsymbol{\xi}) = \dfrac{1}{4\pi r}$ in three-dimensional space - where r is the Euclidean distance between the field point $\boldsymbol{x}$ and the source point $\boldsymbol{\xi}$ of the fundamental solution. Due to the dependence of this fundamental solution only on r the approximating function is generally chosen to be some radial function *i.e.,* $f_j = f_j(r)$. Several other options for f_j have been tried (Partridge et al. 1992) but it has been found that in general the most accurate results were generated using some radial function. For both two and three-dimensional problems Wrobel, Brebbia & Nardini (1986) recommended choosing f_j from the series

$$f_j = 1 + r_j + r_j^2 + \ldots + r_j^m \tag{7.40}$$

where r_j is the distance between the field point (node j) and the DR-BEM collocation point (node i). They showed that accurate results can be achieved using some combination of terms from this series. Generally the same approximating function f_j is used at all the collocation points so in this thesis, for simplicity, the form of approximating functions f_j will be referred to by a single f.

Choosing f to be a function of only one variable simplifies the process of determining $\hat{u}$ and $\hat{q}$. For two-dimensional problems, if $f = f(r)$ then the relationship

$$\nabla^2 \hat{u} = f(r) \tag{7.41}$$

can be reduced to the ordinary differential equation

$$\frac{d^2 \hat{u}}{dr^2} + \frac{1}{r} \frac{d\hat{u}}{dr} = f \tag{7.42}$$

Using f defined by Equation (7.40) the corresponding forms of $\hat{u}$ and $\hat{q}$, for two-dimensional

problems, can be shown to be

$$\hat{u} = \frac{r^2}{4} + \frac{r^3}{9} + \ldots + \frac{r^{m+2}}{(m+2)^2} \tag{7.43}$$

$$\hat{q} = \left(r_x \frac{\partial x}{\partial n} + r_y \frac{\partial y}{\partial n} \right) \left(\frac{1}{2} + \frac{r}{3} + \ldots + \frac{r^m}{m+2} \right) \tag{7.44}$$

where $r_x = x_j - x_i$ and $r_y = y_j - y_i$.

Any combination of terms from Equation (7.40) can be used for specifying f. It has been found that in general including higher-order terms leads to little improvement in accuracy (Partridge et al. 1992). The most commonly used form is $f = 1 + r$ as this approximation will generally give accurate results with greater computational efficiency than other choices.

Equation (7.40) was recommended as a basis for the approximating function f due to the particular form of the fundamental solution of Laplace's equation and its dependence on r only. If a different operator is used as the basis of the DR-BEM then it is likely a different form of f will be more appropriate. The choice of f in this case will be discussed in Section 7.3.3.

The performance of the DR-BEM hinges on the choice of the approximating function f. The theory of how to determine the best approximating function is therefore a vital component of the DR-BEM. Unfortunately the approximating function has generally been chosen and used in a rather ad-hoc manner. Recently some more formal analysis of the use of approximating functions has been undertaken.

Golberg & Chen (1994) argued that a formal analysis of the approximating function f can be undertaken using the theory of radial basis functions. Radial basis functions are a generalisation of cubic splines in multi-dimensions. Cubic splines are known to be optimal for one-dimensional interpolation. Therefore, rather than being an arbitrary choice, it seems that choosing f to be a radial function is a logical extension for two or three-dimensional problems. Golberg & Chen showed that, for the Poisson equation, choosing f to be a radial basis function ensures convergence of the DR-BEM.

They also demonstrated that $f = 1 + r$ is a specific member of the group of radial basis functions. The theory of using radial basis functions for multi-dimensional approximation is fairly advanced. It has been shown that $f = r$ is optimal for three-dimensional problems which justifies the use of $f = 1 + r$ when applying the DR-BEM to three-dimensional problems - the constant is included to ensure a non-zero diagonal for $\boldsymbol{F}$. However for two-dimensional problems it has been shown that optimal approximation is attained using the thin plate spline $f = r^2 log r$. This observation lead Golberg & Chen to suggest that choosing f to be a thin plate spline may improve the accuracy of the DR-BEM in two dimensions. Recently Golberg (1995) has published a review of the DR-BEM concentrating on developments since 1990 concerning the numerical evaluation of particular solutions.

Inhomogeneous Equations

If the forcing function b is a function of position only then the differential equation under consideration is simply Poisson's equation. In this case it is not necessary to invert the $\boldsymbol{F}$ matrix as $\boldsymbol{\alpha}$ can simply be calculated from $\boldsymbol{b} = \boldsymbol{F}\boldsymbol{\alpha}$ using Gaussian elimination. Equation (7.39) can be rewritten

as

$$\boldsymbol{Hu} - \boldsymbol{Gq} = \boldsymbol{d} \quad \text{where } \boldsymbol{d} = \left(\boldsymbol{H\hat{U}} - \boldsymbol{G\hat{Q}}\right) \boldsymbol{\alpha} \tag{7.45}$$

By applying boundary conditions Equation (7.45) can be reduced to a linear system $\boldsymbol{Ax} = \boldsymbol{\tau}$ which can be solved to give the unknown nodal values of u and q.

Zheng et al. (1991) and Coleman, Tullock & Phan-Thien (1991) have proposed a method which uses a global shape function to construct an approximate particular solution. As discussed by Polyzos, Dassios & Beskos (1994) this method is essentially equivalent to the DR-BEM. However, Zheng et al. and Coleman et al. suggested several alternative ways of determining the unknown coefficients α_j for inhomogeneous equations. Zheng et al. (1991) used a least-squares method where they minimised the sum of squares

$$S = \sum_{m=1}^{M} \left(b\left(r_m\right) - \sum_{j=1}^{N} \alpha_j f_j\left(r_m\right) \right) \tag{7.46}$$

using singular value decomposition. For large systems they found the computational efficiency could be improved by employing the conjugate gradient method. Coleman et al. (1991) successfully solved inhomogeneous potential and elasticity problems which are governed by operators other than the Laplacian.

Elliptic Problems

If b is a function of the dependent variable then $\boldsymbol{\alpha}$ will also be a function of the dependent variable. Consider, for example, the linear second-order differential equation

$$\nabla^2 u + u = 0 \tag{7.47}$$

In this case $b = -u$ so $\boldsymbol{\alpha} = \boldsymbol{F}^{-1} - \boldsymbol{u}$. Applying the DR-BEM to Equation (7.47), based on the fundamental solution to Laplace's equation, gives

$$\boldsymbol{Hu} - \boldsymbol{Gq} = -\left(\boldsymbol{H\hat{U}} - \boldsymbol{G\hat{Q}}\right) \boldsymbol{F}^{-1} \boldsymbol{u} \tag{7.48}$$

which can be rearranged to give

$$\left(\boldsymbol{H} + \boldsymbol{S}\right) \boldsymbol{u} = \boldsymbol{Gq} \quad \text{where } \boldsymbol{S} = \left(\boldsymbol{H\hat{U}} - \boldsymbol{G\hat{Q}}\right) \boldsymbol{F}^{-1} \tag{7.49}$$

Again, by applying boundary conditions Equation (7.49) can be reduced to a linear system $\boldsymbol{AX} = \boldsymbol{\tau}$ which can be solved to determine the unknown nodal values.

Due to the presence of the fully-populated $\boldsymbol{F}^{-1}$ matrix in Equation (7.49) it is not possible to solve the boundary problem and internal problem separately. Instead the solution can be treated as a coupled problem and the solutions at boundary and internal nodes are generated simultaneously.

Derivative Terms The DR-BEM can also be applied for elliptic problems where b involves derivatives of the dependent variable (Partridge et al. 1992). Consider, for example, the differ-

ential equation

$$\nabla^2 u + \frac{\partial u}{\partial x} = 0 \tag{7.50}$$

In this case applying DR-BEM, using the Laplace fundamental solution, gives

$$\boldsymbol{H u} - \boldsymbol{G q} = -\left(\boldsymbol{H \hat{U}} - \boldsymbol{G \hat{Q}}\right) \boldsymbol{F}^{-1} \frac{\partial \boldsymbol{u}}{\partial \boldsymbol{x}} \tag{7.51}$$

To solve this problem it is necessary to relate the nodal values of u to the nodal values of $\frac{\partial u}{\partial x}$. This is achieved by using interpolation functions to approximate $\boldsymbol{u}$ in a similar manner as was used to approximate b in Equation (7.32). A global approximation function of the form

$$u = \sum_{j=1}^{M} \phi_j \left(x, y\right) \beta_j \tag{7.52}$$

can be used to approximate u where ϕ_j are the chosen interpolation functions and β_j are the unknown coefficients. In system form this can be expressed as

$$\boldsymbol{u} = \boldsymbol{\Phi \beta} \tag{7.53}$$

Although it is not necessary, equating $\boldsymbol{\Phi}$ to $\boldsymbol{F}$ improves the computational efficiency of the method as only one matrix inversion procedure is required. Differentiating Equation (7.53) gives

$$\frac{\partial \boldsymbol{u}}{\partial \boldsymbol{x}} = \frac{\partial \boldsymbol{\Phi}}{\partial \boldsymbol{X}} \boldsymbol{\beta} \tag{7.54}$$

Choosing $\boldsymbol{\Phi} = \boldsymbol{F}$ and inverting Equation (7.53) to give an explicit expression for $\boldsymbol{\beta}$ allows Equation (7.54) to be rewritten as

$$\frac{\partial \boldsymbol{u}}{\partial \boldsymbol{x}} = \frac{\partial \boldsymbol{F}}{\partial \boldsymbol{X}} \boldsymbol{F}^{-1} \boldsymbol{u} \tag{7.55}$$

Equation (7.39) can now be rewritten as

$$\left(\boldsymbol{H} + \boldsymbol{R}\right) \boldsymbol{u} = \boldsymbol{G q} \quad \text{where } \boldsymbol{R} = \left(\boldsymbol{H \hat{U}} - \boldsymbol{G \hat{Q}}\right) \boldsymbol{F}^{-1} \frac{\partial \boldsymbol{F}}{\partial \boldsymbol{X}} \boldsymbol{F}^{-1} \tag{7.56}$$

By applying boundary conditions Equation (7.56) can be reduced to a linear system which can be solved to give the unknown nodal values.

As mentioned earlier, the approximating function f is generally chosen to be $f = 1 + r$. This can lead to numerical problems if derivative terms are included in the forcing function b. As shown in Equation (7.55) derivative terms require derivatives of f to be evaluated. For example, evaluating

the $\dfrac{\partial \boldsymbol{F}}{\partial \boldsymbol{X}}$ matrix requires calculation of $\dfrac{\partial f}{\partial x}$. Using the approximating function $f = 1 + r$ gives

$$\frac{\partial f}{\partial x} = \frac{\partial f}{\partial r}\frac{\partial r}{\partial x} = \frac{\partial f}{\partial r}\frac{r_x}{r} \tag{7.57}$$

This derivative function can become singular, so - as shown by Zhang (1993) - significant numerical error may result. This will especially be the case in problems where collocation points are located close together.

Zhang (1993) suggested two possibilities for avoiding this problem. The first suggestion involved using a mapping procedure to map the governing equation to an equation without convective terms. This method was shown to produce accurate results but is somewhat cumbersome and can only be applied to linear problems. A simpler approach is to choose an approximating function which does not lead to singularities for convective terms. Zhang recommended use of either $f = 1 + r^3$ or $f = 1 + r^2 + r^3$. These approximating functions produce accurate results and can be simply applied for both linear and nonlinear problems. Zhang recommended the adoption of these approximating functions for all use of the DR-BEM.

The same idea of using Equation (7.53) to allow nodal values of u to be associated to its derivatives can be applied to extend the DR-BEM to cases involving higher-order derivatives or cross derivatives of the dependent variable. Appropriate approximating functions need to be chosen to avoid the problem of singularities.

Variable Coefficients   The DR-BEM can be readily extended to equations with variable coefficients. Consider the variable coefficient Helmholtz equation

$$\nabla^2 u + \kappa\left(\boldsymbol{x}\right) u = 0 \tag{7.58}$$

where κ is a function of position - $\kappa = \kappa\left(x, y\right)$ in two dimensions. If the DR-BEM is applied using the known fundamental solution to the Laplace operator then the forcing function is $b = -\kappa u$. Applying the DR-BEM gives

$$\boldsymbol{H u} - \boldsymbol{G q} = \left(\boldsymbol{H \hat{U}} - \boldsymbol{G \hat{Q}}\right)\boldsymbol{F}^{-1}\boldsymbol{b} \tag{7.59}$$

where $\boldsymbol{b}$ is a vector of the nodal values of the forcing function b. The relationship $b = -\kappa u$ can be written in matrix form as $\boldsymbol{b} = -\boldsymbol{K u}$ where $\boldsymbol{K}$ is a diagonal matrix containing the nodal values of $\kappa\left(x, y\right)$ i.e.,

$$\boldsymbol{K} = \begin{bmatrix} \kappa\left(x_1, y_1\right) & 0 & \cdots & 0 \\ 0 & \kappa\left(x_2, y_2\right) & \cdots & 0 \\ \vdots & \vdots & \ddots & \vdots \\ 0 & 0 & \cdots & \kappa\left(x_M, y_M\right) \end{bmatrix} \tag{7.60}$$

where M is the number of collocation points used in applying the DR-BEM.

Using this matrix expression for b Equation (7.59) can be rearranged to give

$$(\boldsymbol{H} + \boldsymbol{SK})\, \boldsymbol{u} = \boldsymbol{Gq} \quad \text{where} \boldsymbol{S} = \left(\boldsymbol{H}\hat{\boldsymbol{U}} - \boldsymbol{G}\hat{\boldsymbol{Q}}\right) \boldsymbol{F}^{-1} \tag{7.61}$$

which is a boundary-only expression for the variable coefficient Helmholtz equation. This method is general and can easily be extended to accommodate variable coefficient derivative terms and a sum of variable coefficient terms.

Formulating the DR-BEM for a General Elliptic Problem In this section it has been shown how the DR-BEM can be applied for elliptic problems with varying forms of b. The DR-BEM can be applied in cases where b involves a sum of terms due to the basic property

$$\int_{\Omega} (b_1 + b_2)\, d\Omega = \int_{\Omega} b_1\, d\Omega + \int_{\Omega} b_2\, d\Omega \tag{7.62}$$

Consider a two-dimensional equation of the form

$$\nabla^2 u\,(x, y) = k\,(x, y)\, u + l\,(x, y)\, \frac{\partial u}{\partial x} + m\,(x, y)\, \frac{\partial u}{\partial y} + n\,(x, y) \tag{7.63}$$

Applying the DR-BEM to this equation gives a matrix system of the form

$$(\boldsymbol{H} - \boldsymbol{R})\, \boldsymbol{u} = \boldsymbol{Gq} + \boldsymbol{Sn} \tag{7.64}$$

where

$$\boldsymbol{S} = \left(\boldsymbol{H}\hat{\boldsymbol{U}} - \boldsymbol{G}\hat{\boldsymbol{Q}}\right) \boldsymbol{F}^{-1} \tag{7.65}$$

$$\boldsymbol{R} = \boldsymbol{S} \left[\boldsymbol{K} + \left(\boldsymbol{L}\frac{\partial \boldsymbol{F}}{\partial \boldsymbol{X}} + \boldsymbol{M}\frac{\partial \boldsymbol{F}}{\partial \boldsymbol{Y}}\right) \boldsymbol{F}^{-1}\right] \tag{7.66}$$

$\boldsymbol{K}$, $\boldsymbol{L}$ and $\boldsymbol{M}$ are diagonal matrices where the diagonals contain the nodal values of k, l and m respectively. $\boldsymbol{n}$ is a vector containing the nodal values of n.

The DR-BEM Using Other Operators

The DR-BEM has been presented in this chapter based on the Laplace operator. However the DR-BEM can be be applied using essentially any operator of appropriate order with known fundamental solution. If an appropriate operator can be found the complexity of the forcing function b can be reduced. This should improve the accuracy of the method. The problem with applying the DR-BEM based on another operator is in choosing the approximating function f. A choice of f which produces accurate results is required but it is also necessary to choose an f for which a particular solution $\hat{u}$ can be determined.

Zhu (1993) has determined the particular solutions necessary for applying the DR-BEM based on the two-dimensional Helmholtz operator.

$$\nabla^2 u + \kappa^2 u = b\,(x, y, u, t) \tag{7.67}$$

Radial functions have generally been used when applying the DR-BEM. Along the lines of Wrobel et al. (1986), Zhu chose an approximating function of the form $f = r^m$ where m is a positive integer. Determining the particular solution $\hat{u}$ requires solving the ordinary differential equation

$$\frac{d^2 \hat{u}}{dr^2} + \frac{1}{r}\frac{d\hat{u}}{dr} + \kappa^2 u = r^m \tag{7.68}$$

which can be achieved using a variation of coefficients method.

Partridge et al. (1992) applied the DR-BEM to the transient convection diffusion equation

$$D\nabla^2 u - v_x \frac{\partial u}{\partial x} - v_y \frac{\partial u}{\partial y} - ku = \frac{\partial u}{\partial t} \tag{7.69}$$

where the material parameters D, v_x, v_y and k are all assumed to be homogeneous. They applied the DR-BEM based on the steady-state convection-diffusion operator

$$D\nabla^2 u - v_x \frac{\partial u}{\partial x} - v_y \frac{\partial u}{\partial y} - ku = 0 \tag{7.70}$$

which has a known fundamental solution.

This analysis requires the determination of a particular solution $\hat{u}$ which satisfies

$$D\nabla^2 \hat{u} - v_x \frac{\partial \hat{u}}{\partial x} - v_y \frac{\partial \hat{u}}{\partial y} - k\hat{u} = f \tag{7.71}$$

Instead of defining a form of the approximating function f and solving for $\hat{u}$ Partridge et al. chose to define $\hat{u}$ and use Equation (7.71) to determine the corresponding approximating function. Although somewhat ad-hoc this approach was found to produce accurate results.

Chapter 8

The BEM for Parabolic PDES

8.1 Time-Stepping Methods

Several approaches have been proposed for applying the BEM to parabolic problems. These methods can be broadly classified into two main approaches. Either some form of time-stepping procedure is used to advance the solution in time, or a semi-analytic technique is used which can directly calculate a solution at a specified time. In this section time-stepping procedures will be considered.

Time-stepping approaches discretise the time domain in some manner and use some form of time marching scheme to advance the solution from one discrete time to the next. The two most commonly used time-stepping methods are the coupled finite difference - BEM and the direct time integration method. These two methods will be outlined in this section for the diffusion equation

$$\nabla^2 u\left(\boldsymbol{x}, t\right) = \frac{1}{\kappa}\frac{\partial u\left(\boldsymbol{x}, t\right)}{\partial t} \tag{8.1}$$

where the diffusivity κ is a material parameter which can be a constant or a function of position.

8.1.1 Coupled Finite Difference - Boundary Element Method

This approach discretises the time-domain in a finite difference form. Consider the variation between a time t^m and a time $t^{m+1} = t^m + \Delta t$. The most common approach (Brebbia et al. 1984b) is to assume that, for sufficiently small Δt, the time derivative can be approximated using a first-order fully implicit finite difference scheme

$$\frac{\partial u\left(\boldsymbol{x}, t^{m+1}\right)}{\partial t} = \frac{u\left(\boldsymbol{x}, t^{m+1}\right) - u\left(\boldsymbol{x}, t^m\right)}{\Delta t} \tag{8.2}$$

which allows the diffusion equation in this time-range to be approximated as

$$\nabla^2 u\left(\boldsymbol{x}, t^{m+1}\right) - \frac{1}{\kappa\Delta t}u\left(\boldsymbol{x}, t^{m+1}\right) + \frac{1}{\kappa\Delta t}u\left(\boldsymbol{x}, t^m\right) = 0 \tag{8.3}$$

Using this finite difference approximation the original parabolic equation has been reduced to an elliptic equation. Using the weighted residuals method an integral equation can be generated from

Equation (8.3).

$$c\left(\boldsymbol{\xi}\right)u^{m+1} + \int\limits_{\Gamma} u^{m+1}\frac{\partial\omega}{\partial n}\,d\Gamma = \int\limits_{\Omega} q^{m+1}\omega d\Gamma + \frac{1}{\kappa\Delta t}\int\limits_{\Omega} u^{m}\omega\,d\Omega \qquad (8.4)$$

where $u^{m+1} = u\left(\boldsymbol{x}, t^{m+1}\right)$ and $u^m = u\left(\boldsymbol{x}, t^m\right)$. The fundamental solution ω is a solution of the modified Helmholtz equation

$$\nabla^2\omega\left(\boldsymbol{x}, \boldsymbol{\xi}\right) - \frac{1}{\kappa\Delta t}\omega\left(\boldsymbol{x}, \boldsymbol{\xi}\right) + \delta\left(\boldsymbol{\xi}\right) = 0 \qquad (8.5)$$

applied at some source point ξ. The fundamental solution of the modified Helmholtz equation is known in both two and three dimensions. If an internal solution is required at a specific time this can be determined explicitly from Equation (8.4) where the fundamental solution is applied at internal point ξ and $c\left(\boldsymbol{\xi}\right) = 1$.

Unfortunately Equation (8.4) contains a domain integral. This integral is generally evaluated by using a domain mesh (Brebbia et al. 1984b). The domain integral does not include any problem unknowns so a fairly coarse domain mesh will generally suffice. Applying the BEM to Equation (8.4) gives

$$\boldsymbol{H}\boldsymbol{u}^{m+1} - \boldsymbol{G}\boldsymbol{q}^{m+1} = \boldsymbol{B}\boldsymbol{u}^m \qquad (8.6)$$

where $\boldsymbol{B}$ is a matrix containing the influence coefficients due to the domain integral. Using Equation (8.6) the solution can be advanced in time. $\boldsymbol{U^0}$ is known from the initial conditions so a solution can be calculated at $t = t_0 + \Delta t$. A solution at internal nodes can then be calculated. The time-stepping procedure can be repeated using the internal solution at $t = t_0 + \Delta t$ as pseudo-initial conditions for the next time-step.

If a constant time-step is used the matrices $\boldsymbol{H}$, $\boldsymbol{G}$ and $\boldsymbol{B}$ can be calculated once and stored. The boundary conditions can be applied to form a solution system of the form $\boldsymbol{A}\boldsymbol{x}^{m+1} = \boldsymbol{\tau}$ where $\boldsymbol{x}^{m+1}$ is the vector of unknown nodal values at time t^{m+1} and $\boldsymbol{\tau}$ is a vector constructed from known nodal values from the previous time-step. For a problem with time-independent boundary conditions at each time-step it is only necessary to update $\boldsymbol{\tau}$ and solve the system for $\boldsymbol{x}^{m+1}$. If a problem has time-dependent boundary conditions the solution system needs to be reformed at each time-step.

This coupled finite difference - boundary element method (FD-BEM) was first proposed by Brebbia & Walker (1980) for the diffusion equation. It was implemented and investigated by Curran, Cross & Lewis (1980). They found that this method will only produce accurate results if Equation (8.2) accurately approximates the time derivative. This will generally require small time-steps to be adopted. Curran et al. investigated the use of a higher-order approximation to the time-derivative. They found that this improved the accuracy of the method. Unfortunately it lead to a deterioration in convergence behaviour.

Tanaka, Matsimoto & Yang (1994) proposed a generalised version of this time-stepping scheme. They approximated the time variation within an interval as

$$u\left(\boldsymbol{x}, t\right) = \phi u\left(\boldsymbol{x}, t^{m+1}\right) + \left(1 - \phi\right)u\left(\boldsymbol{x}, t^m\right) \qquad (8.7)$$

where ϕ, termed the time-scheme parameter, is a constant in the range $0 < \phi \leq 1$. Substituting this approximation and a first-order finite difference approximation of the time derivative into the diffusion equation gives

$$\phi \nabla^2 u^{m+1} + (1 - \phi) \nabla^2 u^m = \frac{u^{m+1} - u^m}{\kappa \Delta t} \tag{8.8}$$

If $\phi = 1$ this approximation of the diffusion equation is equivalent to the standard FD-BEM discussed earlier. An integral equation can be derived from Equation (8.8). Tanaka et al. implemented this method and found it gave accurate results for a range of diffusion problems. They tested the accuracy for a Crank-Nicolson scheme ($\phi = \frac{1}{2}$), a Galerkin scheme ($\phi = \frac{2}{3}$) and a fully implicit scheme ($\phi = 1$). They found that the best results were achieved using a Crank-Nicolson scheme.

8.1.2 Direct Time-Integration Method

Instead of converting the original parabolic equation to an elliptic equation the problem can be treated directly in the time domain by directly integrating over both time and space. The weighted residual statement using this approach is

$$\int_{t_0}^{t_F} \int_{\Omega} \left[\nabla^2 u\left(\boldsymbol{x}, t\right) - \frac{1}{\kappa} \frac{\partial u\left(\boldsymbol{x}, t\right)}{\partial t} \right] \omega\left(\xi, \boldsymbol{x}, t_F, t\right) \, d\Omega \, dt = 0 \tag{8.9}$$

Integrating in time once and in space twice gives

$$c\left(\xi\right) u\left(\xi, t_F\right) + \kappa \int_{t_0}^{t_F} \int_{\Gamma} u \frac{\partial \omega}{\partial n} \, d\Gamma \, dt = \kappa \int_{t_0}^{t_F} \int_{\Gamma} q\omega \, d\Gamma \, dt + \int_{\Omega} u\left(\boldsymbol{x}, t_0\right) \omega \, d\Omega \tag{8.10}$$

where the fundamental solution ω satisfies

$$\kappa \nabla^2 \omega\left(\xi, \boldsymbol{x}, t_F, t\right) + \frac{\partial \omega\left(\xi, \boldsymbol{x}, t_F, t\right)}{\partial t} + \delta\left(\xi\right) \delta\left(t_F\right) = 0 \tag{8.11}$$

This time dependent fundamental solution is known in two and three dimensions. Physically this fundamental solution represents the effect at a field point $\boldsymbol{x}$ at time t of a unit point source applied at a point ξ at time t_F. If an internal solution is required at a specific time this can be determined from Equation (8.10) with $c\left(\xi\right) = 1$.

The variation of u and q with time is unknown so it is still necessary to step in time. However, as the time dependence is included in the fundamental solution, accurate results can be achieved using larger time-steps than with the FD-BEM. Two different time-stepping schemes can be used. Similarly to the FD-BEM, each time-step can be treated as a new problem so that an internal solution is constructed at the end of each time-step to be used as pseudo-initial conditions for the next time-step. Alternatively the time integration process can be restarted at t_0 with increasing numbers of intermediate steps used. These two time-stepping approaches are discussed in detail in Brebbia et al. (1984*b*).

The first method requires a new domain integral to be calculated after each time-step due to

the updated pseudo-initial conditions. The second time-stepping procedure involves only a domain integral at t_0 so, ideally, a domain integral only needs to be calculated once. This, however, will still require the user to create a domain mesh. As mentioned by Brebbia et al. (1984b), in many practical cases the domain integral can be avoided. If the initial conditions are $u_0 = 0$ throughout the body the domain integral equals zero. If the initial conditions satisfy Laplace's equation $\nabla^2 u_0 = 0$ then a Galerkin vector can be found and the domain integral can be expressed as equivalent boundary integrals. This includes many practical cases such as constant initial temperature or an initial linear temperature profile.

Unfortunately, in practice it is not always feasible to restart the integration process at t_0. At each time-step new $\boldsymbol{H}$ and $\boldsymbol{G}$ matrices are required so if many time-steps are required the storage capacity of the computer is likely to be exceeded. This requires the procedure to be restarted at some time where an internal solution is constructed and used as pseudo-initial conditions to repeat the process. Therefore, in practice, both time-stepping methods are likely to require domain integration.

8.2 Laplace Transform Method

An alternative approach which avoids time-stepping is to solve the problem in a transform domain which removes the time dependence of the problem. The parabolic PDE is thus converted to an elliptic problem for which the boundary element method has been shown to generally produce accurate results. Once the solution to the elliptic problem is determined in the transform space a solution in the original space can be attained using an inverse transform procedure. The most appropriate transform approach for parabolic problems is the Laplace transform.

Consider the diffusion equation

$$\nabla^2 u\left(\boldsymbol{x}, t\right) = \frac{1}{\kappa} \frac{\partial u\left(\boldsymbol{x}, t\right)}{\partial t} \tag{8.12}$$

with appropriate boundary and initial conditions. The Laplace transform of $u\left(\boldsymbol{x}, t\right)$ will be symbolised as $U\left(\boldsymbol{x}, \lambda\right)$ and is defined as

$$U\left(\boldsymbol{x}, \lambda\right) = \int_0^\infty e^{-\lambda t} u\left(\boldsymbol{x}, t\right) \, dt \tag{8.13}$$

Applying Laplace transforms to Equation (8.12) gives

$$\nabla^2 U\left(\boldsymbol{x}, \lambda\right) = \frac{1}{\kappa} \left(\lambda U\left(\boldsymbol{x}, \lambda\right) - u_0\left(\boldsymbol{x}\right)\right) \tag{8.14}$$

with transformed boundary conditions. $u_0\left(\boldsymbol{x}\right)$ is the initial conditions of u. Equation (8.14) is an elliptic PDE which can be readily solved using the boundary element method. Once the solution is determined in Laplace transform space this solution can be inverted to give a solution in the time-domain. This inversion procedure requires solutions to be generated for several values of the transform parameter λ.

This method was first proposed by Rizzo & Shippy (1970) and has since been successfully

used by other practitioners (Moridis & Reddell 1991) (Zhu, Satravaha & Lu 1994). Liggett & Liu (1979) compared the Laplace transform method with the time-dependent Green's function method. They noted that the direct method is simpler to apply. However, due to its greater efficiency, they recommended the Laplace transform method for solving diffusion problems.

One limitation of the Laplace transform method is that Equation (8.14) is inhomogeneous so that applying the standard BEM will generate a domain integral involving the initial conditions. Traditionally this domain integral has been calculated by using a domain discretisation (Brebbia et al. 1984b). However, recently Zhu et al. (1994) proposed using the DR-BEM to convert this domain integral term to equivalent boundary integrals. They chose to apply the DR-BEM based on the known fundamental solution to the Laplace operator. Considering Equation (8.14) this means that the DR-BEM will be used to convert the right-hand-side to equivalent domain integrals. Therefore the required DR-BEM approximation is

$$\frac{1}{\kappa}\left(\lambda U\left(\boldsymbol{x},\lambda\right)-u_0\left(\boldsymbol{x}\right)\right)=\sum_{j=1}^{N+L}f_j\alpha_j \tag{8.15}$$

The DR-BEM can now be applied to Equation (8.14), giving a matrix system of the form

$$\left(\boldsymbol{H}-\frac{\lambda}{\kappa}\boldsymbol{S}\right)\boldsymbol{u}-\boldsymbol{G}\boldsymbol{q}=-\frac{1}{\kappa}\boldsymbol{S}\boldsymbol{u_0} \tag{8.16}$$

which can be reduced to a square system by applying boundary conditions. Once the solution is determined for this elliptic equation in the transform space a solution at a given time can be constructed using an inversion process.

This Laplace transform dual reciprocity method (LT-DRM) can easily be extended to equations of the form

$$\nabla^2 u\left(\boldsymbol{x},t\right)=\frac{1}{\kappa}\frac{\partial u\left(\boldsymbol{x},t\right)}{\partial t}+b\left(\boldsymbol{x},u\right) \tag{8.17}$$

in which case a matrix expression of the form

$$\left(\boldsymbol{H}-\boldsymbol{R}-\frac{\lambda}{\kappa}\boldsymbol{S}\right)\boldsymbol{u}-\boldsymbol{G}\boldsymbol{q}=-\frac{1}{\kappa}\boldsymbol{S}\boldsymbol{u_0} \tag{8.18}$$

is generated. Zhu and his colleagues have successfully extended the LT-DRM to solve diffusion problems with nonlinear source terms.

8.3 The DR-BEM For Transient Problems

The DR-BEM can also be applied to parabolic problems. Consider, for example, the diffusion equation

$$\nabla^2 u=\frac{1}{\kappa}\frac{\partial u}{\partial t} \tag{8.19}$$

where the thermal diffusivity, κ, is a constant. In this case the global approximation of b implies a separation of variables such that

$$\frac{\partial u}{\partial t} = \sum_{j=1}^{M} f_j\left(\boldsymbol{x}\right) \alpha_j\left(t\right) \tag{8.20}$$

Using Equation (8.20), Equation (7.39) becomes

$$\boldsymbol{H}\boldsymbol{u} - \boldsymbol{G}\boldsymbol{q} = \frac{1}{\kappa}\left(\boldsymbol{H}\hat{\boldsymbol{U}} - \boldsymbol{G}\hat{\boldsymbol{Q}}\right)\boldsymbol{F}^{-1}\frac{\partial \boldsymbol{u}}{\partial \boldsymbol{t}} \tag{8.21}$$

or

$$\boldsymbol{C}\frac{\partial \boldsymbol{u}}{\partial \boldsymbol{t}} + \boldsymbol{H}\boldsymbol{u} = \boldsymbol{G}\boldsymbol{q} \quad \text{where } \boldsymbol{C} = -\frac{1}{\kappa}\left(\boldsymbol{H}\hat{\boldsymbol{u}} - \boldsymbol{G}\hat{\boldsymbol{Q}}\right)\boldsymbol{F}^{-1} \tag{8.22}$$

Equation (8.22) can be solved using a standard direct time-integration method.

Partridge & Brebbia (1990) recommended using a first-order finite difference approximation to the time derivative

$$\frac{\partial u}{\partial t} = \frac{u^{m+1} - u^m}{\Delta t} \tag{8.23}$$

and linear approximations to u and q within a time-step.

$$u = \left(1 - \phi_u\right)u^m + \phi_u u^{m+1} \tag{8.24}$$

$$q = \left(1 - \phi_q\right)q^m + \phi_q q^{m+1} \tag{8.25}$$

where ϕ_u and ϕ_q are weighting parameters with values in the range $(0, 1]$ and the time-step is between times t^m and $t^{m+1} = t^m + \Delta t$. Substituting these approximations into Equation (8.22) an expression at t^{m+1} can be derived in terms of values at t^m.

$$\left[\frac{1}{\Delta t}\boldsymbol{C} + \phi_u\boldsymbol{H}\right]\boldsymbol{u^{m+1}} - \phi_q\boldsymbol{G}\boldsymbol{q^{m+1}} = \left[\frac{\boldsymbol{c}}{\Delta t} - \left(1 - \phi_u\right)\boldsymbol{H}\right]\boldsymbol{u^m} + \left(1 - \phi_q\right)\boldsymbol{G}\boldsymbol{q^m} \tag{8.26}$$

The values of u^0 and q^0 are known from the initial conditions so a time-stepping procedure can be used. If a constant time-step is used the matrices $\boldsymbol{C}$, $\boldsymbol{H}$ and $\boldsymbol{G}$ only need to be constructed once. Using this two-level time-integration scheme the most common choice of time-scheme parameters is $\phi_u = 0.5, \phi_q = 1.0$.

8.4   The MRM for Transient Problems

The MRM can be applied to the diffusion equation $\nabla^2 u = \frac{1}{\kappa}\frac{\partial u}{\partial t}$ using the fundamental solution of Laplace's equation. In this case the forcing function becomes $b_0 = \frac{1}{\kappa}\frac{\partial u}{\partial t}$ and the recurrence

relationship defined by Equation (7.24) becomes

$$u_{j+1} = \nabla^2 u_j = \frac{\partial^j u}{\partial t^j} \tag{8.27}$$

The higher-order fundamental solutions are known for Laplace's equation. In this case the MRM formulation becomes

$$c\left(\xi\right)u\left(\xi\right) + \sum_{j=0}^{\infty}\int_{\Gamma}\frac{\partial\omega}{\partial n}\frac{\partial^j u}{\partial t^j}\,d\Gamma = \sum_{j=0}^{\infty}\int_{\Gamma}\omega\frac{\partial^j q}{\partial t^j}\,d\Gamma \tag{8.28}$$

The standard BEM numerical procedure can be applied to this boundary integral equation. This gives the matrix system

$$\boldsymbol{H_0 u} + \boldsymbol{H_1 \dot{u}} + \boldsymbol{H_2 \ddot{u}} + \ldots = \boldsymbol{G_0 q} + \boldsymbol{G_1 \dot{q}} + \boldsymbol{G_2 \ddot{q}} + \ldots \tag{8.29}$$

where the matrices $\boldsymbol{H_1}, \boldsymbol{G_1}$ etc are the influence coefficient matrices relating to the higher-order fundamental solutions. This equation can be solved using a time-integration procedure.

The most common approach is to solve this system numerically by discretising the time domain and using a time-stepping procedure. This requires some interpolation between the two time-levels marked by m and $m + 1$. This most common approach is to use a linear approximation to u and q in this time-range

$$u = \left(1 - \phi\right)u^m + \phi u^{m+1} \tag{8.30}$$
$$q = \left(1 - \phi\right)q^m + \phi q^{m+1} \tag{8.31}$$

where ϕ has a value in the range 0 to 1. Differentiating these linear approximations gives

$$\dot{u} = \frac{u^{m+1} - u^m}{\Delta t^m} \tag{8.32}$$
$$\dot{q} = \frac{q^{m+1} - q^m}{\Delta t^m} \tag{8.33}$$

and all the other derivatives vanish.

This allows Equation (8.29) to be simplified to

$$\boldsymbol{H_L u}^{m+1} - \boldsymbol{G_L q}^{m+1} = -\boldsymbol{H_R u}^m + \boldsymbol{G_R q}^m \tag{8.34}$$

where $\boldsymbol{H_L} = \frac{1}{\Delta t^m}\boldsymbol{H_1} + \phi\boldsymbol{H_0}$, $\boldsymbol{H_R} = -\frac{1}{\Delta t^m}\boldsymbol{H_1} + \left(1 - \phi\right)\boldsymbol{H_0}$, $\boldsymbol{G_L} = \frac{1}{\Delta t^m}\boldsymbol{G_1} + \phi\boldsymbol{G_0}$, $\boldsymbol{G_R} = -\frac{1}{\Delta t^m}\boldsymbol{G_1} + \left(1 - \phi\right)\boldsymbol{G_0}$. This approach is termed a first-order approach as it removes all but the first derivatives. A second order approach can be formulated by using quadratic interpolation of u and q within the time-range.

Using Equation (8.34) the solution can be advanced in time. If a constant time-step is used the matrices $\boldsymbol{H_L}, \boldsymbol{H_R}, \boldsymbol{G_L}$ and $\boldsymbol{G_R}$ only need to be constructed once outside the time-stepping loop. If the boundary conditions are not time-dependent the boundary conditions only need to be applied

once.

Bibliography

Brebbia, C. A. & Nowak, A. (1989), A new approach for transforming domain integrals to the boundary, *in* R. Gruber, J. Periaux & R. P. Shaw, eds, 'Proceedings of the Fifth International Symposium on Numerical Methods in Engineering', Computational Mechanics Publications, Springer-Verlag, pp. 73–84.

Brebbia, C. A., Telles, J. C. F. & Wrobel, L. C. (1984*a*), *Boundary Element Techniques*, Springer-Verlag.

Brebbia, C. A., Telles, J. C. F. & Wrobel, L. C. (1984*b*), *Boundary element techniques: Theory and applications in engineering*, Springer-Verlag, New York.

Brebbia, C. A. & Walker, S. (1980), *Boundary Element Techniques In Engineering*, Newnes–Butterworths.

Clements, D. L. & Rizzo, F. (1978), 'A method for the numerical solution of boundary value problems governed by second-order elliptic systems', *Journal of the Institute of Mathematics Applications* **22**, 197–202.

Coleman, C. J., Tullock, D. L. & Phan-Thien, N. (1991), 'An effective boundary element method for inhomogeneous partial differential equations', *Journal of Applied Mathematics and Physics (ZAMP)* **42**, 730–745.

Curran, D. A. S., Cross, M. & Lewis, B. A. (1980), 'Solution of parabolic differential equations by the boundary element method using discretisation in time', *Applied Mathematical Modelling* **4**, 398–400.

Danson, D. J. (1981), A boundary element formulation of problems in linear isotropic elasticity with body forces, *in* C. A. Brebbia, ed., 'Boundary Element Methods', Computational Mechanics Publications and Springer-Verlag, pp. 105–122.

Fairweather, G., Rizzo, F. J., Shippy, D. J. & Wu, Y. S. (1979), 'On the numerical solution of two-dimensional problems by an improved boundary integral equation method', *J. Comput. Phys.* **31**, 96–112.

Gipson, G. S. (1987), *Boundary Element Fundamentals - Basic Concepts And Recent Developments In The Poisson Equation*, Computational Mechanics Publications.

Gipson, G. S., Reible, D. D. & Savant, S. A. (1987), Boundary elements and perturbation theory for certain classes of hyperbolic and parabolic problems, *in* C. A. Brebbia, W. L. Wendland &

G. Kuhn, eds, 'Boundary Elements IX', Computational Mechanics Publications and Springer-Verlag, pp. 115–127.

Golberg, M. A. (1995), 'The numerical evaluation of particular solutions in the BEM - a review', *Boundary Element Communications* .

Golberg, M. A. & Chen, C. S. (1994), 'The theory of radial basis functions applied to the BEM for inhomogeneous partial differential equations', *BE Communications* **5**(2), 57–61.

Huang, Q. & Cruse, T. A. (1993), 'Some remarks on particular solution used in BEM formulation', *Computational Mechanics* **13**, 68–73.

Itagaki, M. & Brebbia, C. A. (1993), 'Generation of higher order fundamental solutions to the two-dimensional modified Helmholtz equation', *Engineering Analysis With Boundary Elements* **11**(1), 87–90.

Lafe, O. E. & Cheng, A. H.-D. (1987), 'A perturbation boundary element code for steady state groundwater flow in heterogeneous aquifers', *Water Resources Research* **23**(6), 1079–1084.

Liggett, J. A. & Liu, P. L.-F. (1979), 'Unsteady flow in confined aquifers: A comparison of two boundary integral methods', *Water Resources Research* **15**(4), 861–866.

Monaco, A. D. & Rangogni, R. (1982), Boundary element method: Processing of the source term of the Poisson equation by means of boundary integrals only, *in* K. P. Holz, U. Meissner, W. Zielke, C. A. Brebbia, G. Pinder & W. Gray, eds, 'Finite Elements In Water Resources IV', Springer-Verlag, pp. 19.29–19.36.

Moridis, G. L. & Reddell, D. L. (1991), The Laplace transform boundary element (LTBE) method for the solution of diffusion-type problems, *in* 'Boundary Elements XIII', Computational Mechanics Publications and Springer-Verlag, pp. 83–97.

Nowak, A. J. (1987), Solution of transient heat conduction problems using boundary-only formulation, *in* C. A. Brebbia, W. L. Wendland & G. Kuhn, eds, 'Boundary Elements IX Vol 3', Computational Mechanics Publications and Springer-Verlag, pp. 265–276.

Nowak, A. J. & Partridge, P. W. (1992), 'Comparison of the dual reciprocity and the multiple reciprocity methods', *Engineering Analysis With Boundary Elements* **10**, 155–160.

Ortner, N. (1987), Construction of fundamental solutions, *in* C. A. Brebbia, ed., 'Topics In Boundary Elements Research', Springer-Verlag, Berlin and New York.

Partridge, P. W. & Brebbia, C. A. (1990), The BEM dual reciprocity method for diffusion problems, *in* 'Computational Methods In Water Resources VIII', Computational Mechanics Publications and Springer-Verlag, pp. 397–403.

Partridge, P. W., Brebbia, C. A. & Wrobel, L. C. (1992), *The Dual Reciprocity Boundary Element Method*, Computational Mechanics Publications and Elsevier Applied Science.

Polyzos, D., Dassios, G. & Beskos, D. E. (1994), 'On the equivalence of dual reciprocity and particular integral approaches in the BEM', *BE Communications* **5**(6), 285–288.

Rangogni, R. (1986), 'Numerical solution of the generalized Laplace equation by coupling the boundary element method and the perturbation method', *Applied Mathematical Modelling* **10**, 266–270.

Rangogni, R. (1991), Solution of variable coefficients PDEs by means of BEM and perturbation technique, *in* 'Boundary Elements XIII', Computational Mechanics Publications and Springer-Verlag.

Rizzo, F. J. & Shippy, D. J. (1970), 'A method of solution for certain problems of heat conduction', *AIAA Journal* **8**(11), 2004–2009.

Tanaka, M., Matsimoto, T. & Yang, Q. F. (1994), 'Time-stepping boundary element method applied to 2-D transient heat conduction problems', *Applied Mathematical Modelling* **18**, 569–576.

Wrobel, L. C., Brebbia, C. A. & Nardini, D. (1986), The dual reciprocity boundary element formulation for transient heat conduction, *in* 'Finite Elements In Water Resources VI', Computational Mechanics Publications and Springer-Verlag.

Wu, J. C. (1985), Boundary element methods and inhomogeneous parabolic equations, *in* C. A. Brebbia & B. J. Noye, eds, 'BETECH 85', Springer-Verlag, pp. 19–30.

Zhang, Y. (1993), On the dual reciprocity boundary element method, Master's thesis, The University of Wollongong.

Zheng, R., Coleman, C. J. & Phan-Thien, N. (1991), 'A boundary element approach for non-homogeneous potential problems', *Computational Mechanics* **7**, 279–288.

Zhu, S. (1993), 'Particular solutions associated with the Helmholtz operator used in DRBEM', *BE Abstracts* **4**(6), 231–233.

Zhu, S., Satravaha, P. & Lu, X. (1994), 'Solving linear diffusion equations with the dual reciprocity method in Laplace space', *Engineering Analysis With Boundary Elements* **13**, 1–10.

Index